NASA TM X-1386

LONGITUDINAL AERODYNAMIC CHARACTERISTICS AT MACH NUMBERS FROM 0.50 TO 1.19 OF A SUPERSONIC TRANSPORT MODEL WITH A MODIFIED M WING

By Edward J. Ray and Robert T. Taylor

Langley Research Center
Langley Station, Hampton, Va.

NATIONAL AERONAUTICS AND SPACE ADMINISTRATION

For sale by the Clearinghouse for Federal Scientific and Technical Information
Springfield, Virginia 22151 – CFSTI price $3.00

LONGITUDINAL AERODYNAMIC CHARACTERISTICS AT MACH NUMBERS FROM 0.50 TO 1.19 OF A SUPERSONIC TRANSPORT MODEL WITH A MODIFIED M WING

By Edward J. Ray and Robert T. Taylor
Langley Research Center

SUMMARY

An investigation has been made at Mach numbers ranging from 0.50 to 1.19 in the Langley high-speed 7- by 10-foot tunnel to determine the longitudinal aerodynamic characteristics of a supersonic transport airplane configuration designated SCAT 18. Longitudinal stability and control effectiveness characteristics were determined for various combinations of model components and the complete configuration with two different horizontal-tail sizes.

The results of the investigation indicated that the addition of the horizontal tails had only a small effect on longitudinal stability of the configuration as a result of the extremely high downwash rate in the region of the tail. Reductions in horizontal-tail control effectiveness were apparent at moderate angles of attack as a result of possible reductions in dynamic pressure with increasing angle of attack in the region of the tail. The highest untrimmed lift-to-drag ratio occurring for the model with the larger horizontal tail was 8.6 at a Mach number of 0.98.

INTRODUCTION

During the past decade the National Aeronautics and Space Administration has directed a considerable amount of aerodynamic research towards the attainment of a commercially acceptable supersonic transport concept capable of cruise flight near a Mach number of 3.0. In 1959, the NASA presented a technical summary to the Federal Aviation Agency which indicated that the cruise phase of commercial supersonic flight was technically feasible for the ranges under consideration. (See ref. 1.)

The conflicting aerodynamic requirements presented by the off-design conditions have led to the study of a variety of configuration concepts. These concepts, designated as supersonic commercial air transports (SCAT) 1 through 19 with variations, have included variable-sweep wing, variable-sweep auxiliary wing panel, and fixed wing

arrangements. A summary and index of the experimental characteristics of the NASA SCAT concepts are contained in reference 2.

One of the major problems associated with the off-design conditions of a supersonic transport configuration with wings whose leading edges are subsonic at cruise has been the attainment of acceptable static longitudinal stability characteristics throughout the entire speed range. Several of the SCAT concepts which have been explored by the NASA have indicated promising performance characteristics but have exhibited undesirable longitudinal stability characteristics at subsonic and transonic Mach numbers. One approach which has been taken to maintain a wing with a reasonably high aspect ratio and a favorable load distribution is the M-wing concept. Subsonic and transonic investigations, references 3 and 4, respectively, have indicated that favorable pitching-moment characteristics might be obtained with an M-wing arrangement.

The purpose of the present investigation is to determine the subsonic and transonic longitudinal aerodynamic characteristics of a warped M-wing supersonic transport configuration designated as SCAT 18. This concept, designed for a cruise Mach number of 2.60, incorporates a slightly cambered fuselage and horizontal tails mounted at a dihedral angle of 8° near the base of the vertical tail. The four simulated engines are mounted below the wing. A similar SCAT 18 arrangement has been tested at supersonic Mach numbers ranging from 2.30 to 2.96 and these results are contained in reference 5.

The present paper presents the static longitudinal results determined for the SCAT 18 concept at Mach numbers ranging from 0.50 to 1.19 which corresponded to a Reynolds number (based on the wing mean aerodynamic chord) range of 2.88×10^6 to 4.50×10^6. In addition, experimental results are included herein which indicate the effects of the various model components on the longitudinal characteristics of the model. Longitudinal stability, control, and performance parameters are presented for the SCAT 18 configuration with two different horizontal-tail sizes. The results of the investigation are presented with a minimum of analysis in order to expedite publication of the basic data.

SYMBOLS

The data contained herein are referred to the wind-axis system. Reference dimensions used in the reduction of these data are indicated in this section. The moment reference point was at fuselage station 28.32 in. (71.93 cm) throughout the investigation. (See fig. 1(a).)

The units used for the physical quantities defined in this paper are given both in U.S. Customary Units and in the International System of Units (SI). Factors relating the two systems are given in reference 6.

c	local chord of airfoil section, in. (cm)
$\bar{c}$	mean aerodynamic chord of wing, 12.32 in. (31.29 cm)
$C_{A,i}$	nacelle internal axial-force coefficient, $\frac{\text{Internal axial force}}{qS}$
C_D	drag coefficient, $\frac{\text{Drag}}{qS}$
$C_{D_{i_t}}$	effective change in drag coefficient caused by unit angular change in horizontal-tail deflection, $\frac{\partial C_D}{\partial i_t}$, per deg
C_L	lift coefficient, $\frac{\text{Lift}}{qS}$
C_{L_α}	lift-curve slope at an angle of attack of 0^o, $\frac{\partial C_L}{\partial \alpha}$
C_m	pitching-moment coefficient, $\frac{\text{Pitching moment}}{qS\bar{c}}$
$C_{m_{C_L}}$	static margin at $C_L = 0$, $\frac{\partial C_m}{\partial C_L}$
$C_{m_{i_t}}$	effective change in pitching-moment coefficient at $C_L = 0$ caused by unit angular change in horizontal-tail deflection, $\frac{\partial C_m}{\partial i_t}$, per deg
$C_{m,o}$	pitching-moment coefficient at zero lift
i_t	horizontal-tail surface deflection measured from model reference line (position trailing edge down), deg
i_w	mean wing incidence, deg
L/D	lift-to-drag ratio
M	Mach number
q	dynamic pressure, lb/ft^2 (N/m^2)

R	Reynolds number based on $\bar{c}$
S	wing reference area including body intercept (see fig. 1(b)), 1.525 ft^2 (0.1417 m^2)
S_t	horizontal-tail area, ft^2 (m^2)
x	coordinate in streamwise direction, positive rearward, in. (cm)
y	coordinate in spanwise direction, $y = 0$ at fuselage center line, in. (cm)
z_u	vertical distance measured from model reference line to upper surface of wing (positive direction up), in. (cm)
z_l	vertical distance measured from model reference line to lower surface of wing (positive direction up), in. (cm)
α	angle of attack, deg
ϵ	average downwash angle (determined from tail-incidence tests), deg
$\frac{d\epsilon}{d\alpha}$	rate of change of downwash angle with angle of attack

Subscripts:

max	maximum
min	minimum

Model components:

B	fuselage
H_L	large horizontal tail
H_S	small horizontal tail
N	engine nacelles
V	vertical tail
W	wing

MODEL

Drawings of the complete model and the various model components are shown in figure 1 and photographs of the model are presented as figure 2. Tables I and II give the geometric characteristics of the model and the coordinates of the wing, respectively.

The wing of the SCAT 18 arrangement consisted of symmetrical NACA 65A-series streamwise airfoil sections varying in thickness from 4.22 percent chord at spanwise station 1.50 in. (3.81 cm) to 3.25 percent chord at spanwise station 3.40 in. (8.64 cm). (See fig. 1(b).) The wing thickness remained constant at 3.25 percent chord outboard to spanwise station 7.31 in. (18.57 cm). The thickness of the wing from spanwise station 7.31 in. (18.57 cm) to the wing tip was 2.82 percent of the wing chord.

The large and small horizontal tails and the vertical tail employed 3-percent-thick circular-arc streamwise airfoil sections. Both of the horizontal-tail arrangements were mounted to the fuselage at a dihedral angle of 8^{o}. The afterbody of the otherwise circular fuselage was modified to provide flat surfaces to accommodate the mounting of the horizontal-tail surfaces. (See fig. 1(a).)

The model of the present study was similar to the basic model utilized in the investigation of reference 5 with the exception of the assumed center-of-gravity location and the simulated engine arrangement. Four individual circular nacelles, having constant internal dimensions, were employed for the present study. Details of the nacelle arrangement are shown in figure 1(c).

TESTS AND CORRECTIONS

The investigation of the modified SCAT 18 model was made in the Langley high-speed 7- by 10-foot tunnel at Mach numbers of 0.50, 0.79, 0.89, 0.98, 1.01, and 1.19. The Reynolds number (based on the average temperature) and dynamic pressure, at each of the test Mach numbers are shown in the following table:

M	R	q	
		lb/ft^2	N/m^2
0.50	2.88×10^6	310	14 843
.79	3.80	617	29 542
.89	4.01	704	33 708
.98	4.37	778	37 251
1.01	4.40	794	38 017
1.19	4.50	884	42 326

The model was sting mounted and the forces and moments were measured with an internally mounted six-component strain-gage balance. The angles of attack have been corrected for the bending of the sting and balance combination due to aerodynamic loading.

Transition strips of No. 60 carborundum grains were applied near the leading edge of the airfoil, 1 inch (2.54 cm) behind the fuselage nose, and near the leading edge of the outside and inside of the engine nacelles to assure transition to turbulent boundary layer.

The internal skin friction of the four straight-through engine-nacelle simulators was computed and the experimental axial-force data were corrected at each test Mach number by the computed internal axial-force coefficient $C_{A,i}$ presented in the following table:

M	$C_{A,i}$
0.50	0.0017
.79	.0015
.89	.0015
.98	.0015
1.01	.0015
1.19	.0014

Nacelle base pressure and fuselage chamber pressure measurements were made and the drag data were adjusted to correspond to a condition of free-stream static pressure at the solid portions of the nacelle bases and in the balance cavity of the fuselage.

Jet-boundary and blockage corrections are negligible for the slotted tunnel configuration and, therefore, were not applied to the data.

PRESENTATION OF RESULTS

The results of the investigation are presented in the following figures:

SUMMARY OF RESULTS

A detailed discussion of results obtained in this investigation of a supersonic transport model with a modified M wing at Mach numbers from 0.50 to 1.19 has been omitted in order to expedite publication of these data. A few observations are made, however, in order to point out some of the more important results obtained.

Longitudinal Stability and Control

Nonlinearities in the variation of pitching-moment coefficient with lift coefficient were exhibited for all the configurations investigated. (See figs. 3 and 4.) The addition of two different horizontal-tail arrangements, differing in size, had only a small effect on the longitudinal stability level of the configuration due to the extremely high downwash rate in the region of the tail. As shown in figure 7, the downwash rate at the tail $d\epsilon/d\alpha$ was about 0.8 throughout the Mach number range of the investigation. In addition, the configurations incorporating the two different horizontal-tail arrangements indicated substantial reduction in longitudinal control effectiveness with increasing angle of attack (fig. 8), probably resulting from reduced dynamic pressure at the tail. Addition of the horizontal tails resulted in sizable positive increments in the zero-lift pitching-moment coefficient due to the misalinement between the effective mean chord planes of the wing and horizontal tail. (See fig. 9.) If the assumed center-of-gravity location were moved forward by about 10 percent of the wing mean aerodynamic chord to a center-of-gravity location similar to the one assumed in the investigation of reference 5, the large horizontal-tail configuration would trim without control deflection at the lift coefficient for maximum lift-to-drag ratio in the subsonic Mach number range. (See figs. 6(a), 6(b), and 6(c).)

Performance

The maximum untrimmed lift-to-drag ratios of the large horizontal-tail configuration varied from 7.6 at a Mach number of 0.50 to a maximum lift-to-drag ratio of 8.6 at a Mach number of 0.98. (See fig. 9.) The transonic drag rise occurred at a Mach number near 0.98. An untrimmed lift-to-drag ratio of about 7.0 was indicated for the

large-tail configuration at the highest test Mach number of 1.19. A maximum untrimmed lift-to-drag ratio of 9.2 was exhibited for the tail-off configuration at a Mach number of 0.98.

Langley Research Center,
National Aeronautics and Space Administration,
Langley Station, Hampton, Va., December 20, 1966,
720-01-00-03-23.

REFERENCES

1. Staff of the Langley Research Center: The Supersonic Transport – A Technical Summary. NASA TN D-423, 1960.

2. Ray, Edward J.: NASA Supersonic Commercial Air Transport (SCAT) Configurations: A Summary and Index of Experimental Characteristics. NASA TM X-1329, 1967.

3. Henderson, William P.: Longitudinal Stability Characteristics of Low-Aspect-Ratio Wings Having Variations in Leading- and Trailing-Edge Contours. NASA TN D-1796, 1964.

4. Loving, Donald L.: Investigation of the Effect of Indentation on an M-Plan-Form-Wing–Body Combination at Transonic Speeds. NACA RM L54F14, 1954.

5. Shrout, Barrett L.; and Corlett, William A.: Aerodynamic Characteristics at Mach 2.30, 2.60, and 2.96 of a Supersonic Transport Model with a Modified M Wing. NASA TM X-1056, 1965.

6. Mechtly, E. A.: The International System of Units – Physical Constants and Conversion Factors. NASA SP-7012, 1964.

TABLE I.- GEOMETRIC CHARACTERISTICS OF MODEL

$\frac{(\text{Volume})^{2/3}}{S}$	0.163
Wing:	
Aspect ratio	1.90
Span, in. (cm)	20.40 (51.82)
Reference area, ft^2 (m^2)	1.525 (0.1417)
Tip chord, in. (cm)	2.44 (6.20)
Mean aerodynamic chord, in. (cm)	12.32 (31.29)
Airfoil section (streamwise)	NACA 65A series
Fuselage:	
Length, in. (cm)	46.63 (118.44)
Fuselage base area, in^2 (cm^2)	4.02 (25.94)
Small horizontal tail:	
Span, in. (cm)	7.23 (18.36)
Area, ft^2 (m^2), both	0.21 (0.020)
Tip chord, in. (cm)	1.53 (3.89)
Root chord, in. (cm)	6.70 (17.02)
Airfoil section (streamwise)	0.03c-thick circular-arc
S_t/S	0.14
Dihedral angle, deg	8.00
Large horizontal tail:	
Span, in. (cm)	9.40 (23.88)
Area, ft^2 (m^2), both	0.32 (0.030)
Tip chord, in. (cm)	1.53 (3.89)
Root chord, in. (cm)	8.10 (20.57)
Airfoil section	0.03c-thick circular-arc
S_t/S	0.21
Dihedral angle, deg	8.00
Engine nacelles (each):	
Length, in. (cm)	7.50 (19.05)
Capture area, in^2 (cm^2)	0.71 (4.58)
Base area, in^2 (cm^2)	1.43 (9.22)

TABLE II.- WING COORDINATES

[All dimensions in inches (cm)]

x	z_u	z_l
y = 1.095 (2.781) x = 0 at model station 22.420 (56.947)		
0	0.300 (0.762)	0.300 (0.762)
.068 (0.173)	.346 (.879)	.261 (.663)
.102 (.259)	.357 (.907)	.253 (.643)
.169 (.429)	.374 (.950)	.240 (.610)
.339 (.861)	.404 (1.026)	.218 (.554)
.677 (1.720)	.443 (1.125)	.187 (.475)
1.016 (2.581)	.464 (1.178)	.156 (.396)
1.353 (3.437)	.476 (1.209)	.122 (.310)
2.031 (5.159)	.482 (1.224)	.075 (.190)
2.708 (6.878)	.489 (1.242)	.023 (.058)
3.385 (8.598)	.479 (1.217)	-.023 (-.058)
4.061 (10.315)	.471 (1.196)	-.054 (-.137)
4.738 (12.034)	.462 (1.173)	-.079 (-.201)
5.416 (13.757)	.449 (1.140)	-.096 (-.244)
6.092 (15.474)	.425 (1.080)	-.112 (-.284)
6.769 (17.193)	.403 (1.024)	-.113 (-.287)
7.446 (18.913)	.379 (.963)	-.106 (-.269)
8.122 (20.630)	.345 (.876)	-.102 (-.259)
8.800 (22.352)	.321 (.815)	-.082 (-.208)
9.477 (24.072)	.293 (.744)	-.059 (-.150)
10.154 (25.791)	.260 (.660)	-.037 (-.094)
10.830 (27.508)	.227 (.576)	-.110 (-.025)
11.507 (29.228)	.192 (.488)	.015 (.038)
12.185 (30.950)	.158 (.488)	.038 (.096)
12.861 (32.667)	.123 (.401)	.062 (.157)
13.538 (34.386)	.089 (.226)	.086 (.218)
y = 1.500 (3.810) x = 0 at model station 22.835 (58.001)		
0	0.438 (1.112)	0.438 (1.112)
.064 (0.162)	.481 (1.222)	.396 (1.006)
.097 (.246)	.491 (1.247)	.386 (.980)
.162 (.411)	.505 (1.283)	.371 (.942)
.323 (.820)	.530 (1.346)	.345 (.876)
.646 (1.641)	.551 (1.400)	.294 (.747)
.968 (2.459)	.572 (1.453)	.264 (.670)
1.291 (3.279)	.583 (1.481)	.232 (.589)
1.937 (4.920)	.606 (1.539)	.190 (.483)
2.582 (6.558)	.612 (1.554)	.146 (.371)
3.228 (8.199)	.610 (1.549)	.109 (.277)
3.874 (9.840)	.604 (1.534)	.079 (.201)
4.519 (11.478)	.600 (1.524)	.059 (.150)
5.165 (13.119)	.590 (1.499)	.045 (.114)
5.810 (14.757)	.567 (1.440)	.030 (.076)
6.456 (16.398)	.538 (1.366)	.023 (.058)
7.102 (18.039)	.505 (1.283)	.020 (.051)
7.747 (19.677)	.480 (1.219)	.034 (.086)
8.393 (21.318)	.441 (1.120)	.038 (.096)
9.039 (22.959)	.402 (1.021)	.050 (.127)
9.684 (24.597)	.369 (.937)	.073 (.185)
10.330 (26.238)	.334 (.848)	.095 (.241)
10.975 (27.876)	.296 (.752)	.117 (.297)
11.621 (29.517)	.262 (.665)	.141 (.358)
12.267 (31.158)	.226 (.574)	.165 (.419)
12.912 (32.796)	.189 (.480)	.187 (.475)

x	z_u	z_l
y = 2.040 (5.182) x = 0 at model station 22.101 (56.137)		
0	0.642 (1.631)	0.642 (1.631)
.067 (0.170)	.684 (1.737)	.599 (1.521)
.100 (.254)	.694 (1.763)	.589 (1.496)
.167 (.424)	.709 (1.801)	.575 (1.460)
.334 (.848)	.734 (1.864)	.549 (1.394)
.667 (1.694)	.767 (1.948)	.510 (1.295)
1.000 (2.540)	.784 (1.991)	.476 (1.209)
1.334 (3.388)	.798 (2.027)	.446 (1.133)
2.001 (5.082)	.819 (2.080)	.403 (1.024)
2.667 (6.774)	.814 (2.068)	.349 (.886)
3.335 (8.471)	.812 (2.062)	.313 (.795)
4.001 (10.162)	.802 (2.037)	.276 (.701)
4.668 (11.857)	.785 (1.994)	.245 (.622)
5.335 (13.551)	.757 (1.923)	.222 (.564)
6.002 (15.245)	.728 (1.849)	.192 (.488)
6.668 (16.937)	.690 (1.753)	.175 (.444)
7.336 (18.633)	.648 (1.646)	.157 (.399)
8.002 (20.325)	.600 (1.524)	.154 (.391)
8.669 (22.019)	.559 (1.420)	.157 (.399)
9.336 (23.713)	.509 (1.293)	.158 (.401)
10.003 (25.408)	.455 (1.156)	.159 (.404)
10.669 (27.099)	.406 (1.031)	.168 (.427)
11.337 (28.796)	.367 (.932)	.188 (.478)
12.003 (30.488)	.317 (.805)	.196 (.498)
12.670 (32.181)	.275 (.698)	.214 (.544)
13.337 (33.876)	.233 (.592)	.231 (.587)
y = 2.551 (6.480) x = 0 at model station 20.528 (52.141)		
0	0.906 (2.301)	0.906 (2.301)
.073 (0.185)	.949 (2.410)	.864 (2.194)
.110 (.279)	.959 (2.436)	.854 (2.169)
.183 (.465)	.972 (2.469)	.838 (2.128)
.365 (.927)	.996 (2.530)	.810 (2.057)
.731 (1.857)	1.025 (2.604)	.768 (1.951)
1.096 (2.784)	1.040 (2.642)	.732 (1.859)
1.461 (3.711)	1.052 (2.672)	.701 (1.780)
2.193 (5.570)	1.051 (2.670)	.635 (1.613)
2.923 (7.424)	1.021 (2.593)	.555 (1.410)
3.654 (9.281)	.991 (2.517)	.490 (1.245)
4.384 (11.135)	.949 (2.410)	.423 (1.074)
5.115 (12.992)	.908 (2.306)	.367 (.932)
5.846 (14.849)	.857 (2.177)	.313 (.795)
6.577 (16.706)	.806 (2.047)	.274 (.696)
7.307 (18.560)	.753 (1.913)	.238 (.604)
8.038 (20.416)	.702 (1.783)	.217 (.551)
8.768 (22.271)	.651 (1.654)	.203 (.516)
9.500 (24.130)	.598 (1.519)	.195 (.495)
10.230 (25.984)	.547 (1.389)	.194 (.493)
10.961 (27.841)	.496 (1.260)	.198 (.503)
11.691 (29.695)	.444 (1.128)	.205 (.521)
12.422 (31.552)	.392 (.996)	.212 (.538)
13.153 (33.409)	.341 (.866)	.220 (.559)
13.884 (35.265)	.289 (.734)	.228 (.579)
14.614 (37.120)	.237 (.602)	.235 (.597)

TABLE II.- WING COORDINATES – Continued

x	z_u	z_l
y = 6.121 (15.547) x = 0 at model station 26.289 (66.774)		
0	0.841 (2.136)	0.841 (2.136)
.049 (0.124)	.867 (2.202)	.815 (2.070)
.074 (.188)	.873 (2.217)	.809 (2.055)
.124 (.315)	.881 (2.238)	.802 (2.037)
.249 (.632)	.896 (2.276)	.786 (1.996)
.497 (1.262)	.919 (2.334)	.767 (1.948)
.745 (1.892)	.938 (2.382)	.754 (1.915)
.993 (2.522)	.951 (2.416)	.741 (1.882)
1.490 (3.785)	.964 (2.448)	.718 (1.824)
1.987 (5.047)	.977 (2.482)	.701 (1.780)
2.483 (6.307)	.976 (2.479)	.680 (1.727)
2.980 (7.569)	.972 (2.469)	.660 (1.676)
3.477 (8.832)	.962 (2.443)	.642 (1.631)
3.973 (10.091)	.944 (2.398)	.620 (1.575)
4.470 (11.354)	.921 (2.339)	.603 (1.532)
4.966 (12.614)	.893 (2.268)	.592 (1.504)
5.463 (13.876)	.862 (2.189)	.574 (1.458)
5.960 (15.138)	.825 (2.096)	.561 (1.425)
6.456 (16.398)	.783 (1.989)	.544 (1.382)
6.954 (17.663)	.748 (1.900)	.539 (1.369)
7.449 (18.920)	.712 (1.808)	.536 (1.361)
7.946 (20.183)	.669 (1.699)	.528 (1.341)
8.443 (21.445)	.618 (1.570)	.521 (1.323)
8.940 (22.708)	.580 (1.473)	.509 (1.293)
9.436 (23.967)	.536 (1.361)	.500 (1.270)
9.933 (25.230)	.498 (1.265)	.496 (1.260)
y = 6.462 (16.413) x = 0 at model station 27.339 (69.441)		
0	0.795 (2.019)	0.795 (2.019)
.045 (0.114)	.817 (2.075)	.772 (1.961)
.068 (.173)	.823 (2.090)	.766 (1.946)
.114 (.290)	.831 (2.111)	.758 (1.925)
.227 (.576)	.846 (2.149)	.745 (1.892)
.454 (1.153)	.869 (2.207)	.731 (1.857)
.681 (1.730)	.888 (2.256)	.721 (1.831)
.908 (2.306)	.908 (2.306)	.717 (1.821)
1.362 (3.459)	.922 (2.342)	.697 (1.770)
1.816 (4.613)	.926 (2.352)	.673 (1.709)
2.270 (5.766)	.931 (2.365)	.658 (1.671)
2.726 (6.924)	.922 (2.342)	.638 (1.620)
3.180 (8.077)	.916 (2.327)	.624 (1.585)
3.634 (9.230)	.903 (2.294)	.607 (1.542)
4.087 (10.381)	.881 (2.238)	.590 (1.499)
4.542 (11.537)	.858 (2.179)	.568 (1.443)
4.996 (12.690)	.827 (2.100)	.565 (1.435)
5.449 (13.840)	.798 (2.027)	.555 (1.410)
5.903 (14.994)	.766 (1.946)	.547 (1.389)
6.358 (16.149)	.732 (1.859)	.541 (1.374)
6.812 (17.302)	.698 (1.773)	.536 (1.361)
7.267 (18.458)	.666 (1.692)	.536 (1.361)
7.721 (19.611)	.633 (1.608)	.536 (1.361)
8.175 (20.764)	.592 (1.504)	.527 (1.338)
8.629 (21.918)	.555 (1.410)	.521 (1.323)
9.083 (23.071)	.518 (1.316)	.516 (1.311)

x	z_u	z_l
y = 6.632 (16.845) x = 0 at model station 27.862 (70.770)		
0	0.765 (1.943)	0.765 (1.943)
.043 (0.109)	.787 (1.999)	.743 (1.887)
.065 (.165)	.792 (2.012)	.738 (1.874)
.109 (.277)	.800 (2.032)	.731 (1.857)
.216 (.053)	.814 (2.068)	.720 (1.829)
.432 (1.097)	.836 (2.123)	.704 (1.788)
.650 (1.651)	.855 (2.172)	.695 (1.765)
.866 (2.200)	.868 (2.205)	.686 (1.742)
1.298 (3.297)	.885 (2.248)	.669 (1.699)
1.731 (4.397)	.893 (2.268)	.653 (1.659)
2.164 (5.496)	.894 (2.271)	.636 (1.615)
2.597 (6.596)	.893 (2.268)	.621 (1.577)
3.030 (7.696)	.885 (2.248)	.606 (1.539)
3.463 (8.796)	.872 (2.215)	.590 (1.499)
3.895 (9.893)	.862 (2.189)	.585 (1.486)
4.329 (10.996)	.842 (2.139)	.566 (1.438)
4.761 (12.093)	.811 (2.060)	.561 (1.425)
5.194 (13.193)	.782 (1.986)	.551 (1.400)
5.627 (14.292)	.754 (1.915)	.547 (1.389)
6.060 (15.392)	.718 (1.824)	.540 (1.372)
6.493 (16.492)	.689 (1.750)	.535 (1.359)
6.925 (17.590)	.656 (1.666)	.534 (1.356)
7.358 (18.689)	.619 (1.572)	.526 (1.336)
7.792 (19.792)	.578 (1.468)	.517 (1.313)
8.224 (20.889)	.544 (1.382)	.512 (1.300)
8.656 (21.986)	.514 (1.306)	.512 (1.300)
y = 6.802 (17.277) x = 0 at model station 28.385 (72.098)		
0	0.742 (1.885)	0.742 (1.885)
.041 (0.104)	.764 (1.940)	.723 (1.836)
.062 (.157)	.771 (1.958)	.720 (1.829)
.104 (.264)	.784 (1.991)	.717 (1.821)
.207 (.526)	.803 (2.040)	.712 (1.808)
.415 (1.054)	.825 (2.096)	.699 (1.775)
.622 (1.580)	.848 (2.154)	.696 (1.768)
.828 (2.103)	.862 (2.189)	.688 (1.748)
1.243 (3.157)	.878 (2.230)	.672 (1.707)
1.657 (4.209)	.887 (2.253)	.656 (1.666)
2.071 (5.260)	.887 (2.253)	.641 (1.628)
2.487 (6.317)	.887 (2.253)	.627 (1.592)
2.900 (7.366)	.876 (2.225)	.609 (1.547)
3.314 (8.418)	.867 (2.202)	.598 (1.519)
3.729 (9.472)	.855 (2.172)	.590 (1.499)
4.144 (10.526)	.832 (2.113)	.577 (1.466)
4.559 (11.580)	.813 (2.065)	.573 (1.455)
4.972 (12.629)	.789 (2.004)	.568 (1.443)
5.387 (13.683)	.763 (1.938)	.564 (1.432)
5.802 (14.737)	.731 (1.857)	.557 (1.415)
6.215 (15.786)	.699 (1.775)	.553 (1.405)
6.630 (16.840)	.671 (1.704)	.553 (1.405)
7.044 (17.892)	.639 (1.623)	.550 (1.397)
7.459 (18.946)	.604 (1.534)	.545 (1.384)
7.873 (19.997)	.570 (1.448)	.540 (1.372)
8.287 (21.049)	.538 (1.366)	.536 (1.361)

TABLE II.- WING COORDINATES – Continued

x	z_u	z_l
y = 3.400 (8.636) x = 0 at model station 17.915 (45.504)		
0.145 (0.368)	1.234 (3.134)	1.234 (3.134)
.229 (.582)	1.276 (3.241)	1.192 (3.028)
.270 (.686)	1.284 (3.261)	1.179 (2.995)
.354 (.899)	1.297 (3.294)	1.163 (2.954)
.564 (1.432)	1.312 (3.332)	1.126 (2.860)
.982 (2.494)	1.315 (3.340)	1.058 (2.687)
1.401 (3.558)	1.293 (3.284)	.985 (2.502)
1.819 (4.620)	1.264 (3.210)	.912 (2.316)
2.656 (6.746)	1.204 (3.058)	.788 (2.002)
3.494 (8.875)	1.145 (2.908)	.680 (1.727)
4.330 (10.998)	1.086 (2.758)	.585 (1.486)
5.168 (13.127)	1.027 (2.608)	.501 (1.272)
6.005 (15.253)	.967 (2.456)	.427 (1.084)
6.842 (17.379)	.908 (2.306)	.364 (.924)
7.678 (19.502)	.849 (2.156)	.313 (.795)
8.371 (21.262)	.790 (2.007)	.274 (.696)
9.208 (23.388)	.731 (1.857)	.246 (.625)
10.044 (25.512)	.671 (1.704)	.224 (.569)
10.882 (27.640)	.612 (1.554)	.210 (.533)
11.720 (29.769)	.553 (1.405)	.200 (.508)
12.556 (31.892)	.494 (1.255)	.196 (.498)
13.393 (34.018)	.434 (1.102)	.196 (.498)
14.230 (36.144)	.375 (.952)	.196 (.498)
15.068 (38.273)	.316 (.803)	.195 (.495)
15.904 (40.396)	.257 (.653)	.195 (.495)
16.741 (42.522)	.197 (.500)	.194 (.493)
y = 3.741 (9.502) x = 0 at model station 18.964 (48.169)		
0	1.187 (3.015)	1.187 (3.015)
.079 (0.201)	1.227 (3.116)	1.146 (2.911)
.118 (.300)	1.234 (3.134)	1.135 (2.883)
.198 (.503)	1.245 (3.162)	1.118 (2.840)
.398 (1.011)	1.265 (3.213)	1.089 (2.766)
.795 (2.019)	1.284 (3.261)	1.041 (2.644)
1.192 (3.028)	1.283 (3.259)	.991 (2.517)
1.589 (4.036)	1.274 (3.236)	.941 (2.390)
2.383 (6.053)	1.226 (3.114)	.831 (2.111)
3.178 (8.072)	1.170 (2.971)	.730 (1.854)
3.972 (10.089)	1.109 (2.817)	.633 (1.608)
4.767 (12.108)	1.048 (2.662)	.549 (1.394)
5.562 (14.127)	.987 (2.507)	.474 (1.204)
6.354 (16.139)	.927 (2.354)	.410 (1.041)
7.149 (18.158)	.866 (2.200)	.356 (.904)
7.944 (20.178)	.806 (2.047)	.316 (.803)
8.738 (22.194)	.744 (1.890)	.284 (.721)
9.533 (24.214)	.683 (1.735)	.259 (.658)
10.327 (26.230)	.623 (1.582)	.240 (.610)
11.122 (28.250)	.562 (1.427)	.228 (.579)
11.916 (30.267)	.501 (1.272)	.219 (.556)
12.711 (32.286)	.440 (1.118)	.213 (.541)
13.504 (34.300)	.380 (.965)	.210 (.533)
14.300 (36.322)	.319 (.810)	.204 (.518)
15.094 (38.339)	.259 (.658)	.201 (.510)
15.889 (40.358)	.197 (.500)	.194 (.493)

x	z_u	z_l
y = 4.081 (10.366) x = 0 at model station 20.011 (50.828)		
0	1.160 (2.946)	1.160 (2.946)
.075 (0.190)	1.198 (3.043)	1.121 (2.847)
.113 (.287)	1.207 (3.066)	1.113 (2.827)
.188 (.478)	1.220 (3.099)	1.100 (2.794)
.376 (.955)	1.238 (3.144)	1.072 (2.723)
.752 (1.910)	1.264 (3.210)	1.033 (2.624)
1.128 (2.865)	1.278 (3.246)	1.002 (2.545)
1.503 (3.818)	1.278 (3.246)	.962 (2.443)
2.256 (5.730)	1.264 (3.210)	.888 (2.256)
3.008 (7.640)	1.231 (3.127)	.812 (2.062)
3.759 (9.548)	1.188 (3.018)	.737 (1.872)
4.512 (11.460)	1.137 (2.888)	.665 (1.689)
5.265 (13.373)	1.077 (2.736)	.591 (1.501)
6.016 (15.281)	1.015 (2.578)	.525 (1.334)
6.767 (17.188)	.947 (2.405)	.465 (1.181)
7.520 (19.101)	.879 (2.233)	.417 (1.059)
8.272 (21.011)	.810 (2.057)	.374 (.950)
9.024 (22.921)	.742 (1.885)	.342 (.869)
9.775 (24.828)	.674 (1.712)	.313 (.795)
10.528 (26.741)	.606 (1.539)	.290 (.737)
11.279 (28.649)	.538 (1.366)	.271 (.688)
12.032 (30.561)	.470 (1.194)	.257 (.653)
12.784 (32.471)	.402 (1.021)	.242 (.615)
13.536 (34.381)	.334 (.848)	.225 (.572)
14.287 (36.289)	.266 (.676)	.210 (.533)
15.040 (38.202)	.197 (.500)	.195 (.495)
y = 5.102 (12.959) x = 0 at model station 23.153 (58.809)		
0	0.987 (2.507)	0.987 (2.507)
.062 (0.157)	1.019 (2.588)	.956 (2.428)
.094 (.239)	1.028 (2.611)	.949 (2.410)
.156 (.396)	1.039 (2.639)	.939 (2.385)
.312 (.792)	1.060 (2.692)	.922 (2.342)
.624 (1.585)	1.093 (2.776)	.901 (2.288)
.937 (2.380)	1.114 (2.830)	.884 (2.245)
1.249 (3.172)	1.126 (2.860)	.864 (2.194)
1.872 (4.755)	1.132 (2.875)	.822 (2.088)
2.498 (6.345)	1.128 (2.865)	.781 (1.984)
3.121 (7.927)	1.115 (2.832)	.741 (1.882)
3.746 (9.515)	1.089 (2.766)	.698 (1.773)
4.370 (11.100)	1.065 (2.705)	.662 (1.681)
4.995 (12.687)	1.033 (2.624)	.626 (1.590)
5.619 (14.272)	.995 (2.527)	.594 (1.509)
6.244 (15.860)	.953 (2.421)	.568 (1.443)
6.868 (17.445)	.902 (2.291)	.541 (1.374)
7.492 (19.030)	.849 (2.156)	.515 (1.308)
8.117 (20.617)	.796 (2.022)	.496 (1.260)
8.741 (22.202)	.738 (1.874)	.479 (1.217)
9.365 (23.787)	.683 (1.735)	.462 (1.173)
9.989 (25.372)	.622 (1.580)	.444 (1.128)
10.614 (26.960)	.562 (1.427)	.427 (1.084)
11.239 (28.547)	.499 (1.267)	.410 (1.041)
11.862 (30.129)	.452 (1.148)	.407 (1.034)
12.487 (31.717)	.400 (1.016)	.398 (1.011)

TABLE II.- WING COORDINATES – Concluded

x	z_u	z_l
y = 7.142 (18.141) x = 0 at model station 29.429 (74.750)		
0	0.696 (1.768)	0.695 (1.765)
.038 (0.096)	.716 (1.819)	.676 (1.717)
.057 (.145)	.720 (1.829)	.672 (1.707)
.096 (.244)	.727 (1.846)	.665 (1.689)
.192 (.488)	.738 (1.874)	.654 (1.661)
.384 (.975)	.759 (1.928)	.643 (1.633)
.576 (1.463)	.777 (1.974)	.635 (1.613)
.767 (1.948)	.792 (2.012)	.630 (1.600)
1.151 (2.924)	.809 (2.055)	.618 (1.570)
1.534 (3.896)	.814 (2.068)	.601 (1.526)
1.918 (4.872)	.818 (2.078)	.589 (1.496)
2.302 (5.847)	.816 (2.073)	.575 (1.460)
2.685 (6.820)	.814 (2.068)	.568 (1.443)
3.069 (7.795)	.806 (2.047)	.557 (1.415)
3.452 (8.768)	.797 (2.024)	.552 (1.402)
3.836 (9.743)	.775 (1.968)	.538 (1.366)
4.220 (10.719)	.760 (1.930)	.537 (1.364)
4.603 (11.692)	.739 (1.877)	.534 (1.356)
4.987 (12.667)	.710 (1.803)	.524 (1.331)
5.371 (13.643)	.686 (1.742)	.524 (1.331)
5.754 (14.615)	.660 (1.676)	.524 (1.331)
6.138 (15.590)	.632 (1.605)	.523 (1.328)
6.521 (16.563)	.601 (1.526)	.518 (1.316)
6.905 (17.539)	.574 (1.458)	.518 (1.316)
7.288 (18.512)	.544 (1.382)	.516 (1.311)
7.672 (19.487)	.516 (1.311)	.514 (1.306)
y = 8.162 (20.731) x = 0 at model station 31.690 (80.493)		
0	0.396 (1.006)	0.396 (1.006)
.084 (0.213)	.413 (1.049)	.387 (.983)
.281 (.714)	.436 (1.107)	.395 (1.003)
.479 (1.217)	.459 (1.166)	.404 (1.026)
.676 (1.717)	.480 (1.219)	.410 (1.041)
.874 (2.220)	.497 (1.262)	.413 (1.049)
1.071 (2.720)	.513 (1.303)	.413 (1.049)
1.269 (3.223)	.532 (1.351)	.417 (1.059)
1.466 (3.724)	.541 (1.374)	.412 (1.046)
1.747 (4.437)	.555 (1.410)	.411 (1.044)
2.039 (5.179)	.568 (1.443)	.406 (1.031)
2.330 (5.918)	.574 (1.458)	.401 (1.018)
2.621 (6.657)	.579 (1.471)	.396 (1.006)
2.912 (7.396)	.578 (1.468)	.391 (.993)
3.203 (8.136)	.574 (1.458)	.385 (.978)
3.495 (8.877)	.568 (1.443)	.382 (.970)
3.786 (9.616)	.563 (1.430)	.383 (.973)
4.077 (10.356)	.547 (1.389)	.379 (.963)
4.368 (11.095)	.533 (1.354)	.377 (.958)
4.659 (11.834)	.520 (1.321)	.380 (.965)
4.951 (12.576)	.498 (1.265)	.376 (.955)
5.242 (13.314)	.485 (1.232)	.382 (.970)
5.533 (14.054)	.462 (1.173)	.379 (.963)
5.824 (14.793)	.447 (1.135)	.384 (.975)
6.116 (15.535)	.424 (1.077)	.383 (.973)
6.407 (16.274)	.407 (1.034)	.385 (.978)
6.698 (17.013)	.387 (.983)	.384 (.975)

x	z_u	z_l
y = 9.183 (23.325) x = 0 at model station 35.162 (89.312)		
0	0.350 (0.889)	0.350 (0.889)
.057 (0.145)	.363 (.922)	.347 (.881)
.192 (.488)	.383 (.973)	.357 (.907)
.327 (.830)	.395 (1.003)	.357 (.907)
.462 (1.173)	.409 (1.039)	.361 (.917)
.596 (1.514)	.423 (1.074)	.366 (.930)
.731 (1.857)	.437 (1.110)	.368 (.935)
.866 (2.200)	.443 (1.125)	.370 (.940)
1.001 (2.542)	.452 (1.148)	.369 (.937)
1.193 (3.030)	.464 (1.178)	.365 (.927)
1.391 (3.533)	.465 (1.181)	.360 (.914)
1.590 (4.039)	.476 (1.209)	.357 (.907)
1.789 (4.544)	.481 (1.222)	.356 (.904)
1.988 (5.050)	.487 (1.237)	.358 (.909)
2.187 (5.555)	.487 (1.237)	.358 (.909)
2.385 (6.058)	.485 (1.232)	.358 (.909)
2.584 (6.563)	.481 (1.222)	.358 (.909)
2.783 (7.069)	.474 (1.204)	.359 (.912)
2.981 (7.572)	.469 (1.191)	.362 (.919)
3.180 (8.077)	.462 (1.173)	.367 (.932)
3.379 (8.583)	.456 (1.158)	.373 (.947)
3.578 (9.088)	.449 (1.140)	.378 (.950)
3.777 (9.594)	.441 (1.120)	.384 (.975)
3.975 (10.096)	.428 (1.087)	.385 (.978)
4.175 (10.604)	.417 (1.059)	.389 (.988)
4.373 (11.107)	.404 (1.026)	.390 (.991)
4.572 (11.613)	.395 (1.003)	.395 (1.003)
y = 10.202 (25.913) x = 0 at model station 38.628 (98.115)		
0	0.215 (0.546)	0.215 (0.546)
.031 (0.079)	.223 (.566)	.213 (.541)
.103 (.262)	.234 (.594)	.219 (.556)
.174 (.442)	.244 (.620)	.224 (.569)
.247 (.627)	.254 (.645)	.228 (.579)
.319 (.810)	.263 (.668)	.231 (.587)
.392 (.996)	.271 (.688)	.236 (.599)
.463 (1.176)	.279 (.709)	.238 (.604)
.535 (1.359)	.287 (.729)	.240 (.610)
.638 (1.620)	.294 (.747)	.241 (.612)
.744 (1.890)	.300 (.762)	.241 (.612)
.850 (2.159)	.304 (.772)	.241 (.612)
.957 (2.431)	.307 (.780)	.240 (.610)
1.062 (2.697)	.309 (.785)	.240 (.610)
1.169 (2.969)	.310 (.787)	.241 (.612)
1.275 (3.238)	.310 (.787)	.243 (.617)
1.381 (3.508)	.309 (.785)	.244 (.620)
1.488 (3.780)	.306 (.777)	.245 (.622)
1.594 (4.049)	.303 (.770)	.247 (.627)
1.700 (4.318)	.300 (.762)	.249 (.632)
1.807 (4.590)	.296 (.752)	.251 (.638)
1.913 (4.859)	.291 (.739)	.254 (.645)
2.019 (5.128)	.287 (.729)	.258 (.655)
2.125 (5.398)	.283 (.719)	.260 (.660)
2.231 (5.667)	.278 (.706)	.263 (.668)
2.338 (5.938)	.274 (.696)	.266 (.676)
2.444 (6.208)	.270 (.686)	.267 (.678)

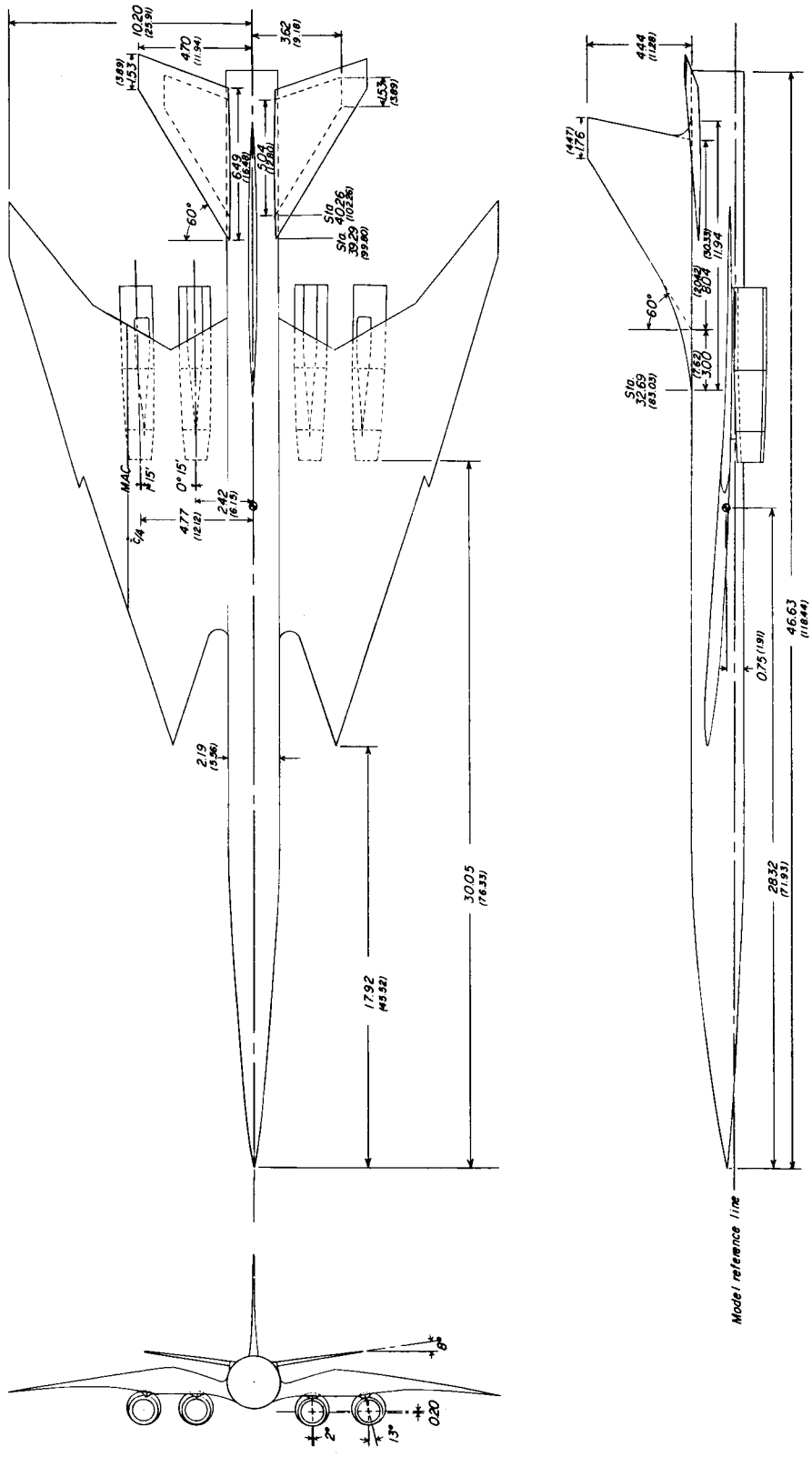

(a) Three-view drawing of complete model.

Figure 1.- Details of model. All dimensions in inches (cm) unless otherwise specified.

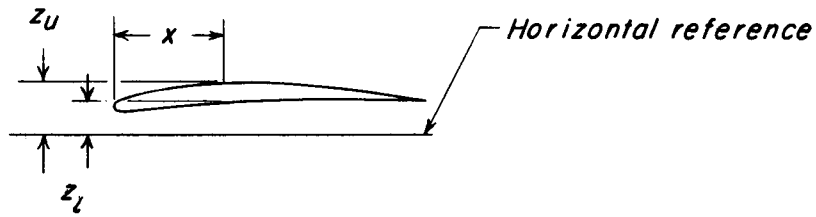

Typical wing section

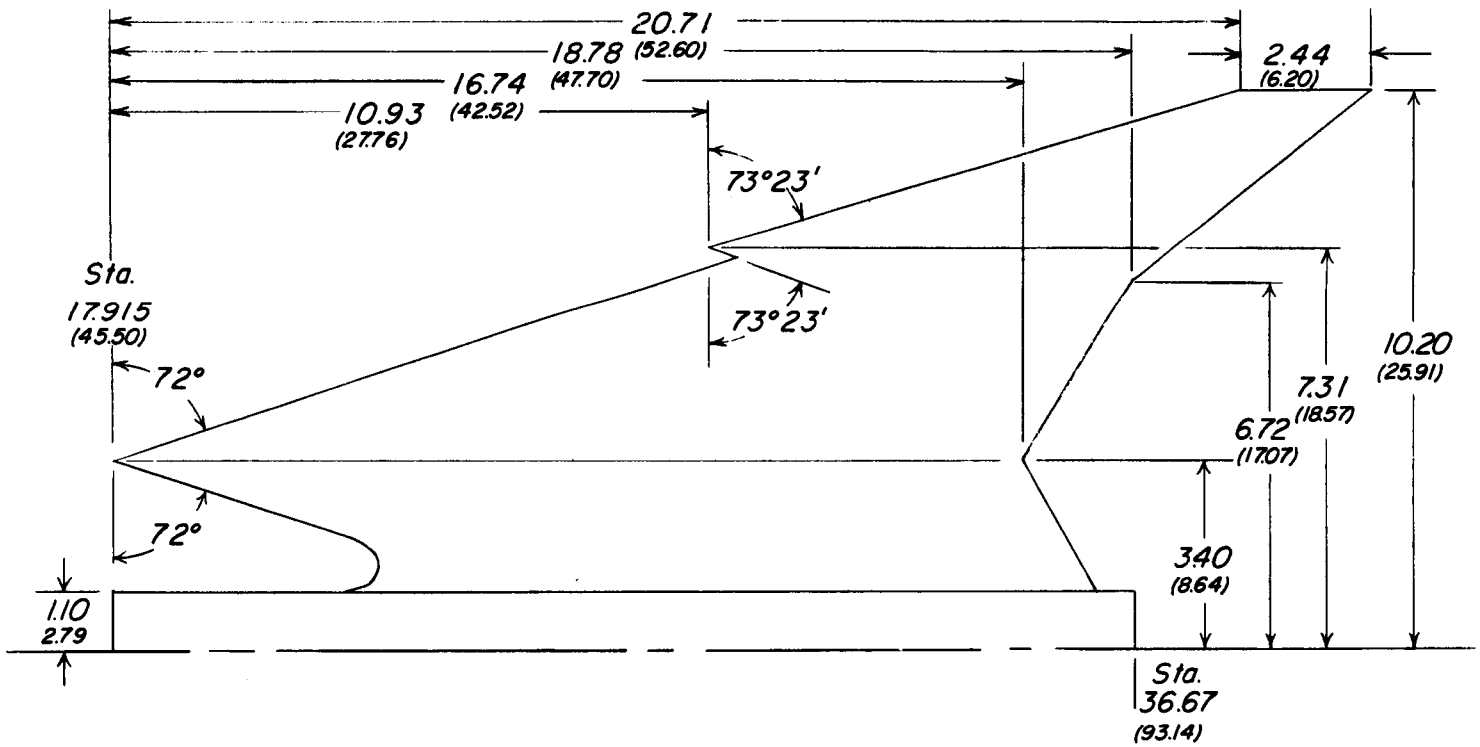

(b) Details of wing.

Figure 1.- Continued.

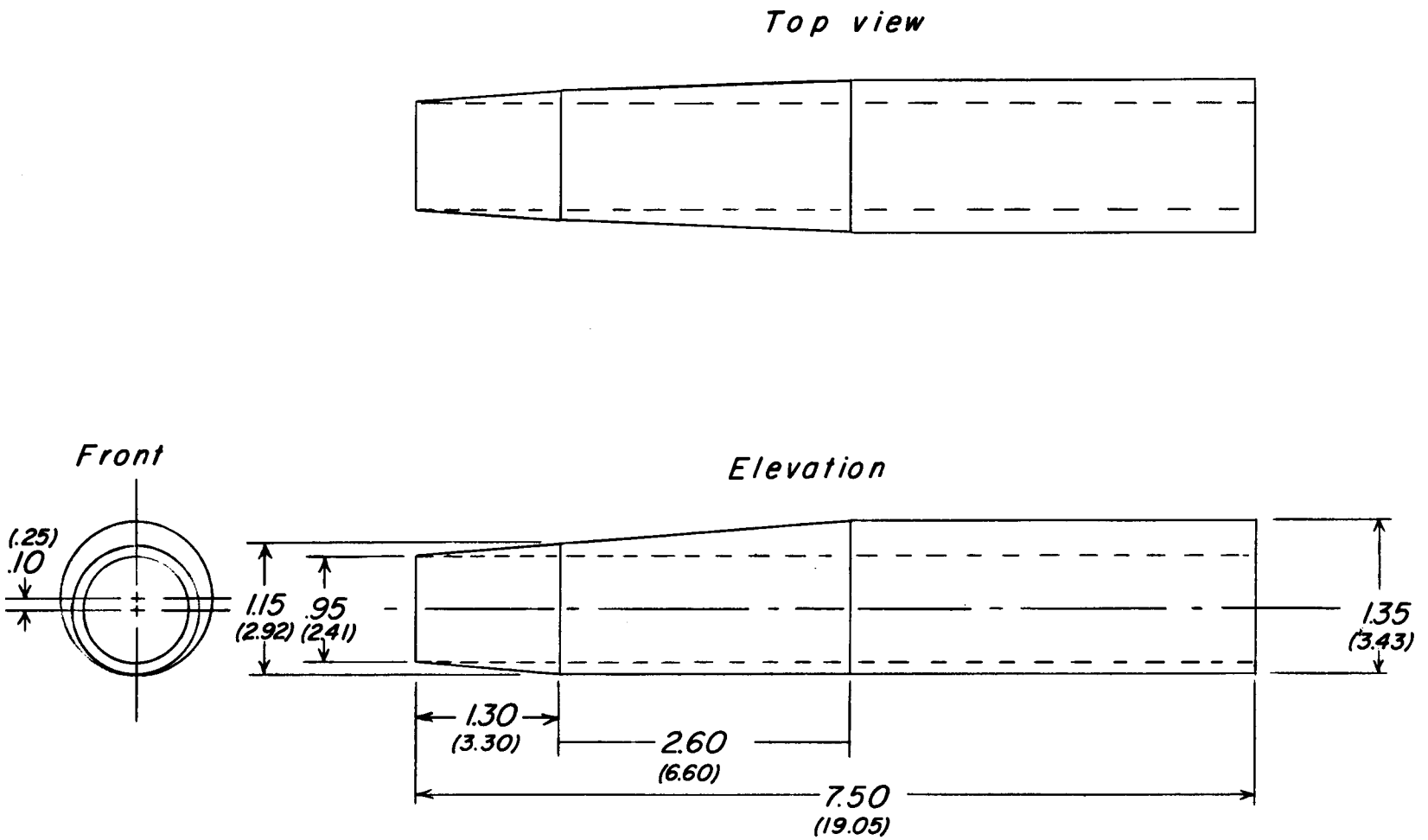

(c) Details of nacelle.

Figure 1.- Continued.

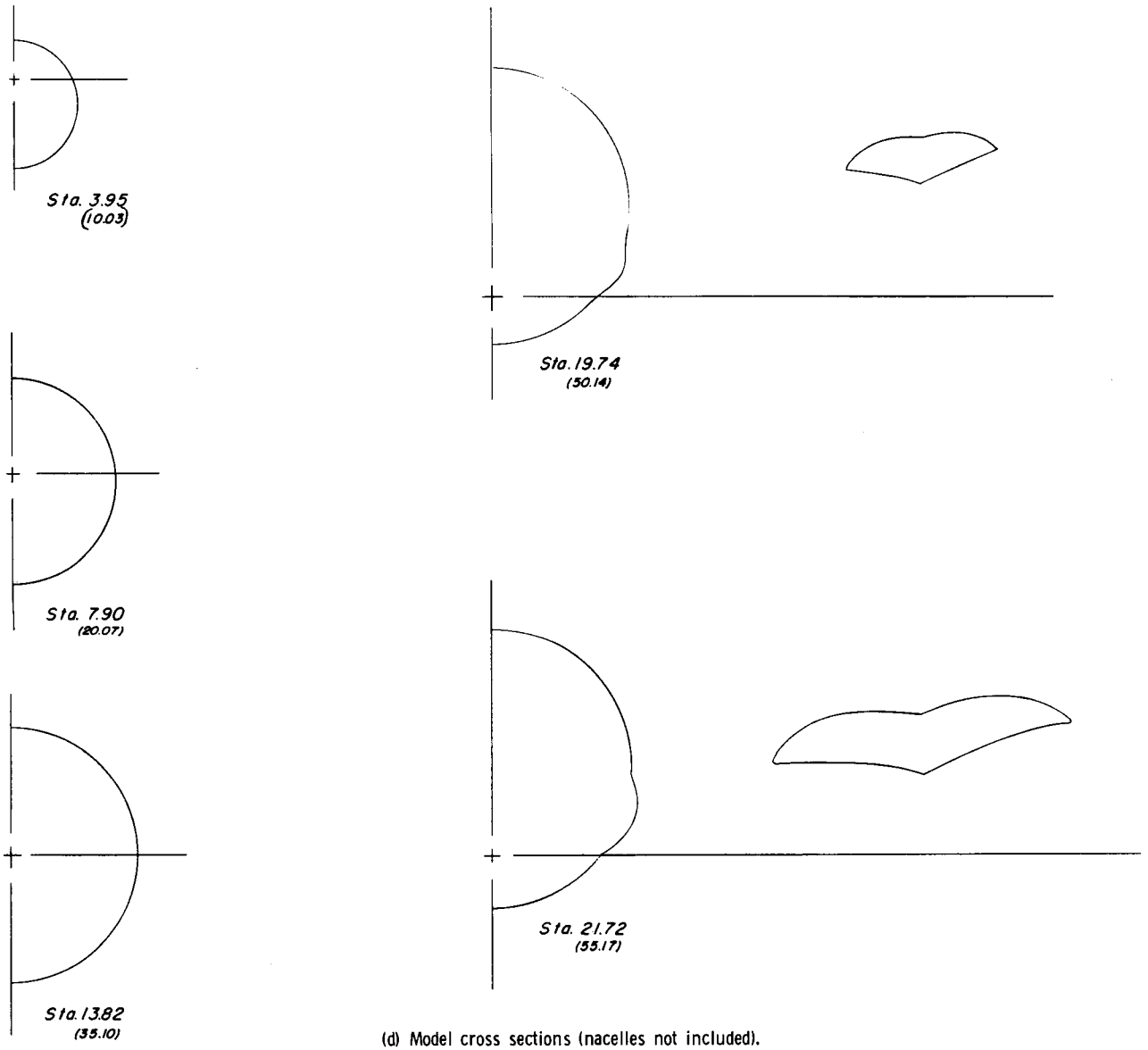

(d) Model cross sections (nacelles not included).

Figure 1.- Continued.

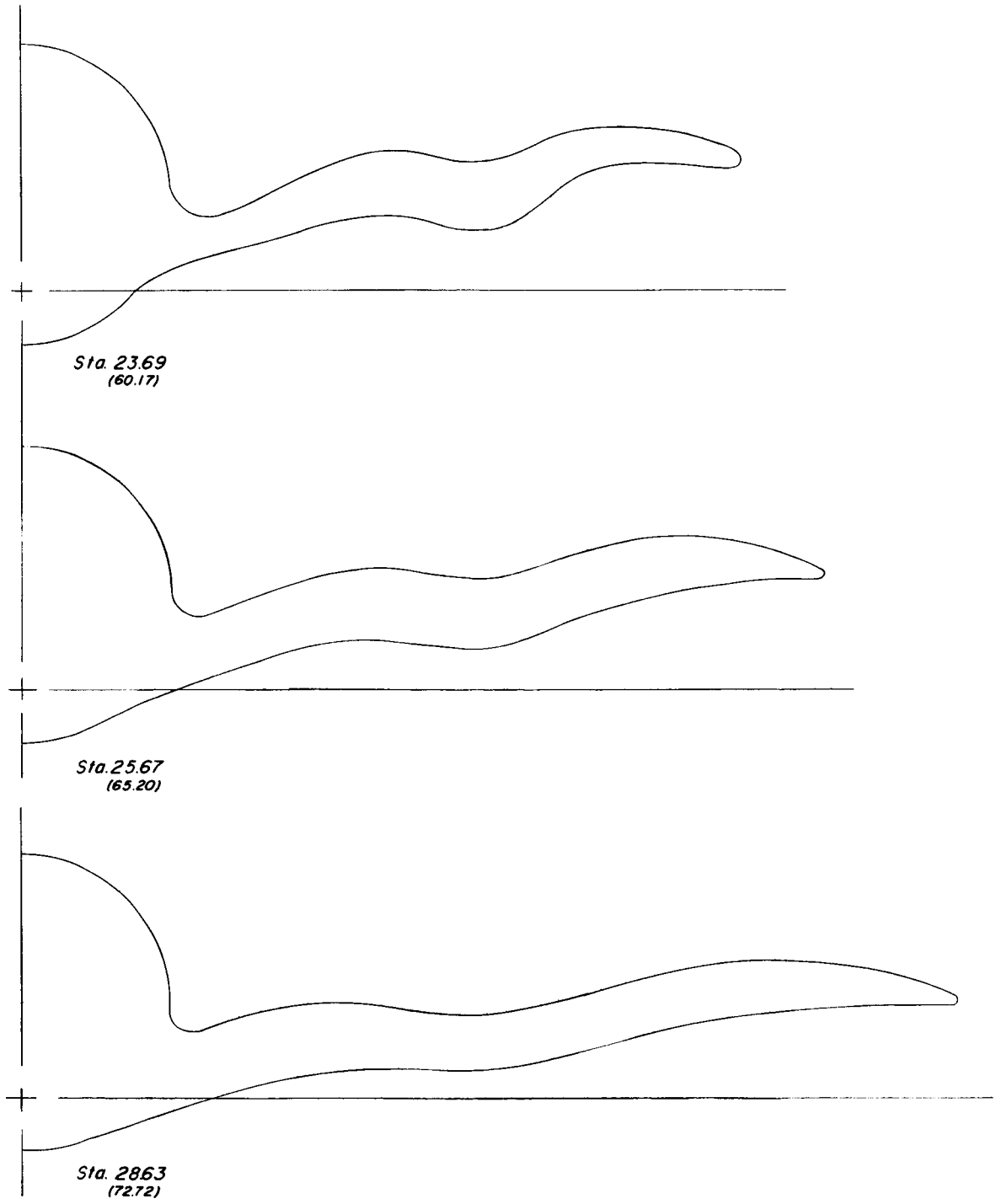

(d) Continued.

Figure 1.- Continued.

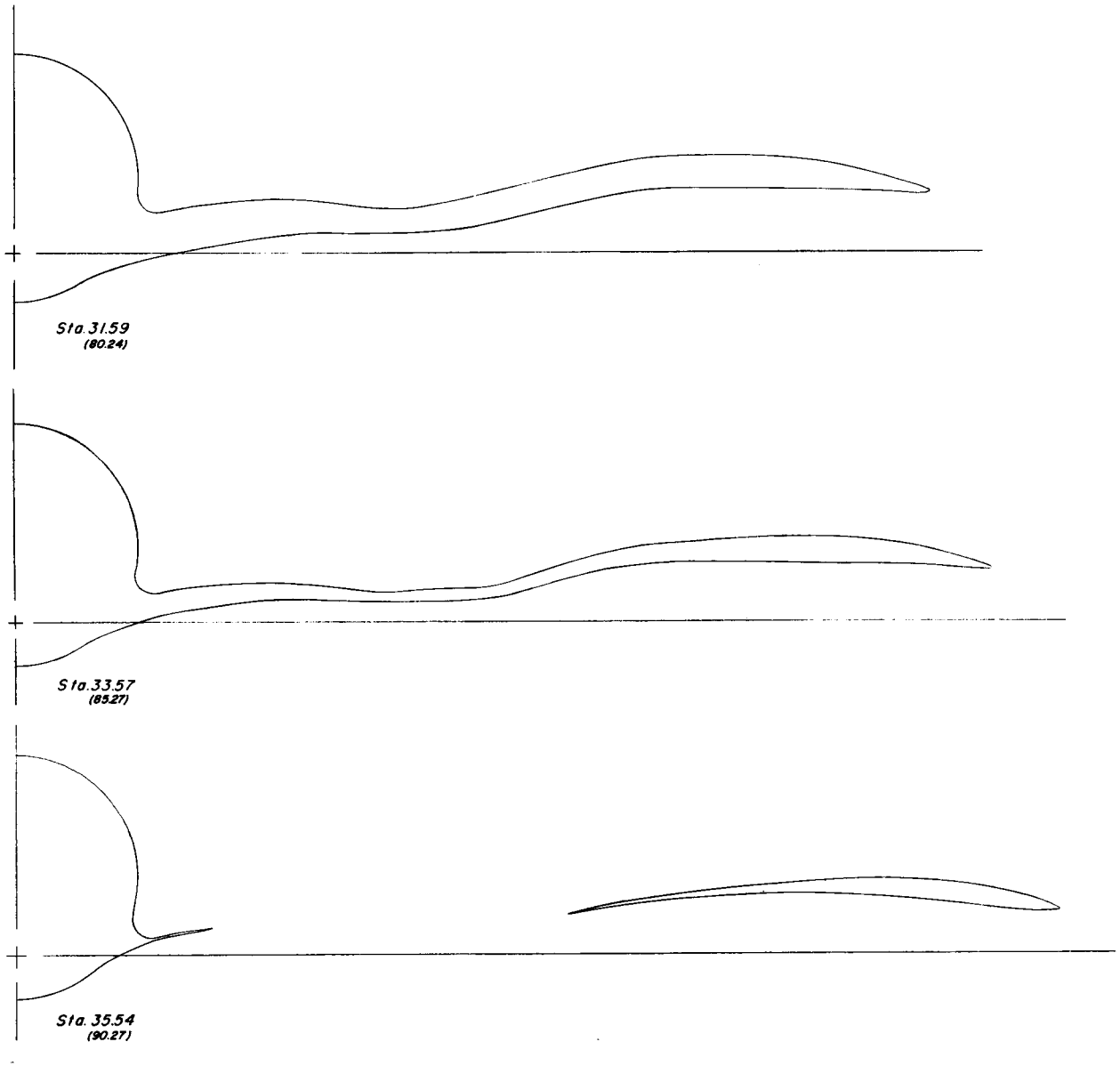

(d) Concluded.

Figure 1.- Concluded.

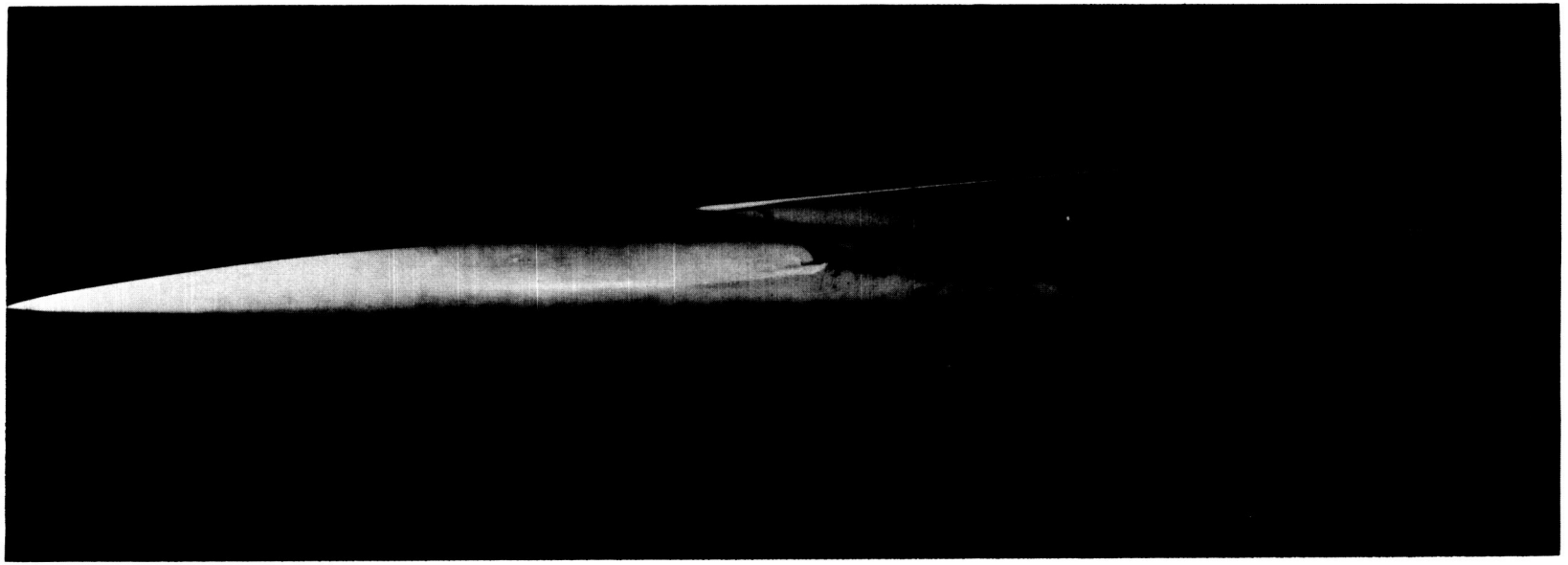

L-64-2780

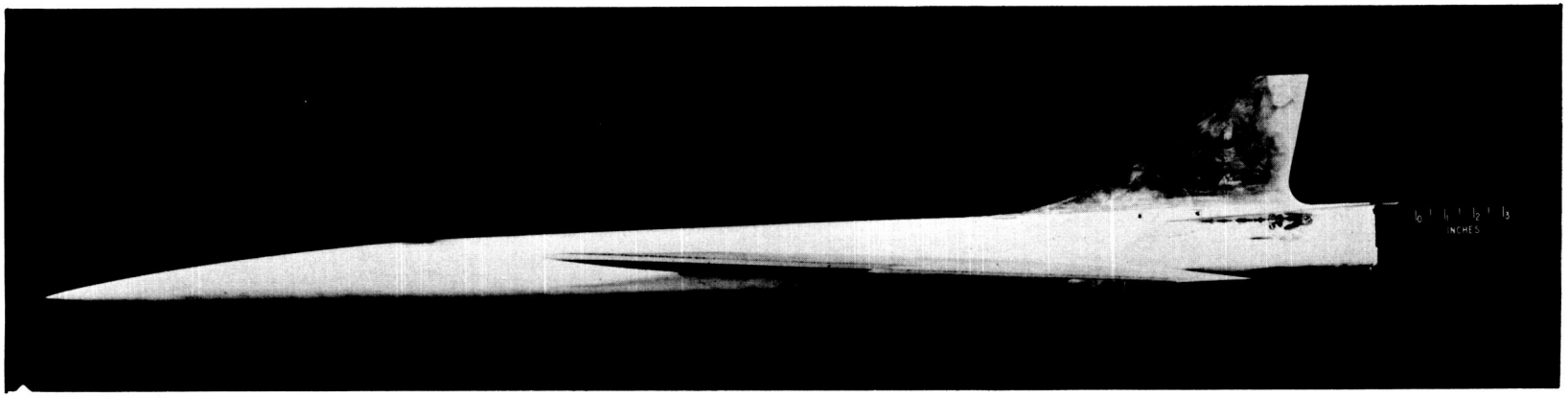

L-64-2779

Figure 2.- Photographs of model.

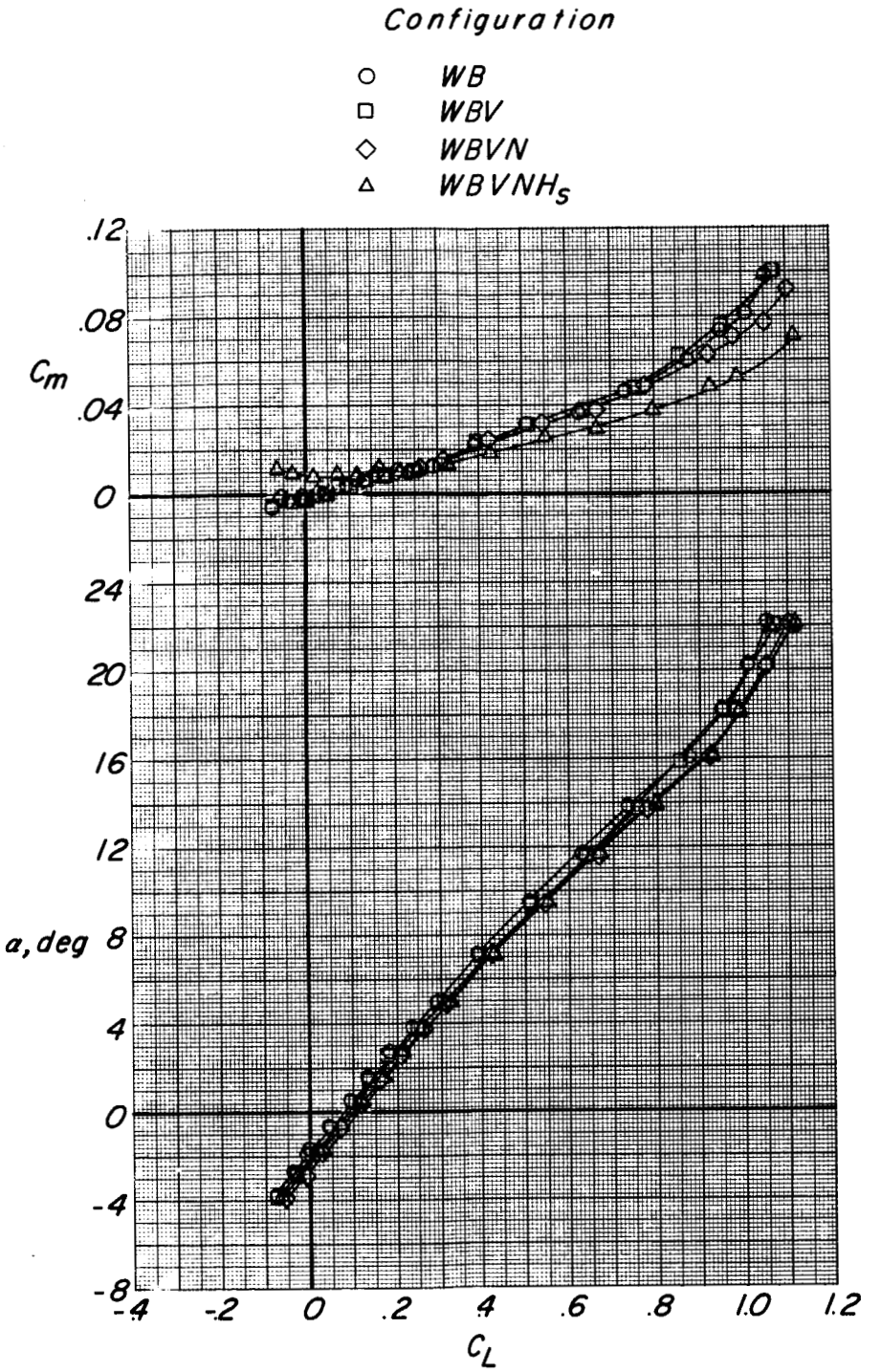

(a) M = 0.50.

Figure 3.- Effect of components on the longitudinal characteristics of the model at Mach numbers from 0.50 to 1.19.

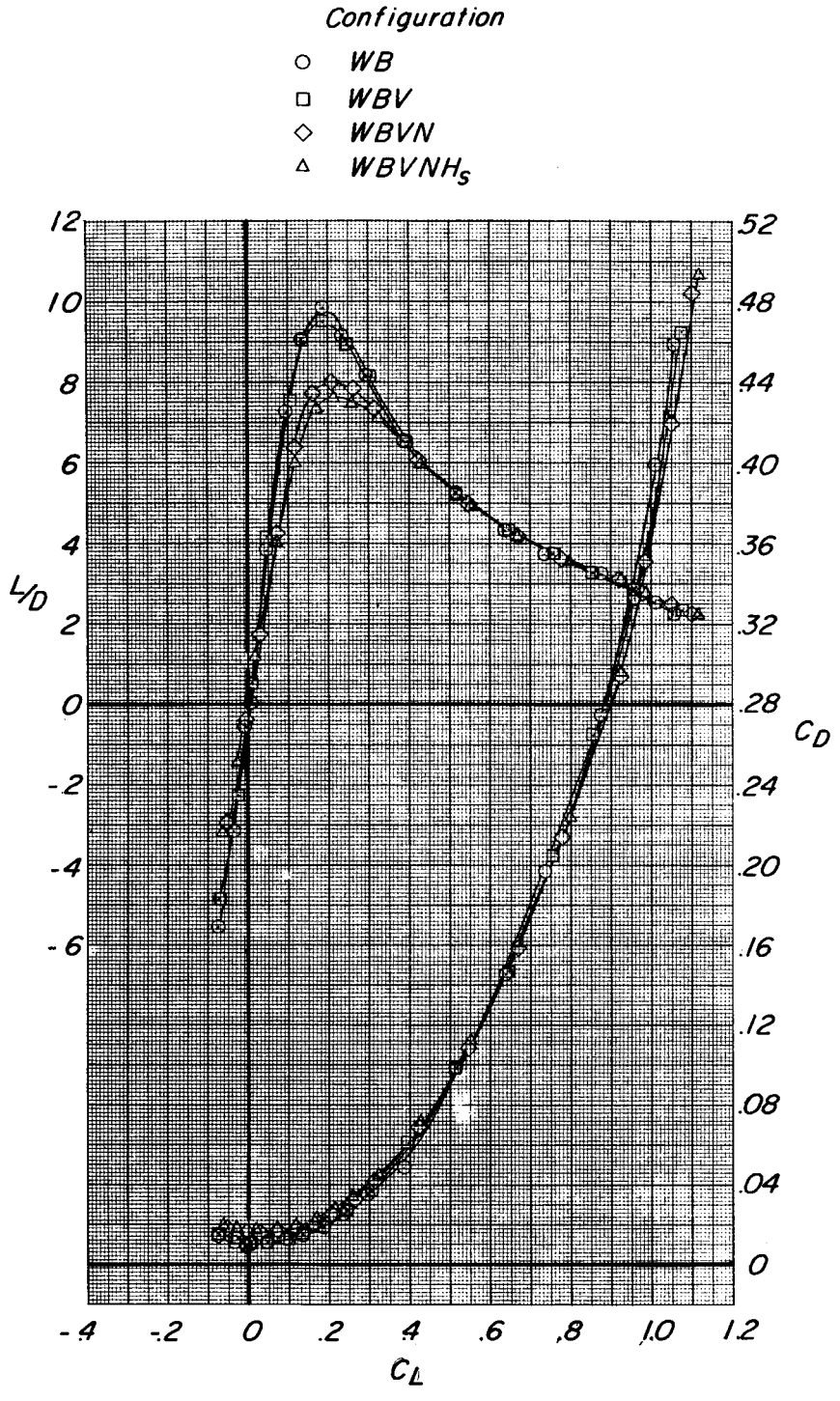

(a) Concluded.

Figure 3.- Continued.

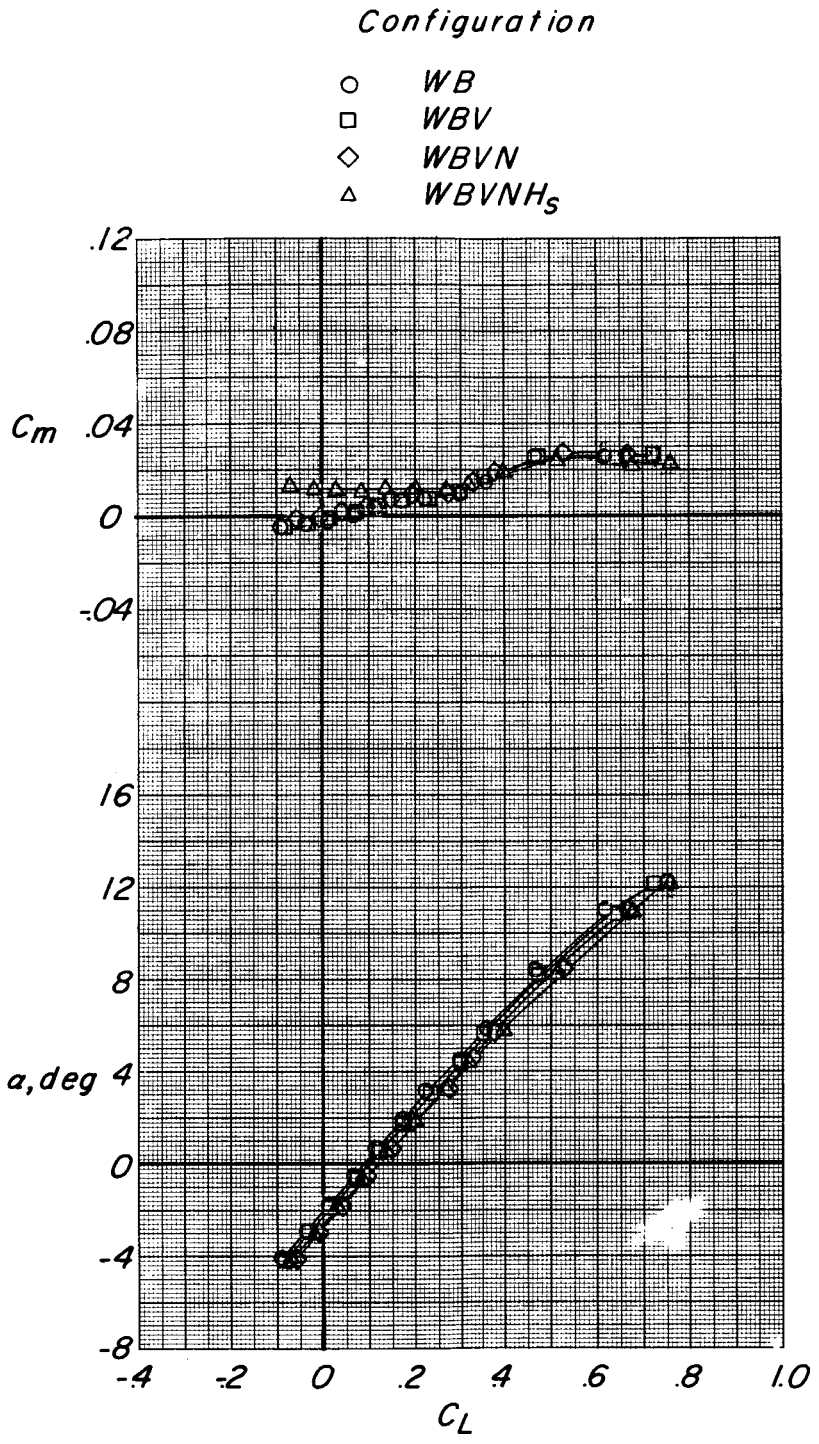

(b) M = 0.79.

Figure 3.- Continued.

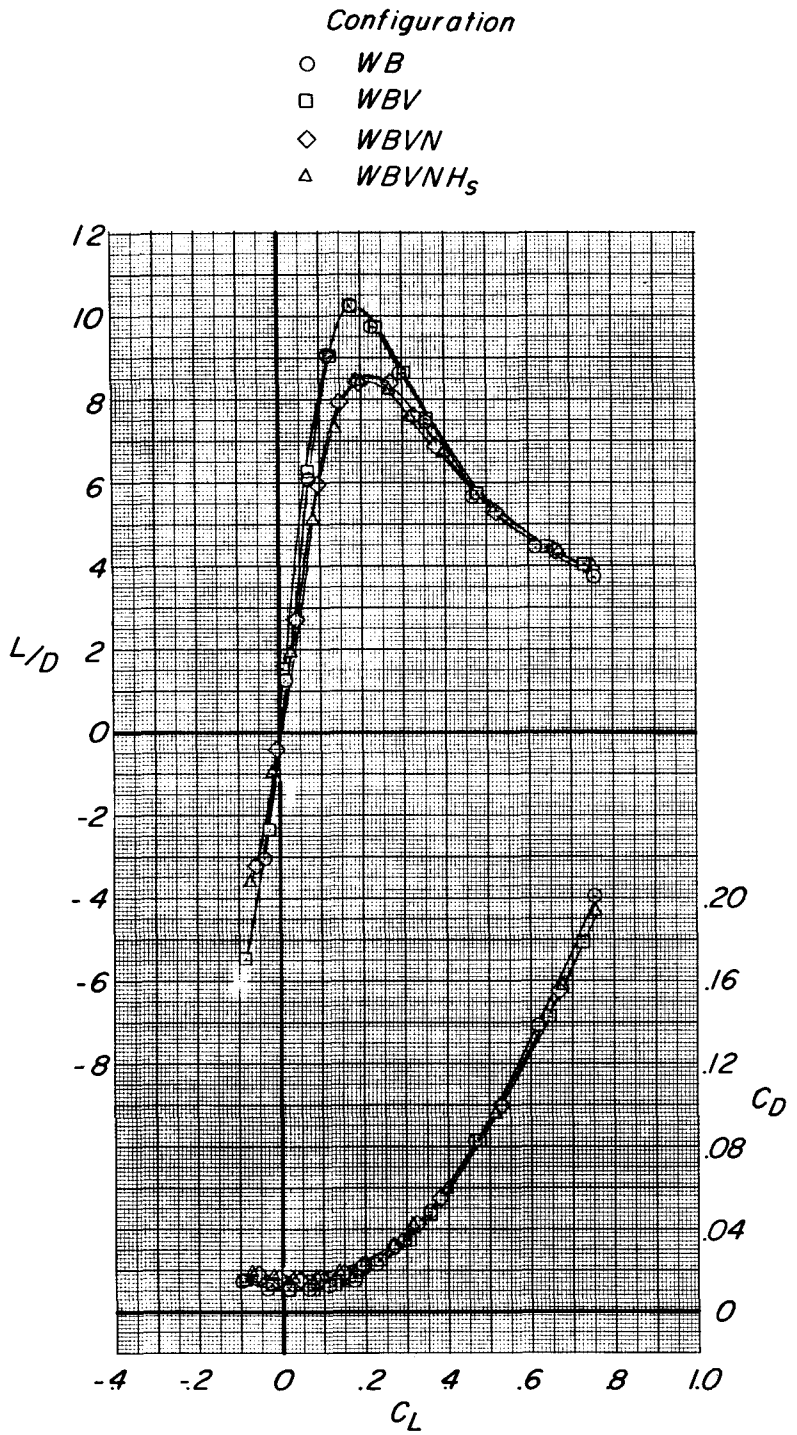

(b) Concluded.

Figure 3.- Continued.

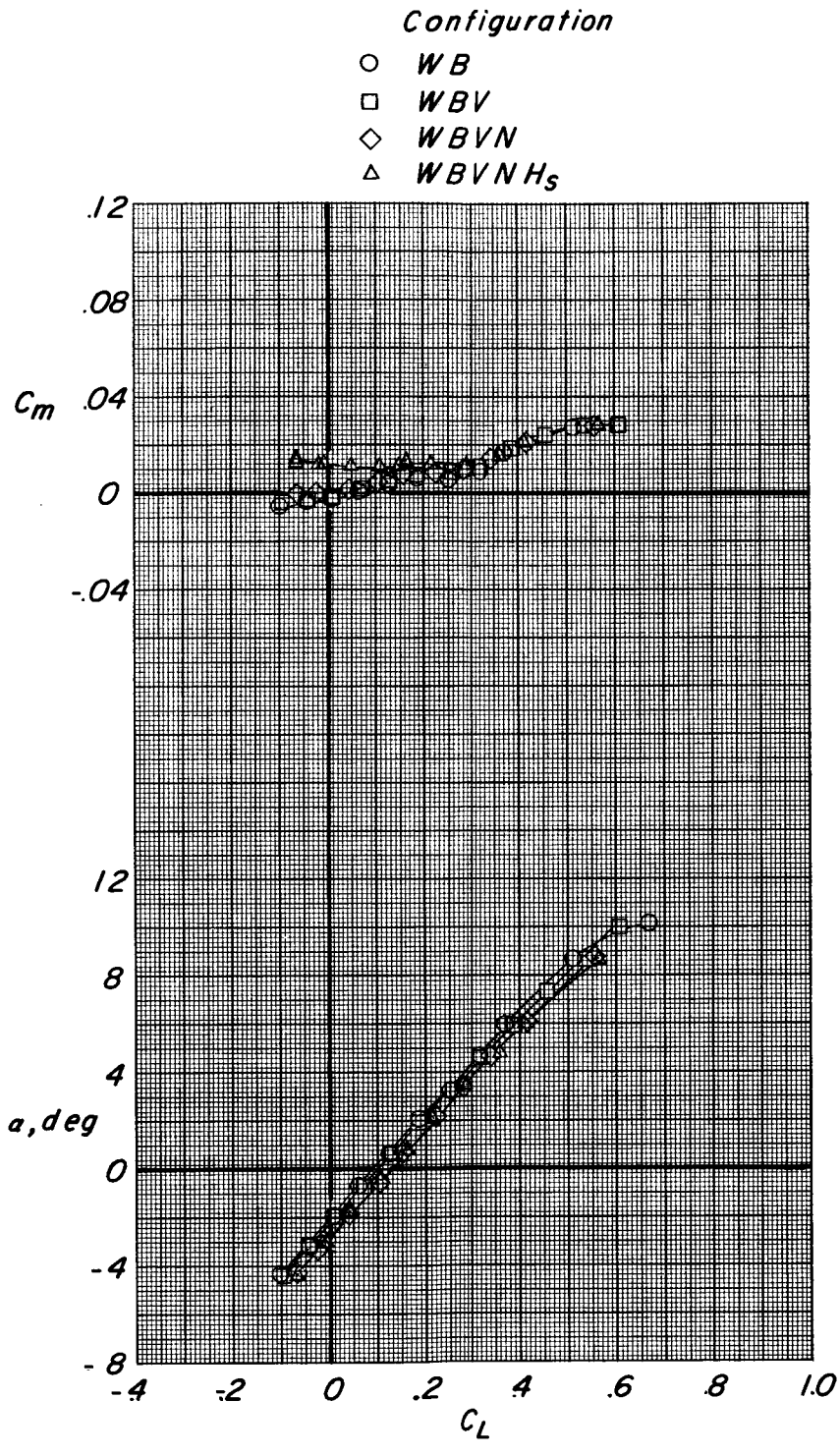

(c) M = 0.89.

Figure 3.- Continued.

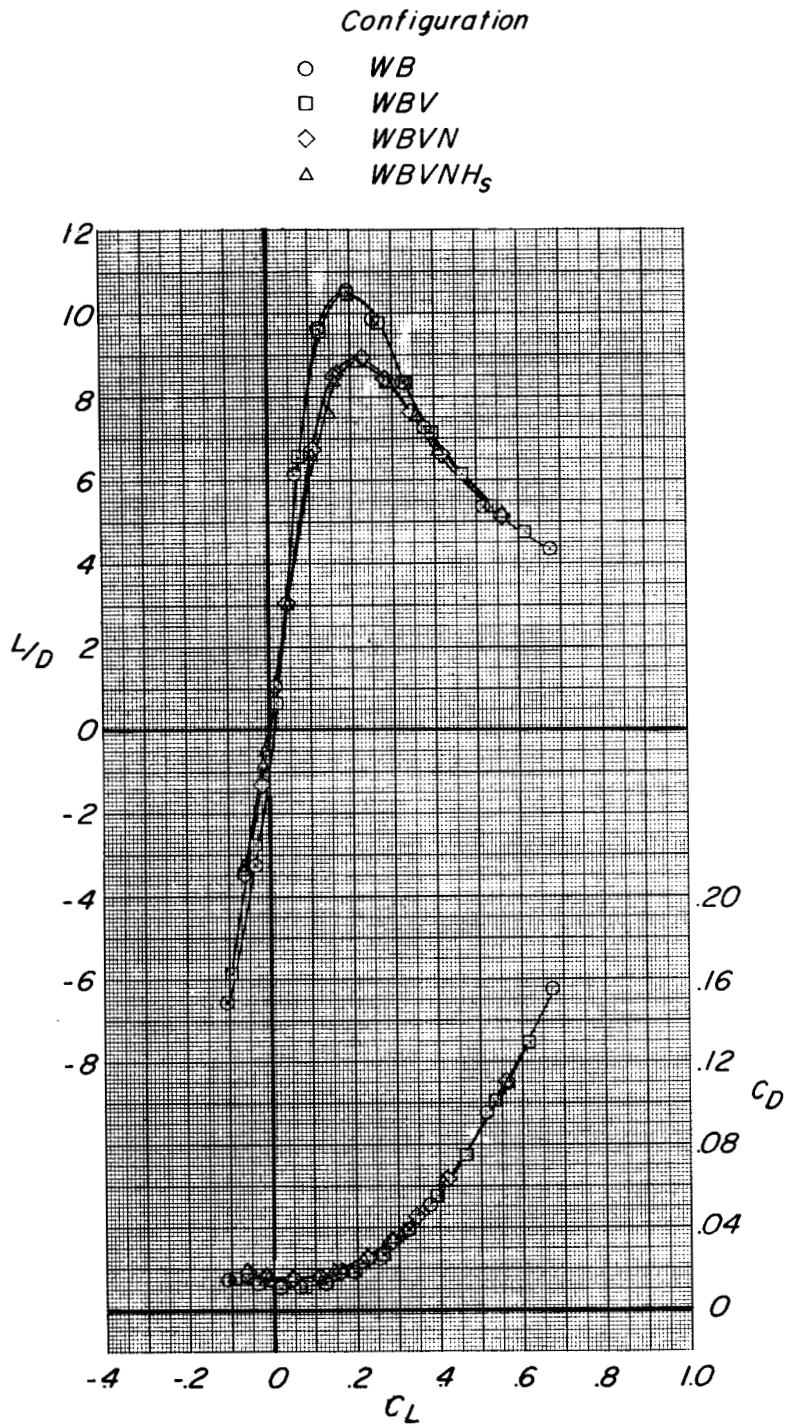

(c) Concluded.

Figure 3.- Continued.

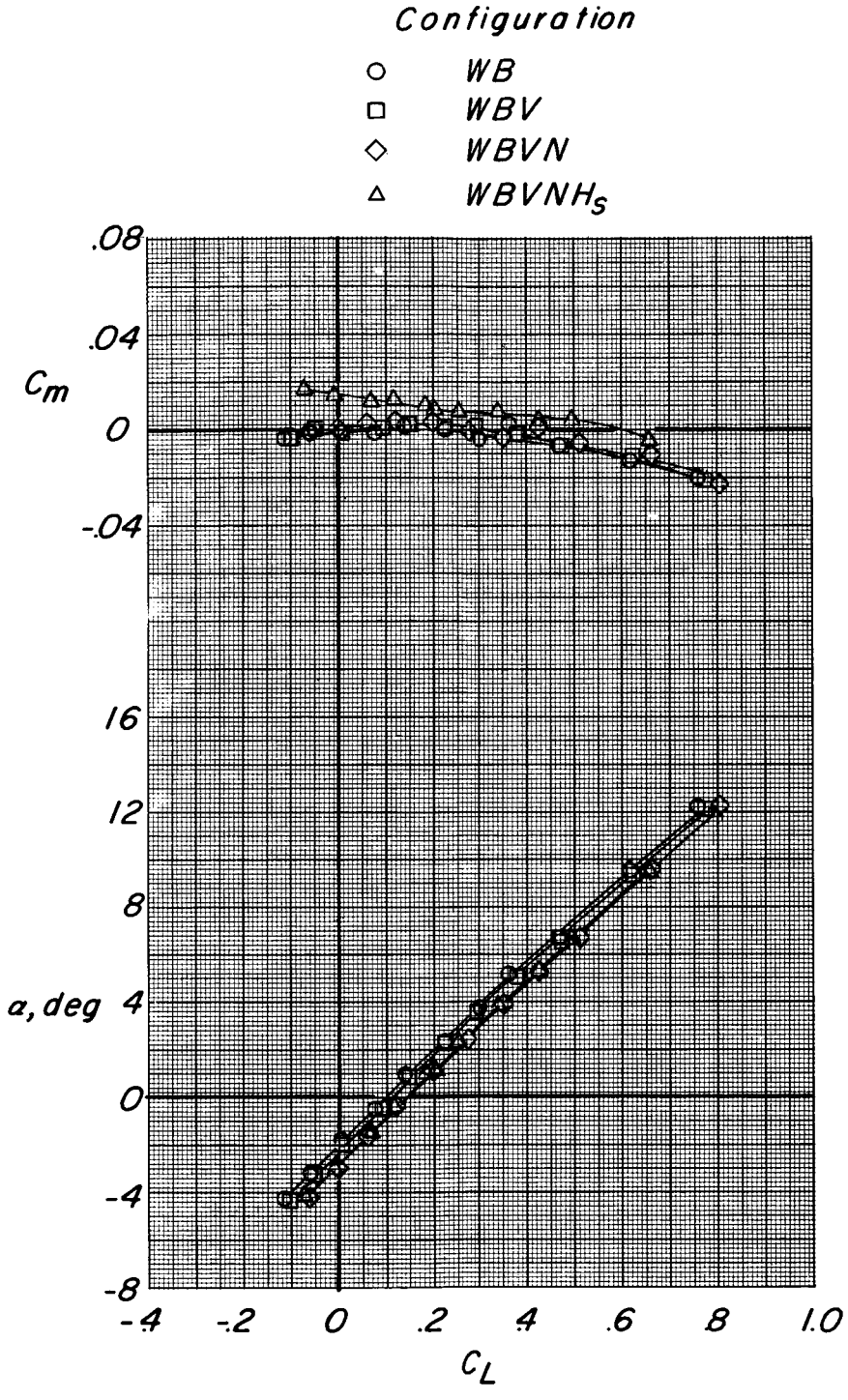

(d) M = 0.98.

Figure 3.- Continued.

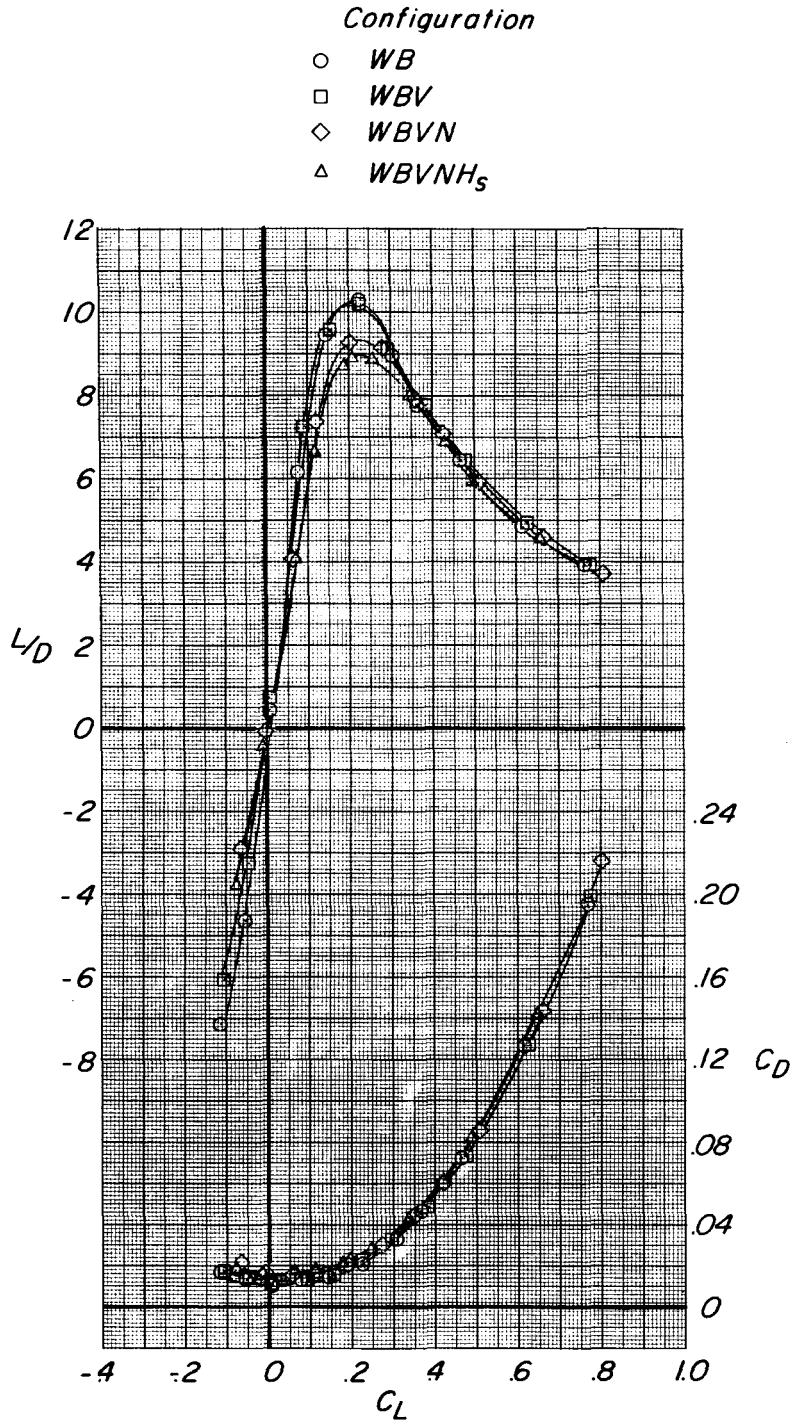

(d) Concluded.

Figure 3.- Continued.

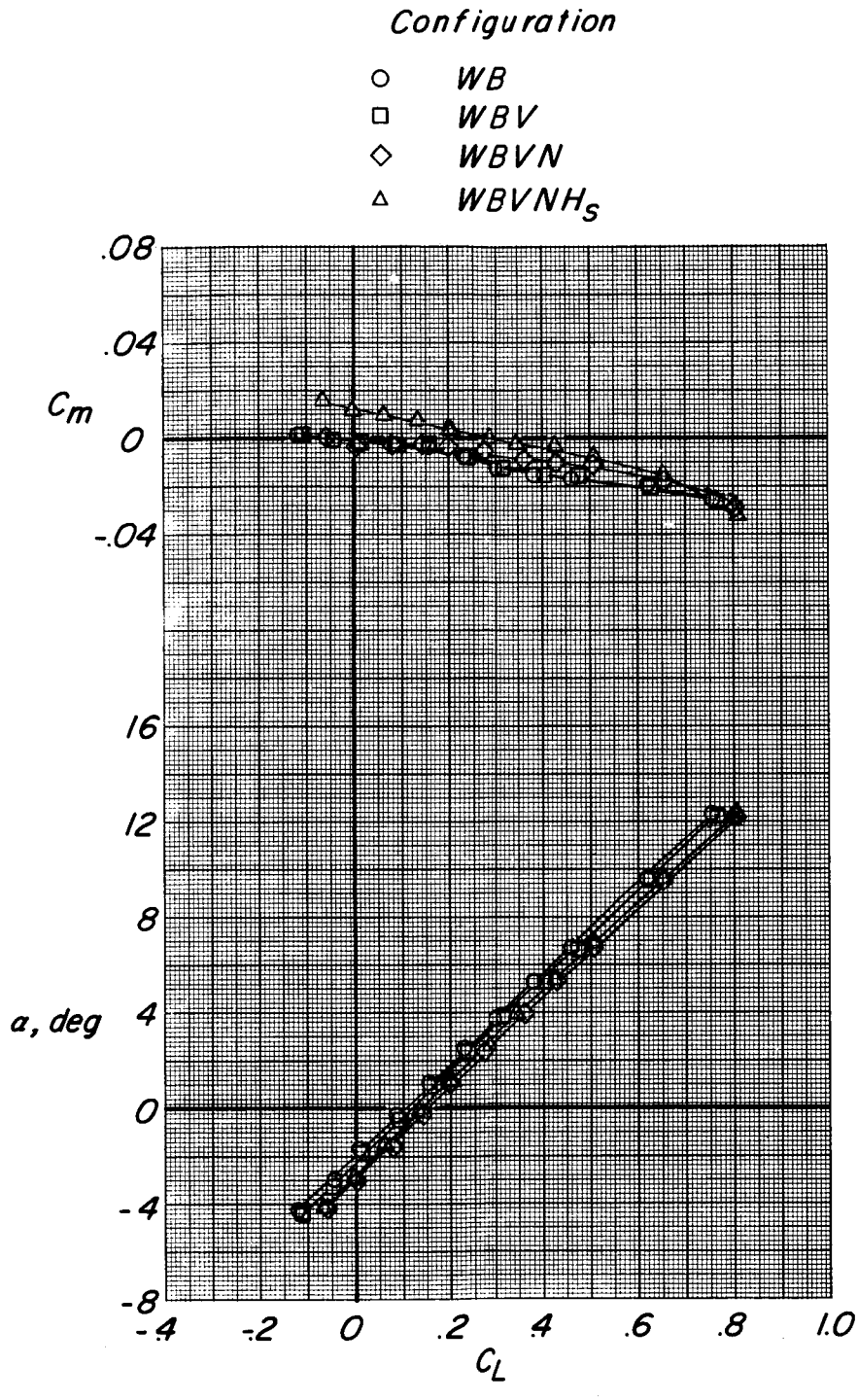

(e) M = 1.01.

Figure 3.- Continued.

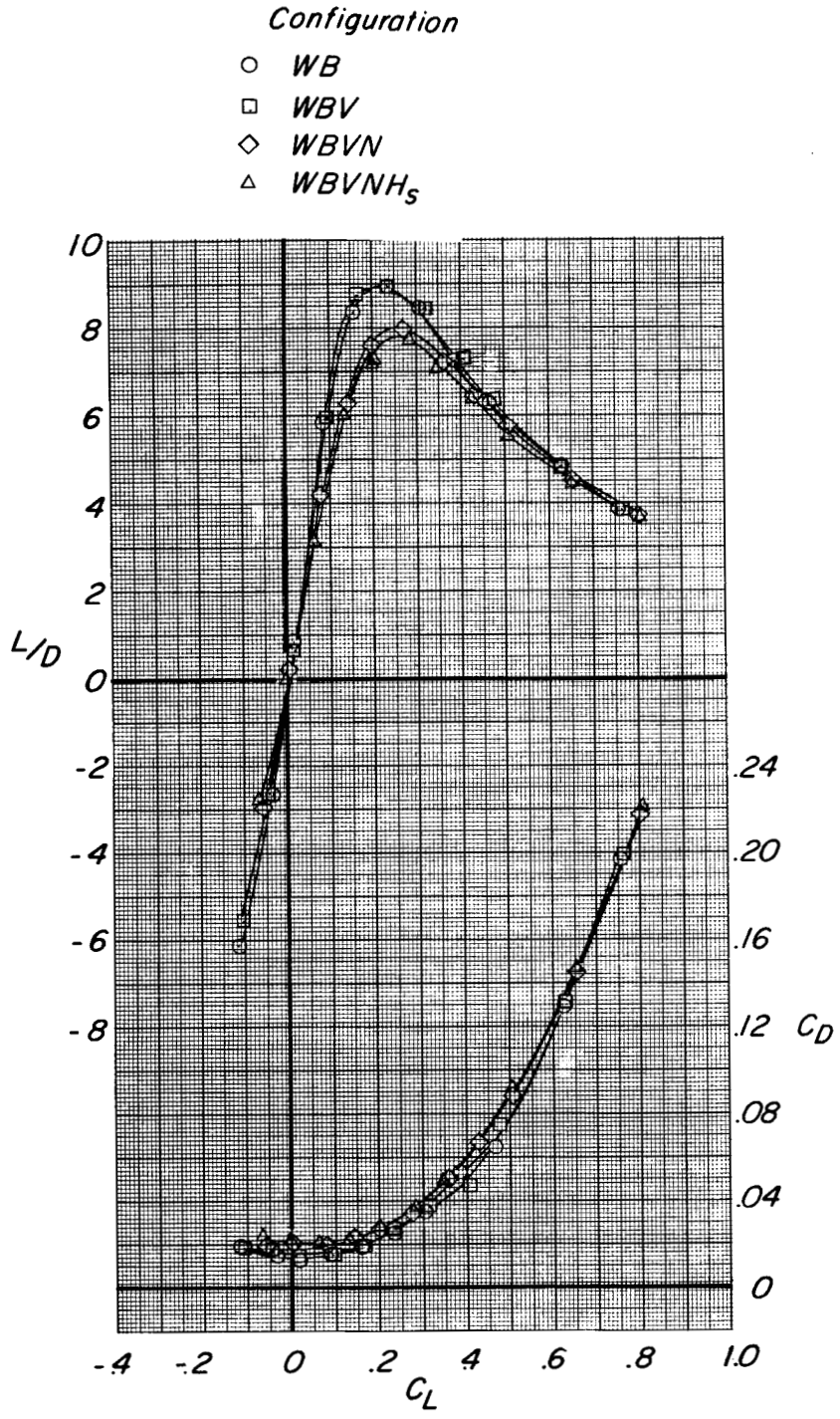

(e) Concluded.

Figure 3.- Continued.

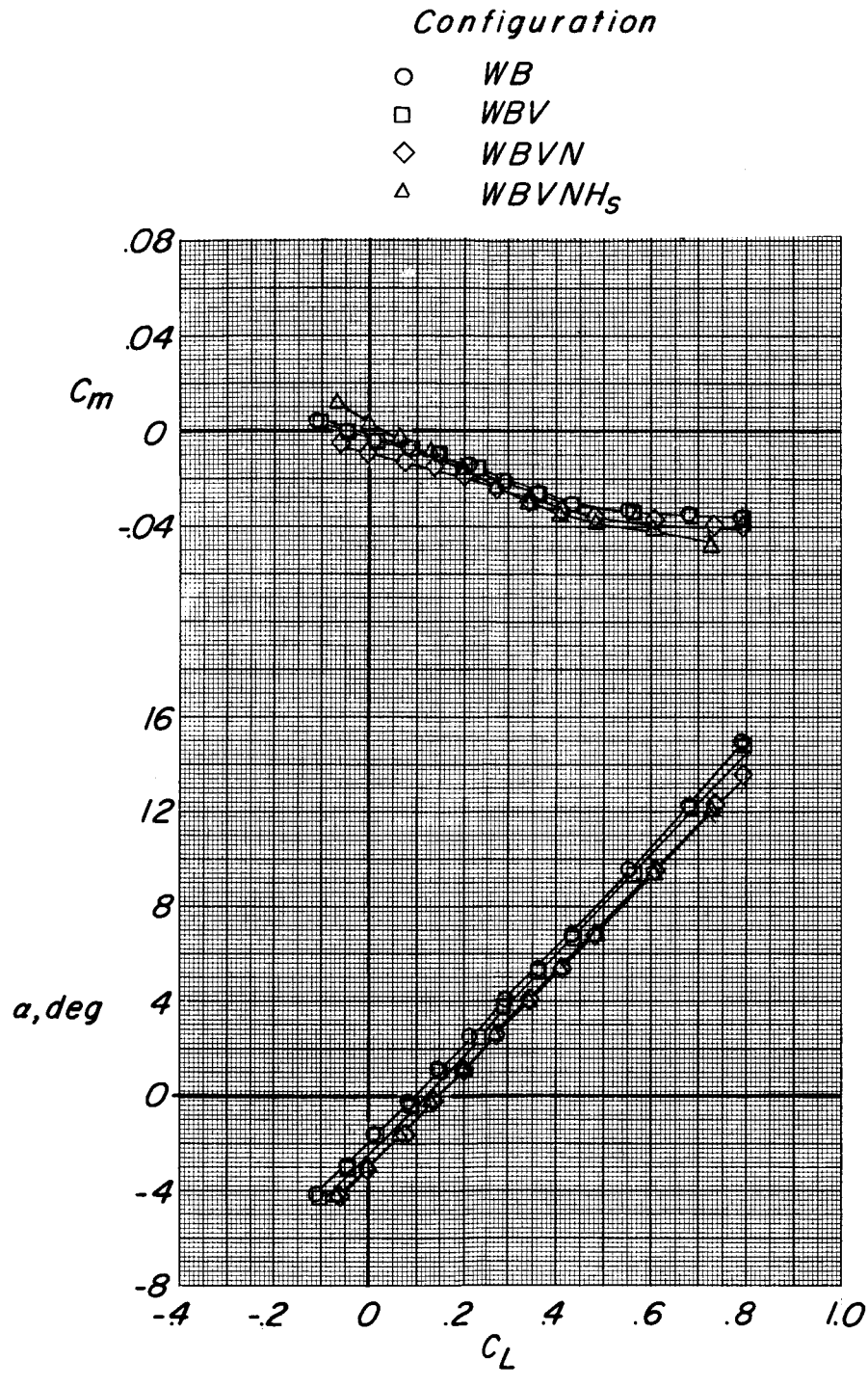

(f) M = 1.19.

Figure 3.- Continued.

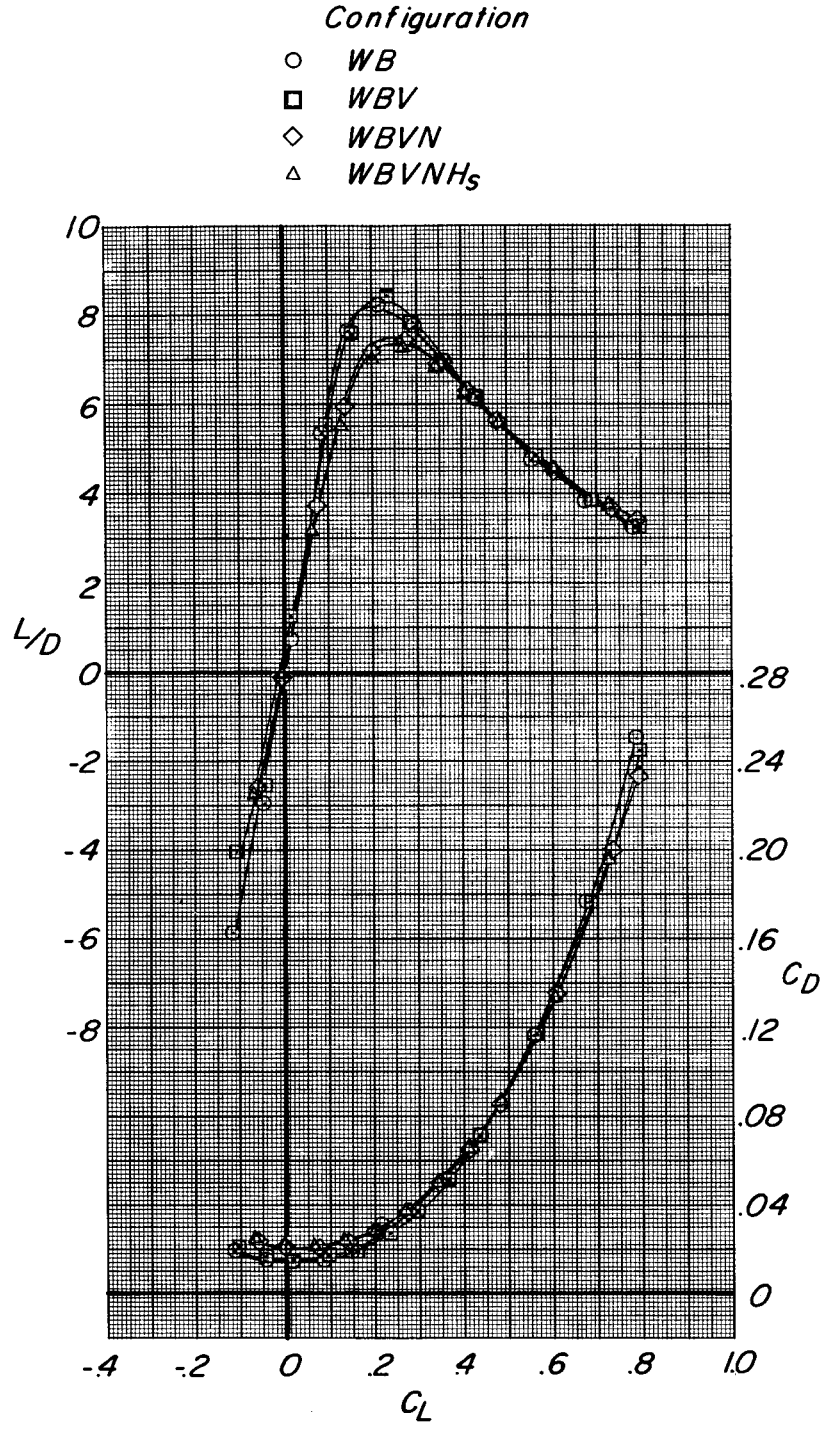

(f) Concluded.

Figure 3.- Concluded.

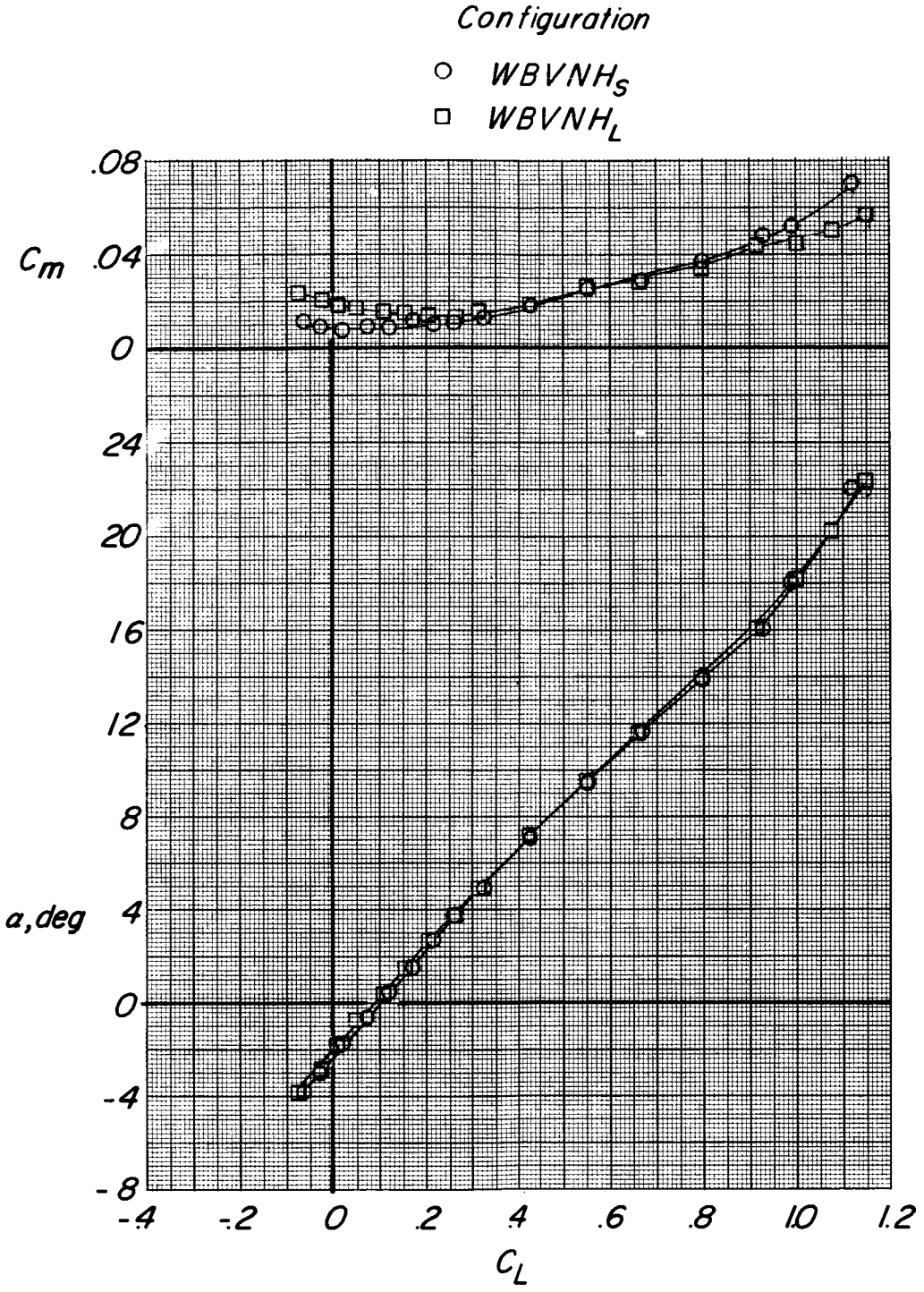

(a) M = 0.50.

Figure 4.- Effect of horizontal-tail size on the longitudinal characteristics of the model at Mach numbers of 0.50 to 1.19.

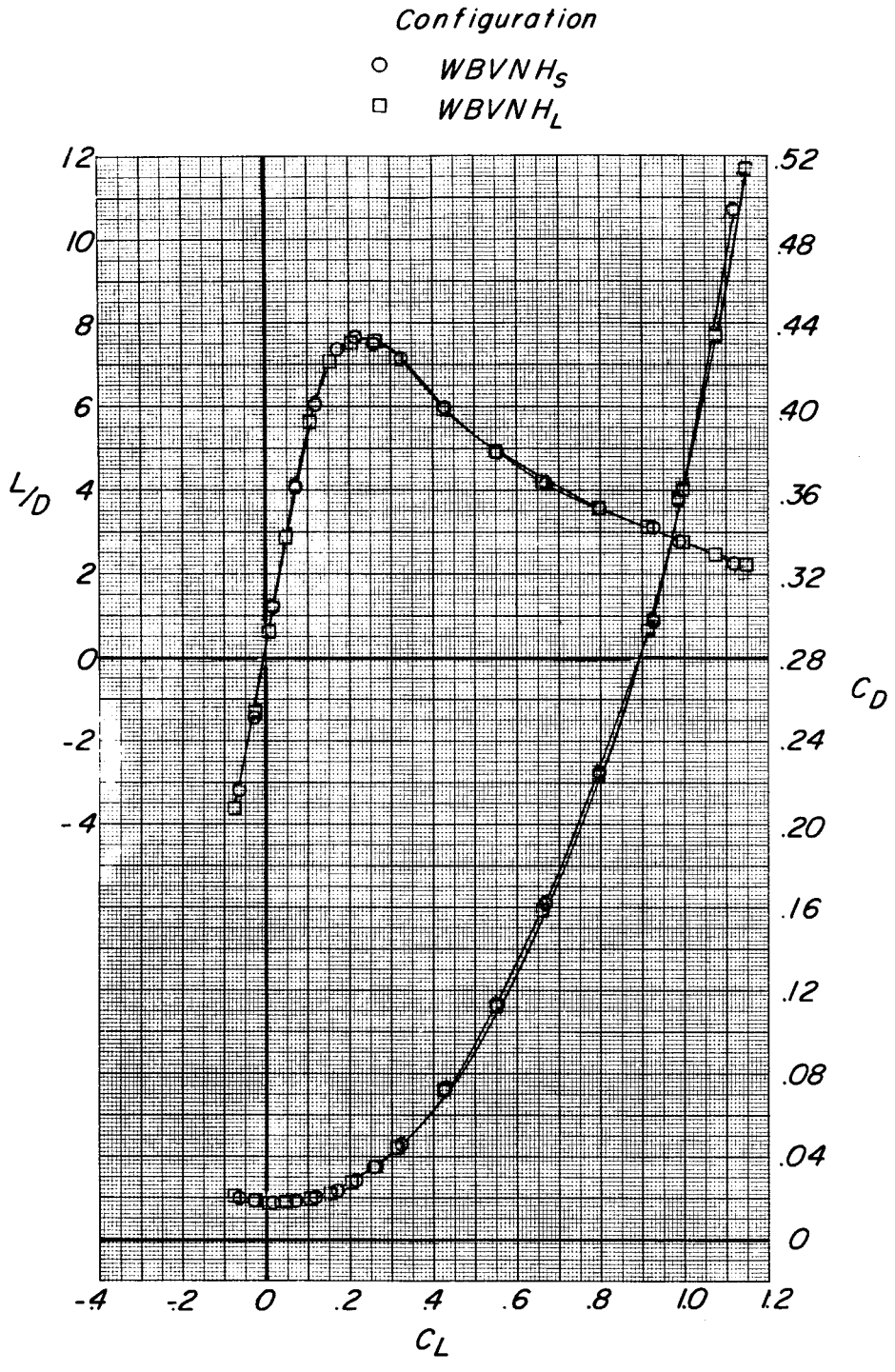

(a) Concluded.

Figure 4.- Continued.

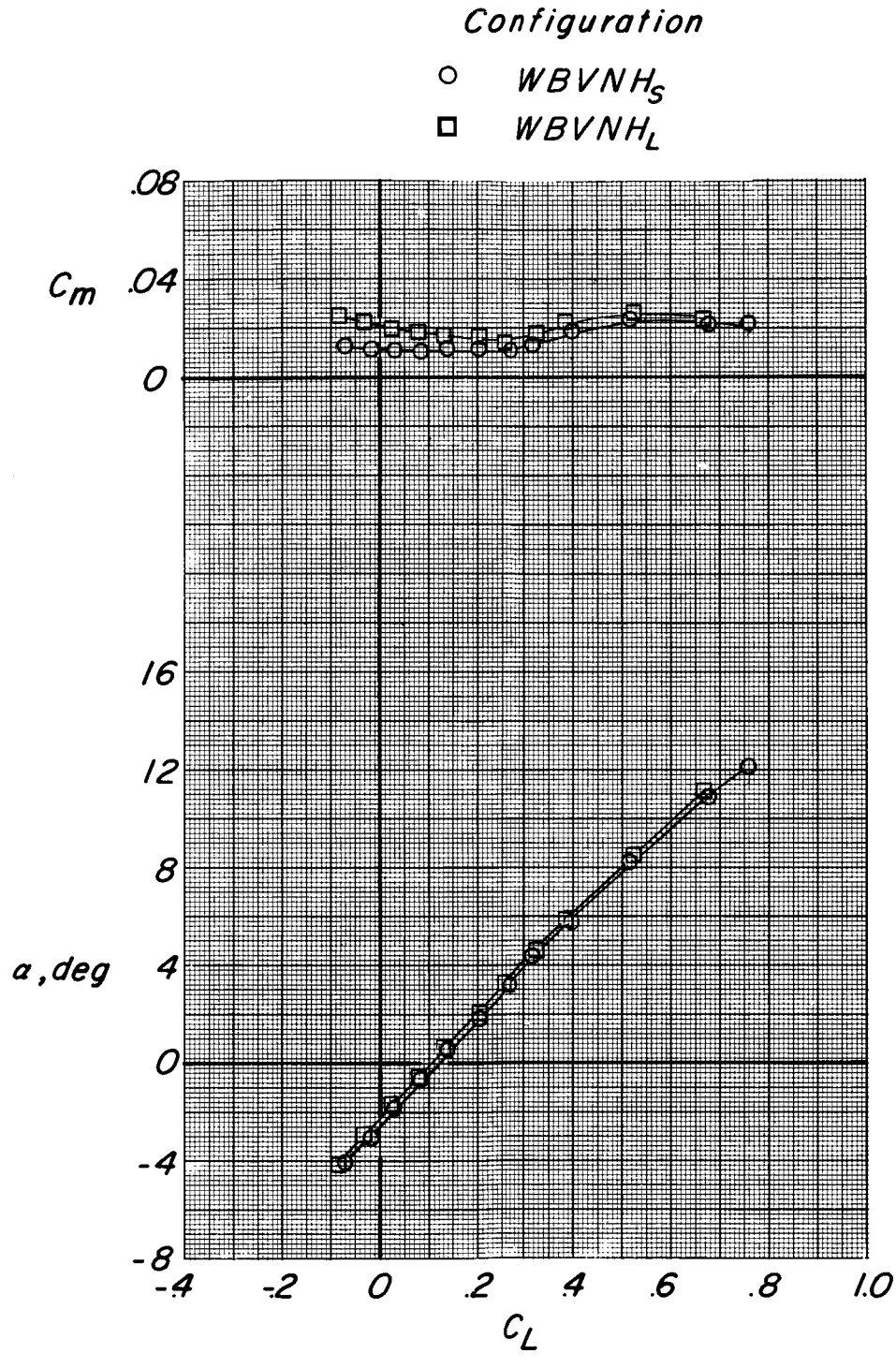

(b) M = 0.79.

Figure 4.- Continued.

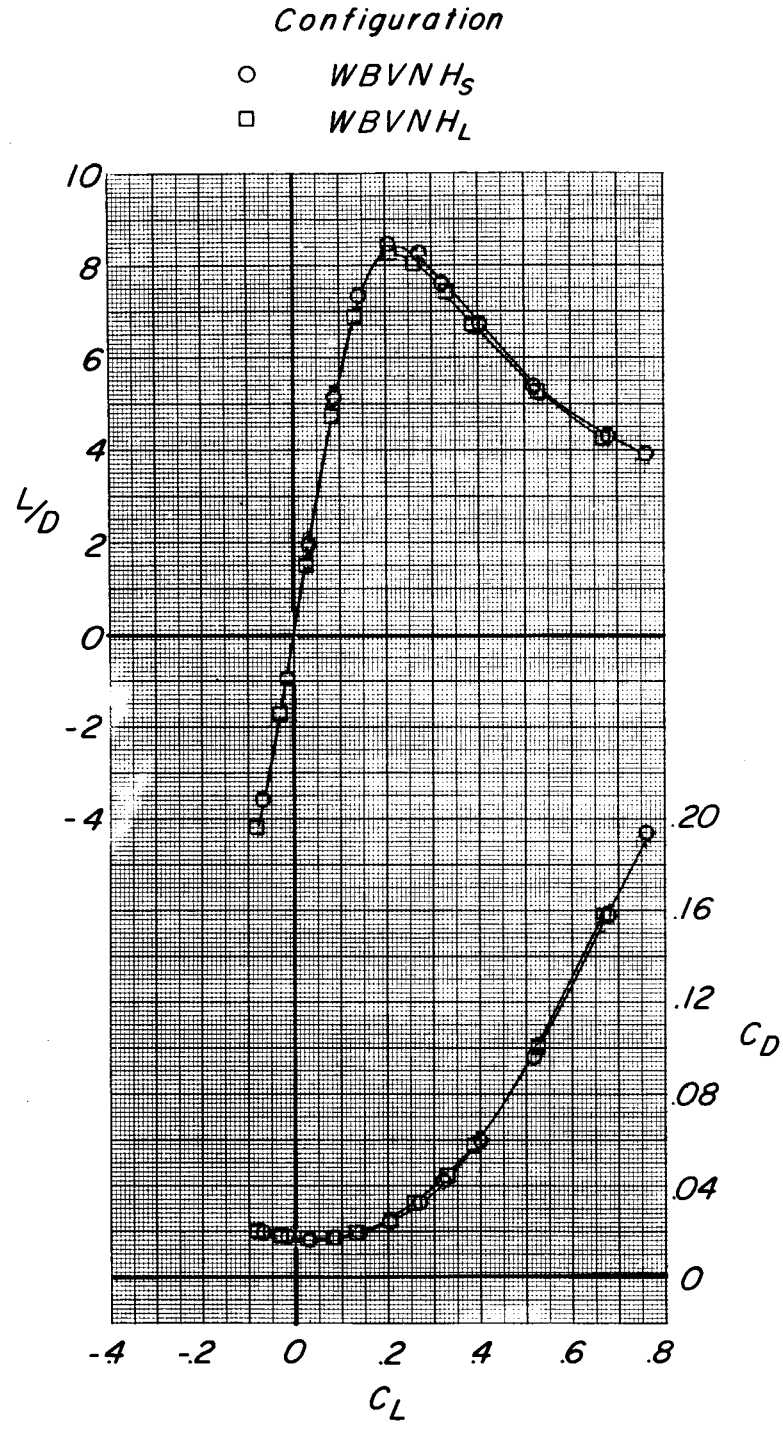

(b) Concluded.

Figure 4.- Continued.

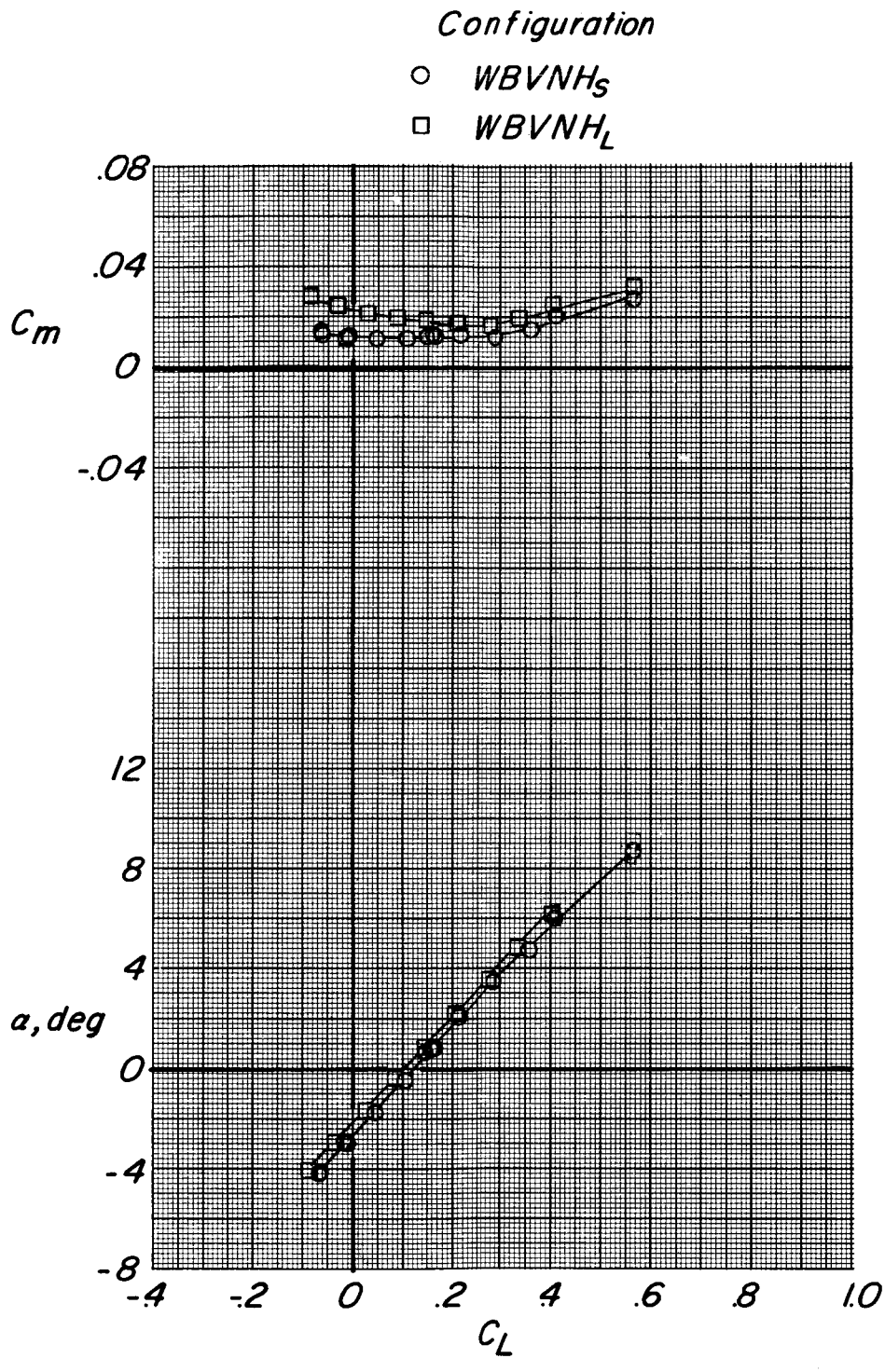

(c) M = 0.89.

Figure 4.- Continued.

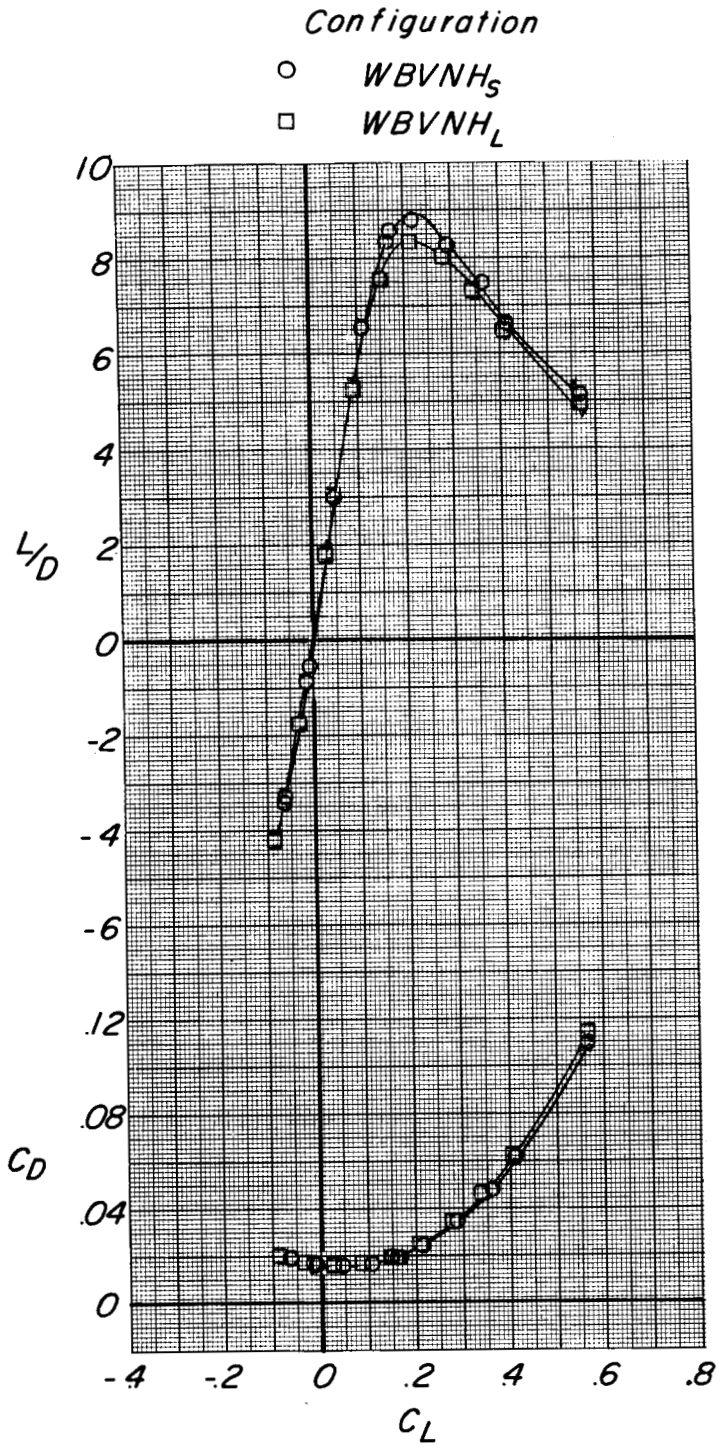

(c) Concluded.

Figure 4.- Continued.

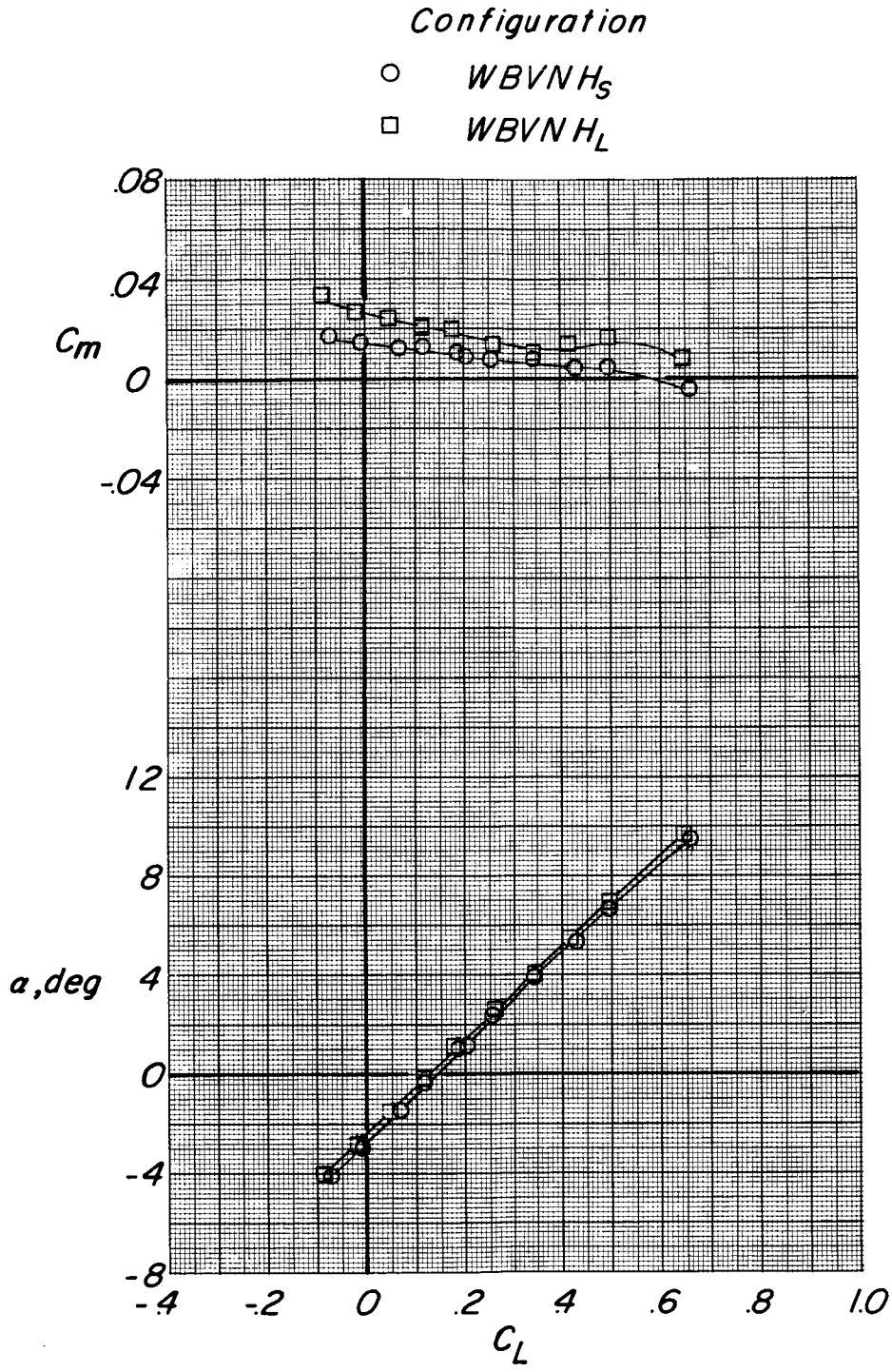

(d) M = 0.98.

Figure 4.- Continued.

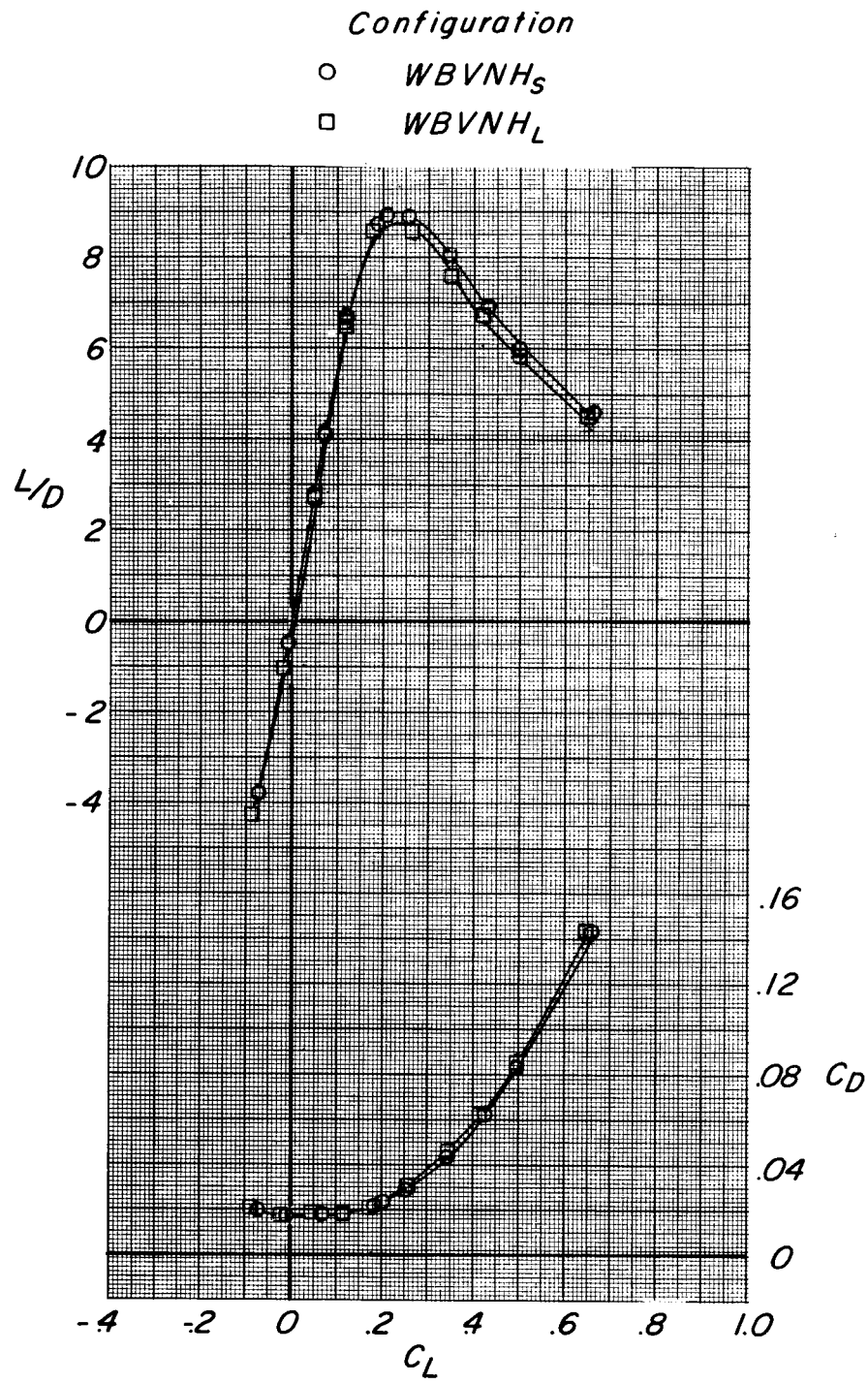

(d) Concluded.

Figure 4.- Continued.

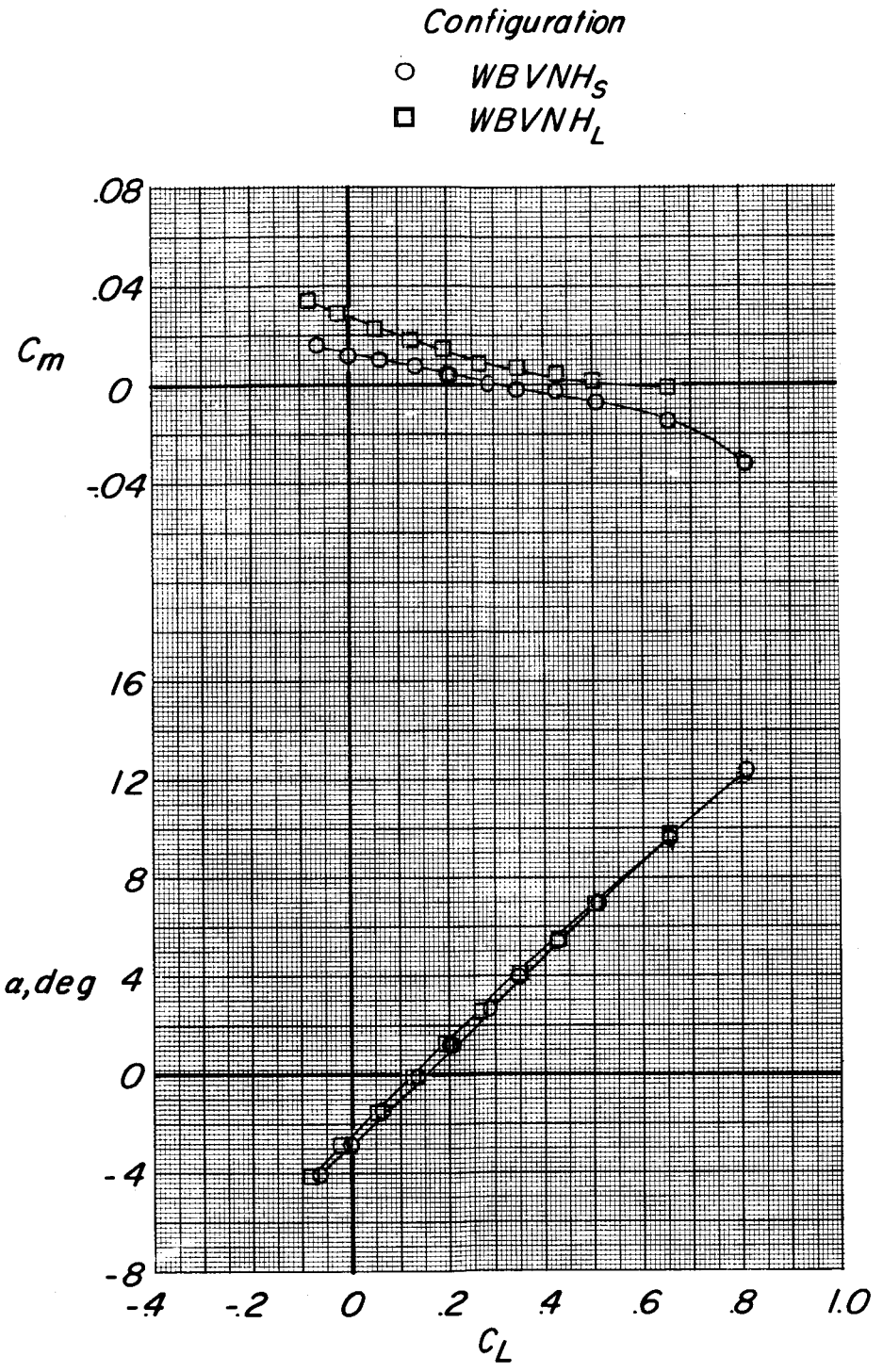

(e) M = 1.01.

Figure 4.- Continued.

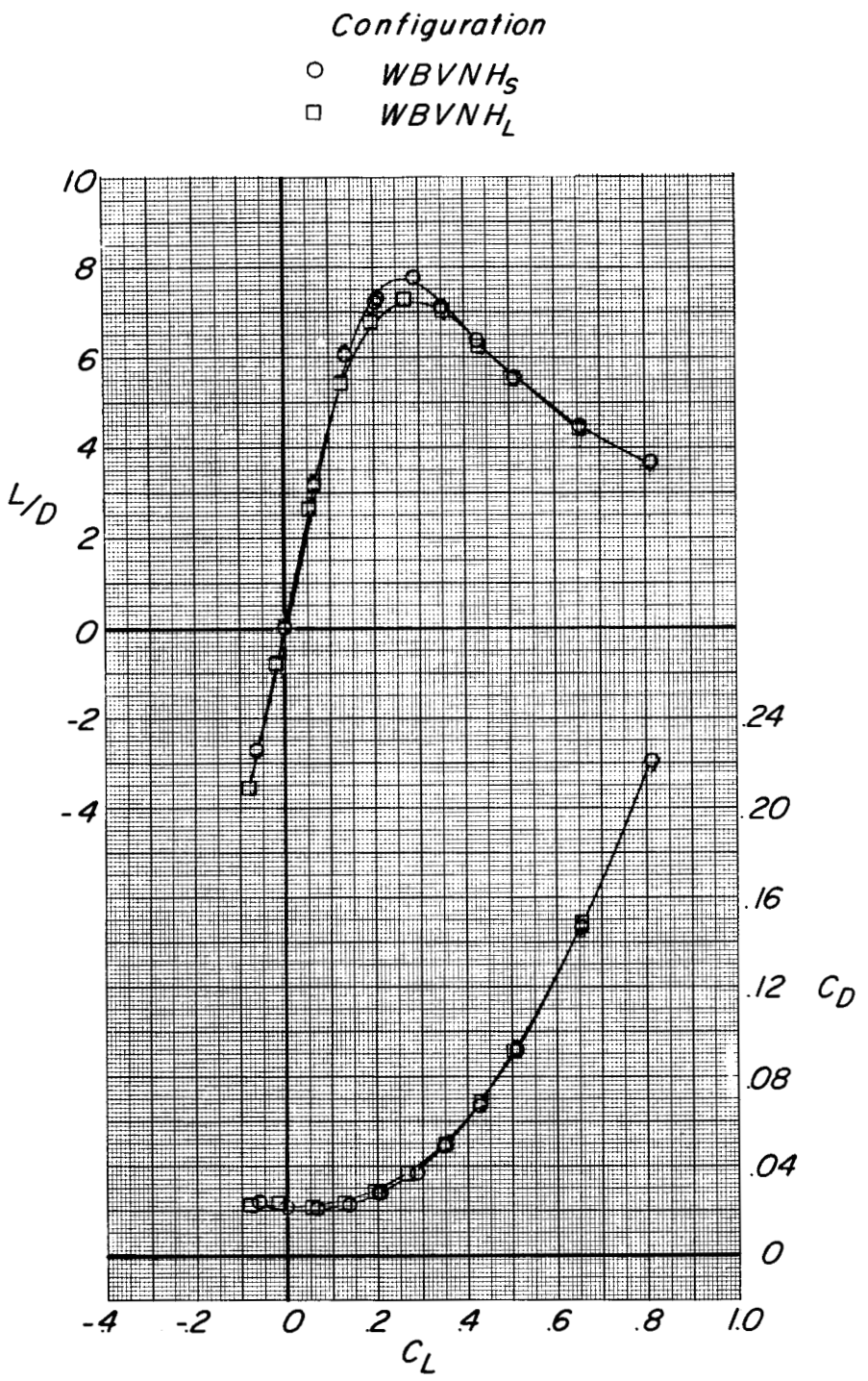

(e) Concluded.

Figure 4.- Continued.

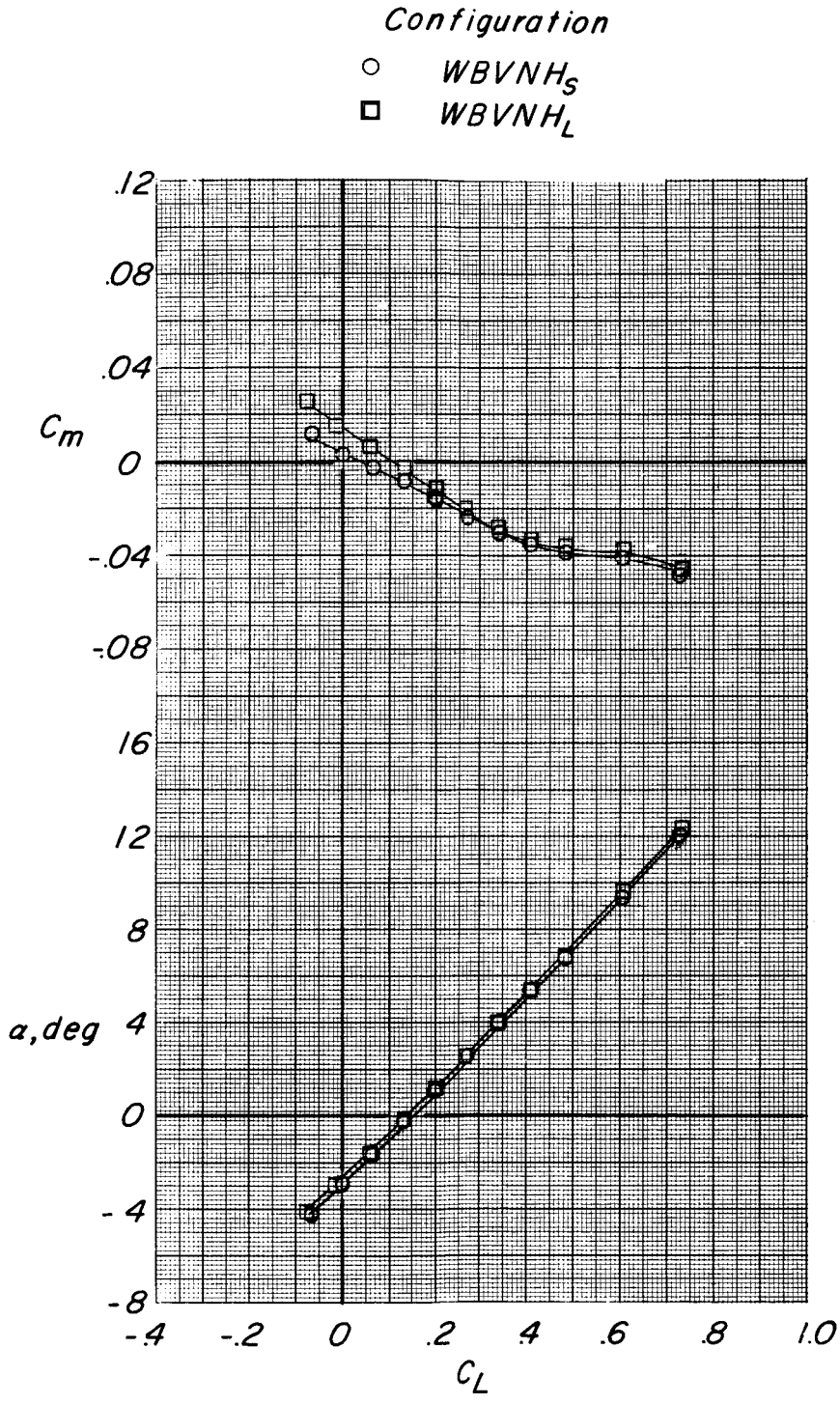

(f) M = 1.19.

Figure 4.- Continued.

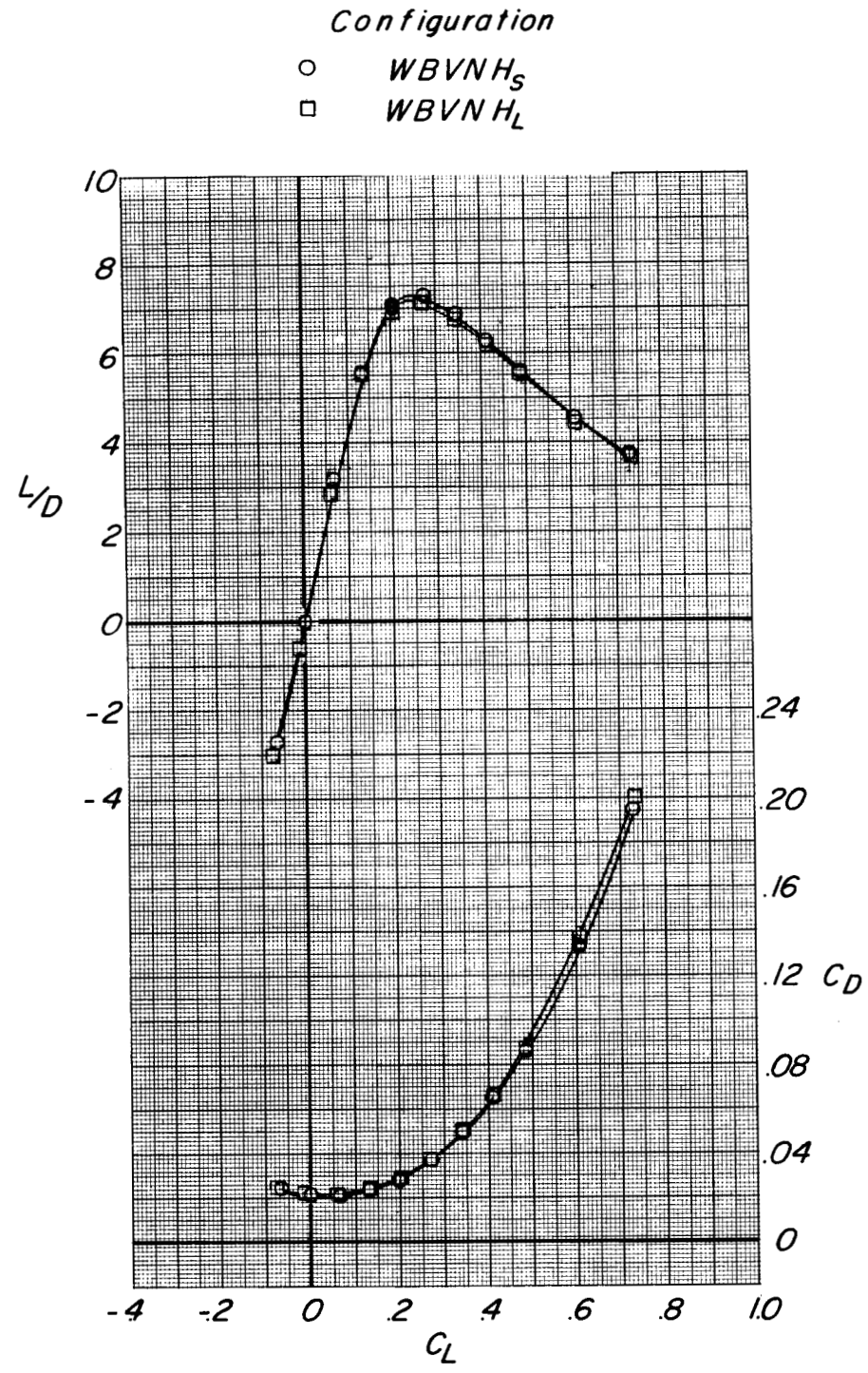

(f) Concluded.

Figure 4.- Concluded.

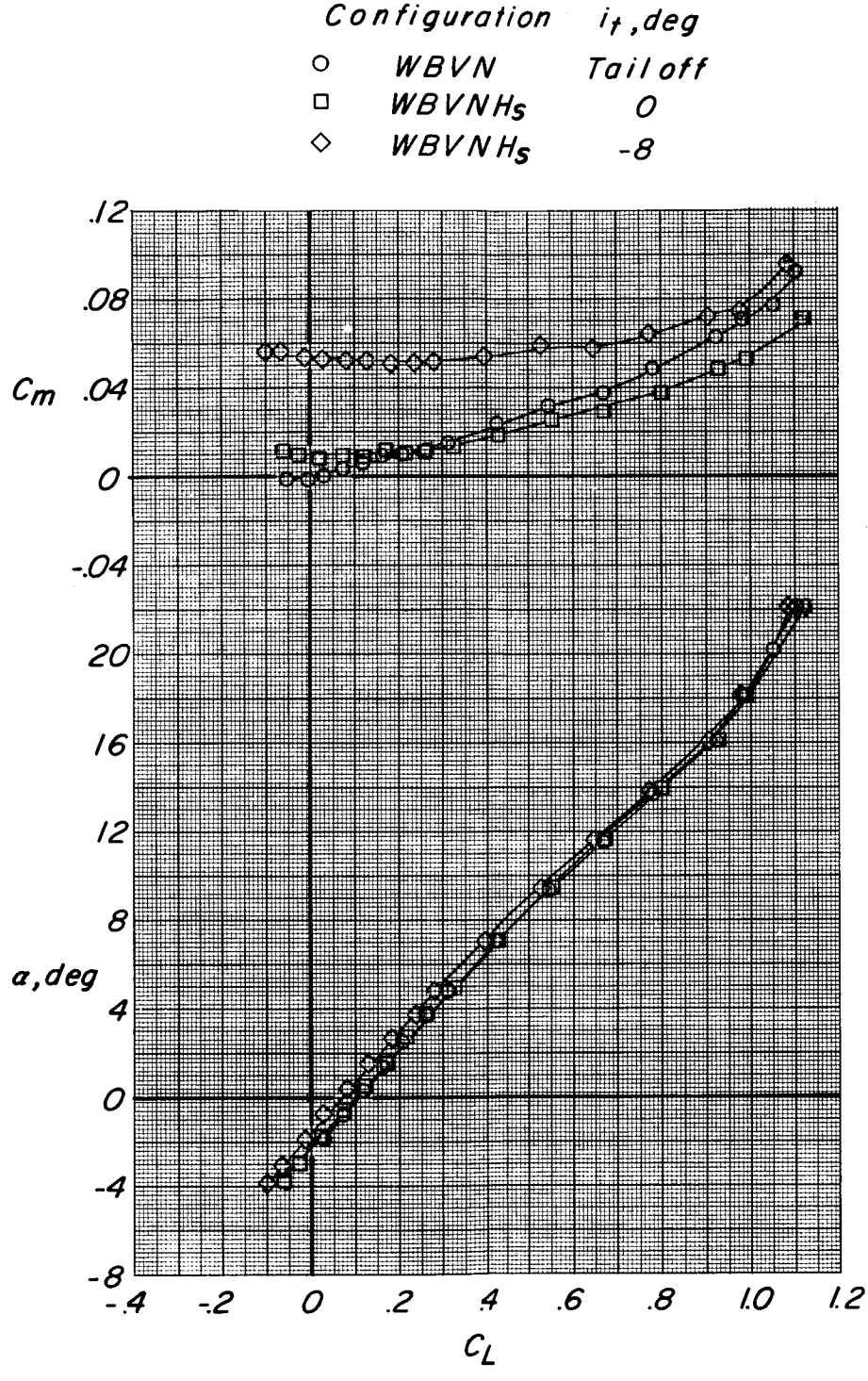

(a) M = 0.50.

Figure 5.- Effect of horizontal-tail deflection on the longitudinal characteristics of the model with the small horizontal tail.

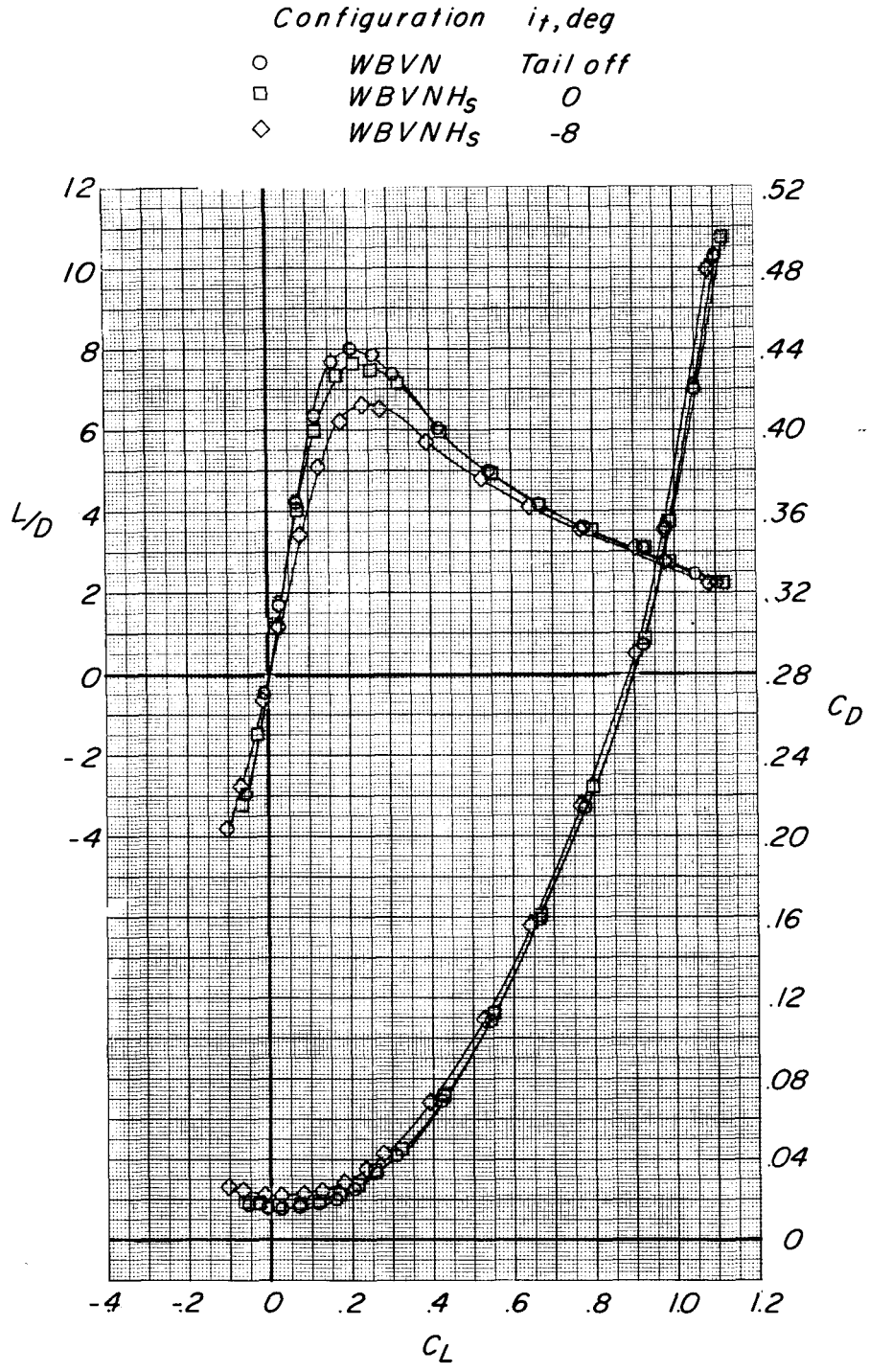

(a) Concluded.

Figure 5.- Continued.

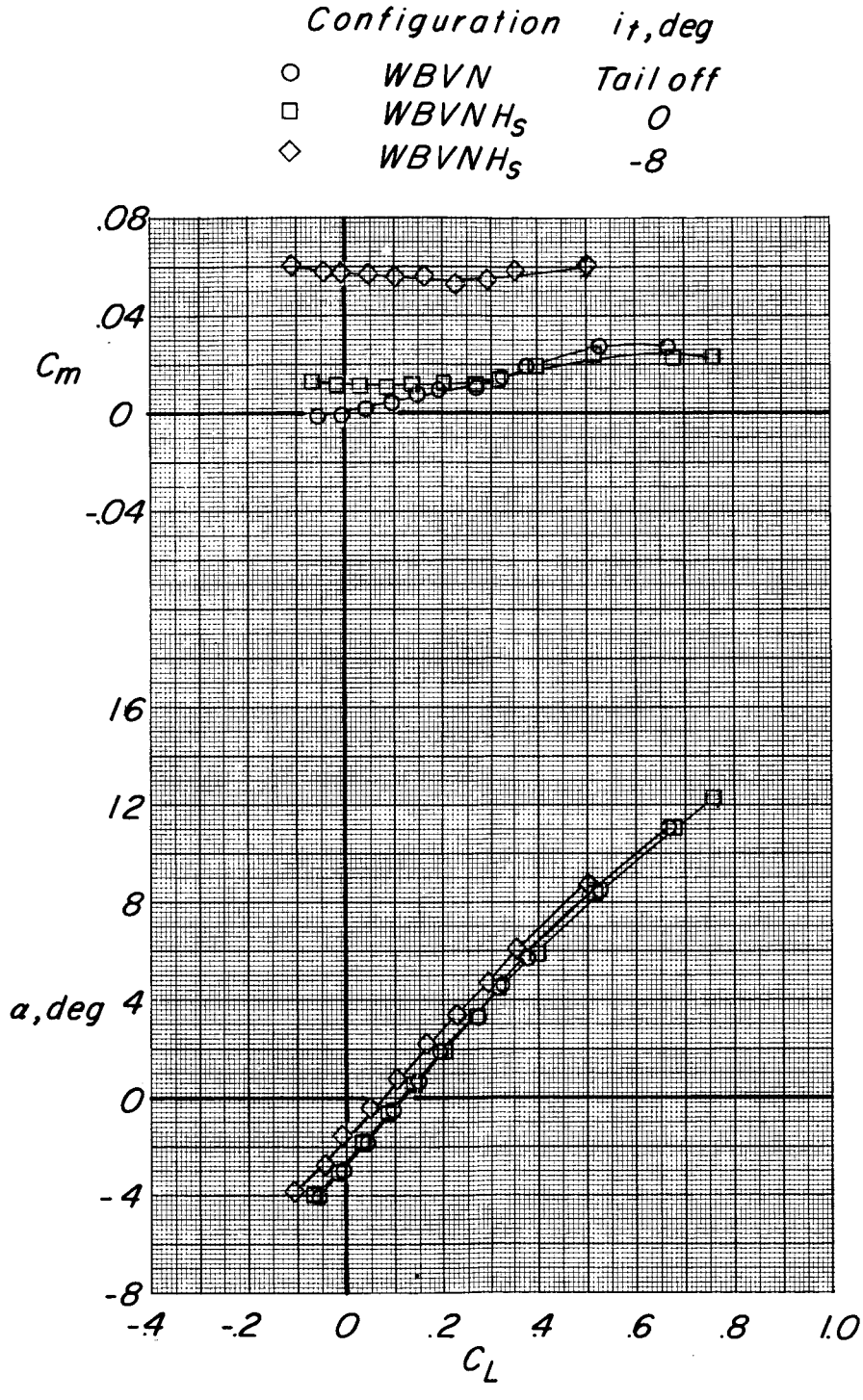

(b) M = 0.79.

Figure 5.- Continued.

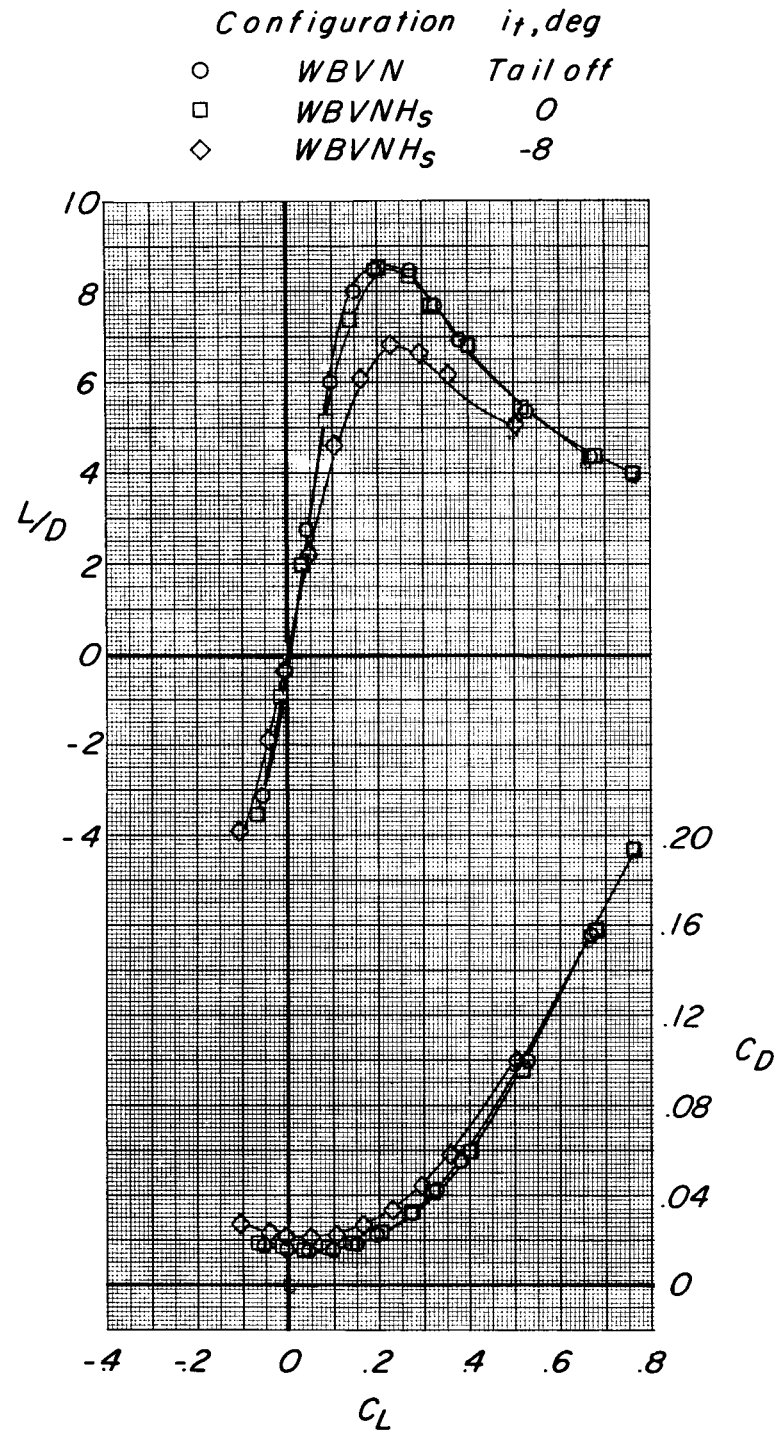

(b) Concluded.

Figure 5.- Continued.

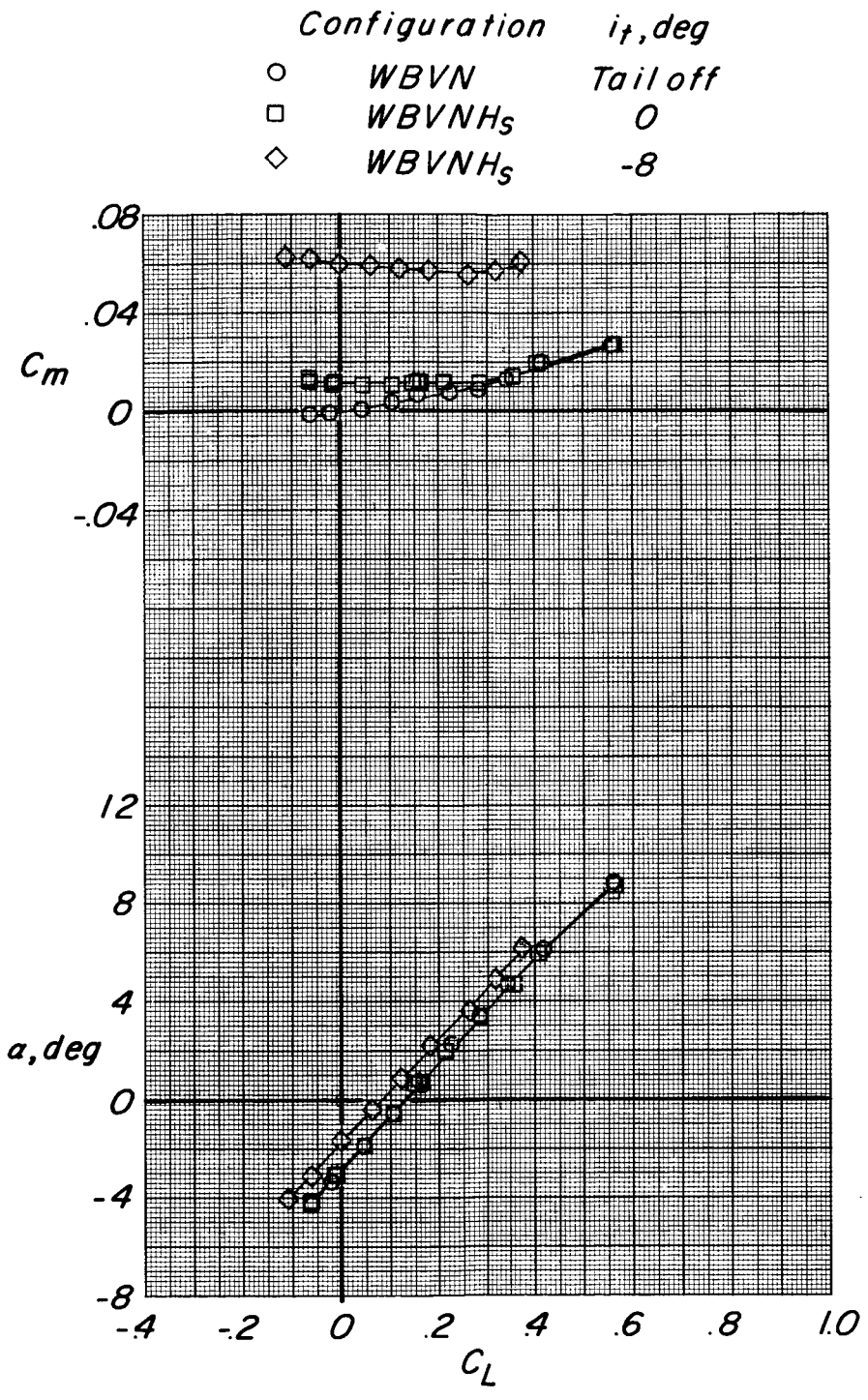

(c) M = 0.89.

Figure 5. Continued.

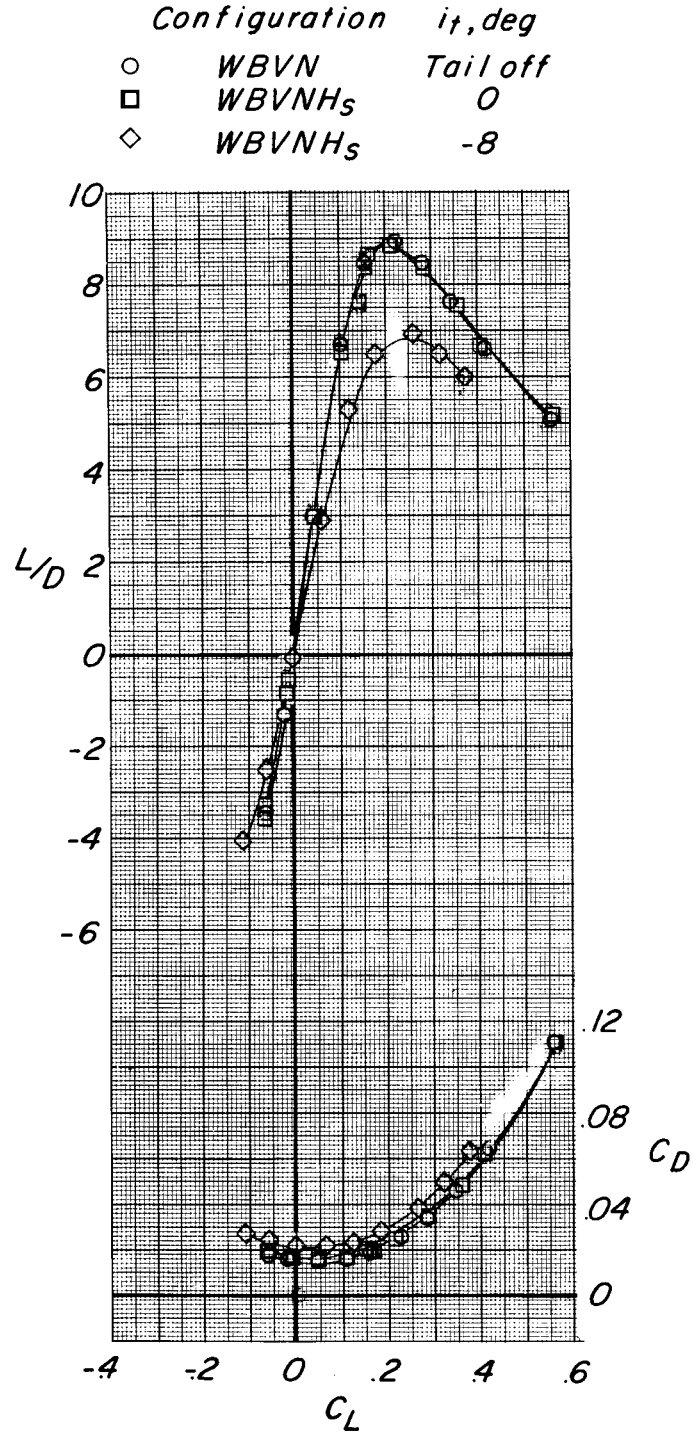

(c) Concluded.

Figure 5.- Continued.

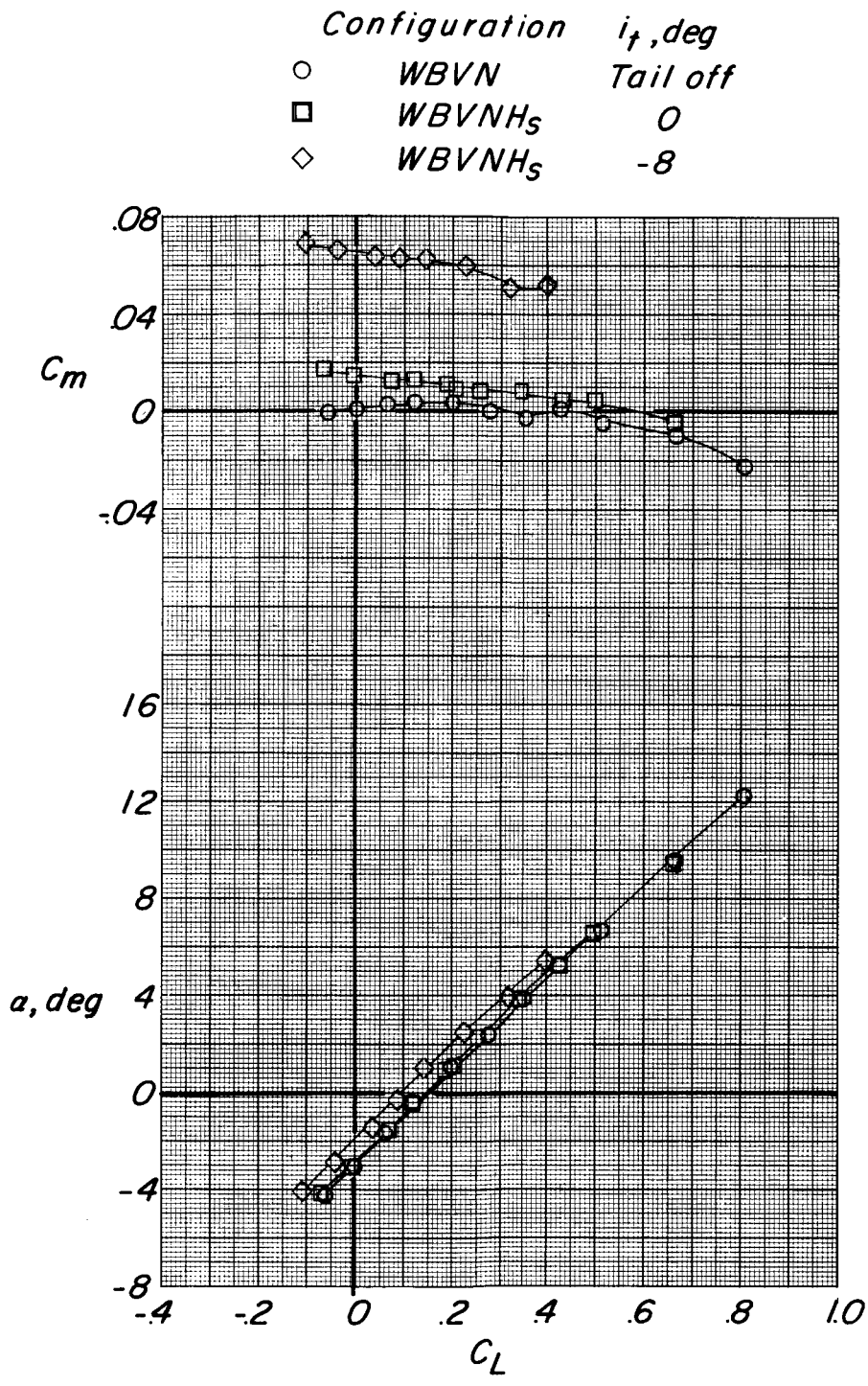

(d) M = 0.98.

Figure 5.- Continued.

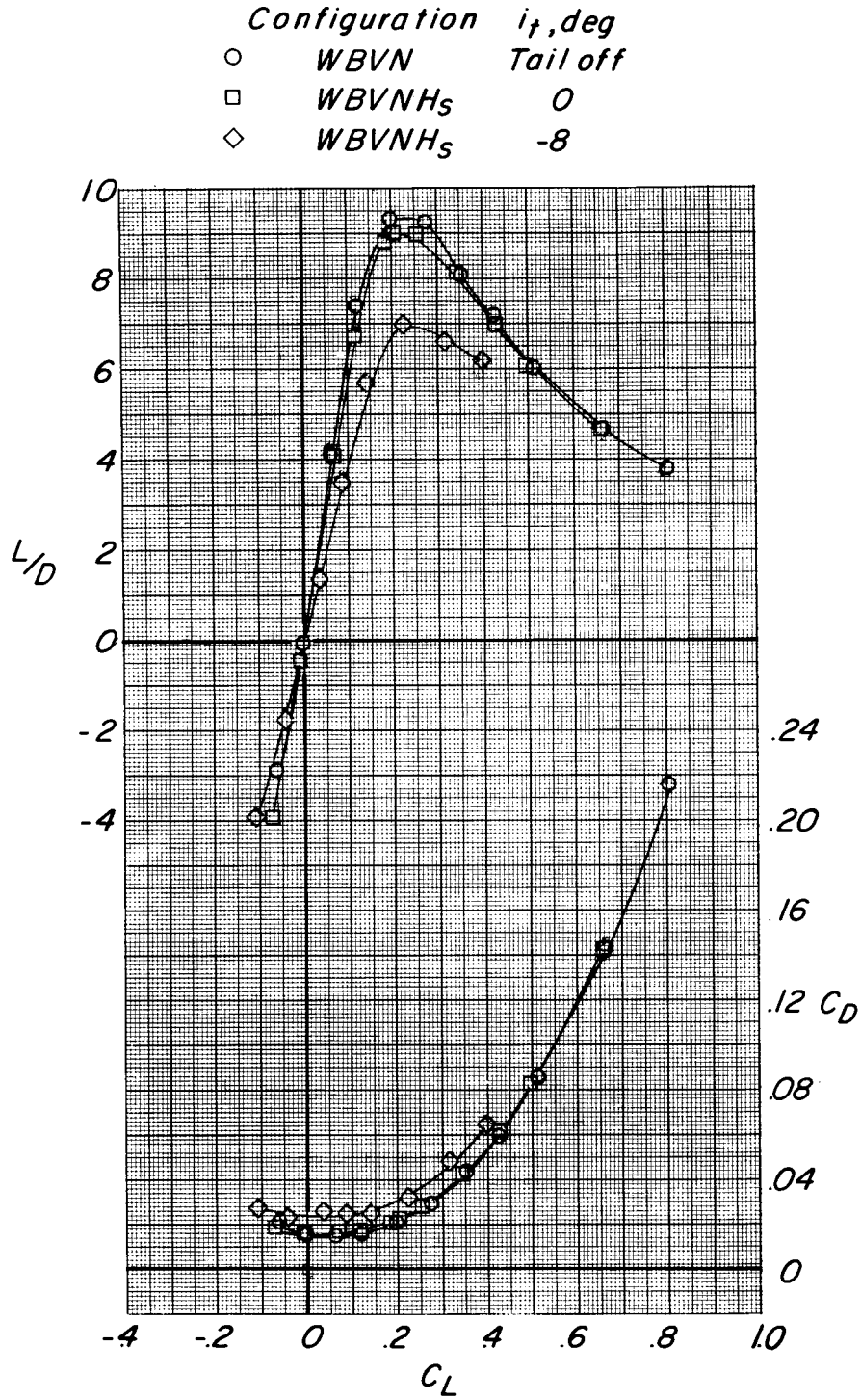

(d) Concluded.

Figure 5.- Continued.

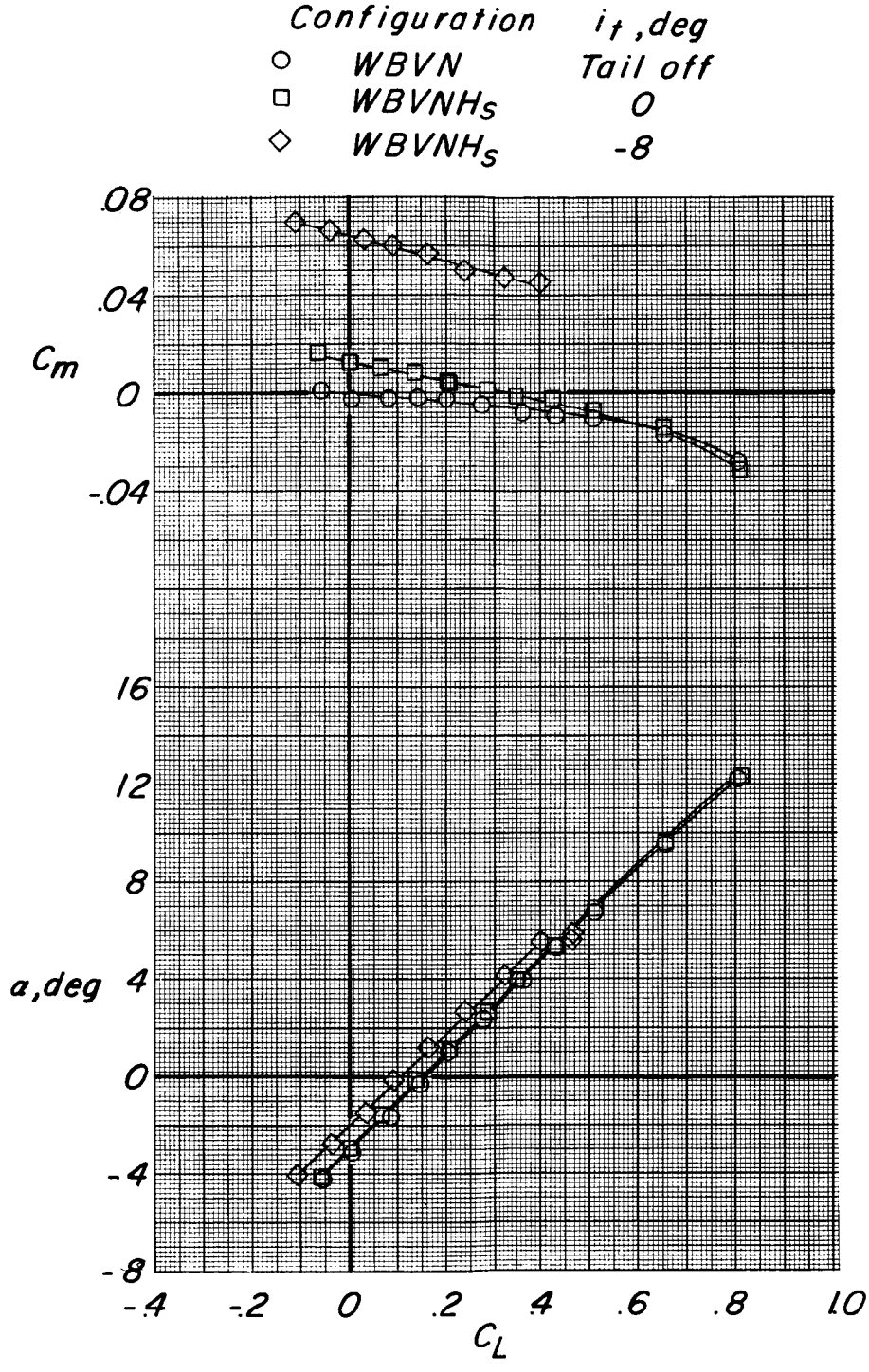

(e) M = 1.01.

Figure 5.- Continued.

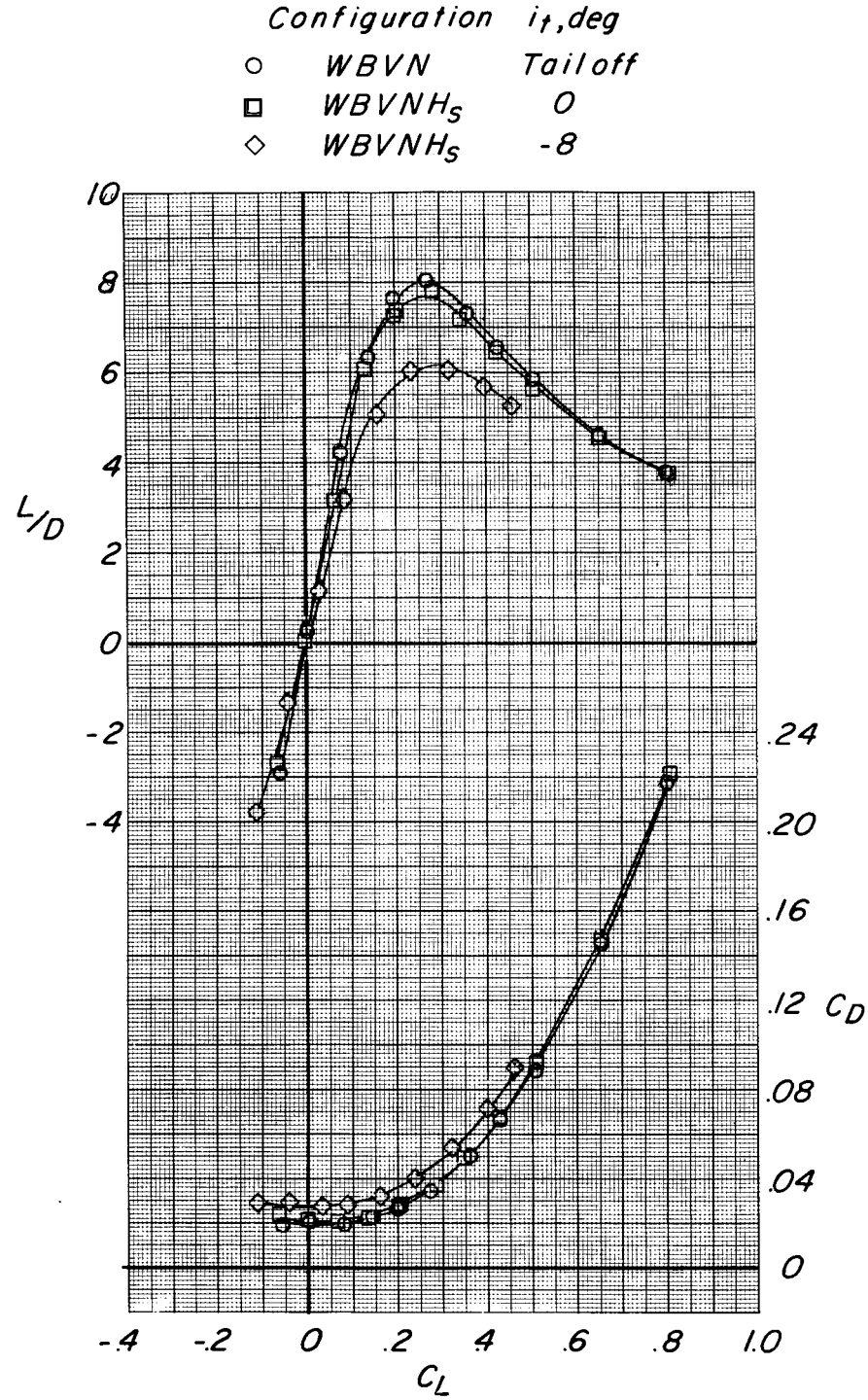

(e) Concluded.

Figure 5.- Continued.

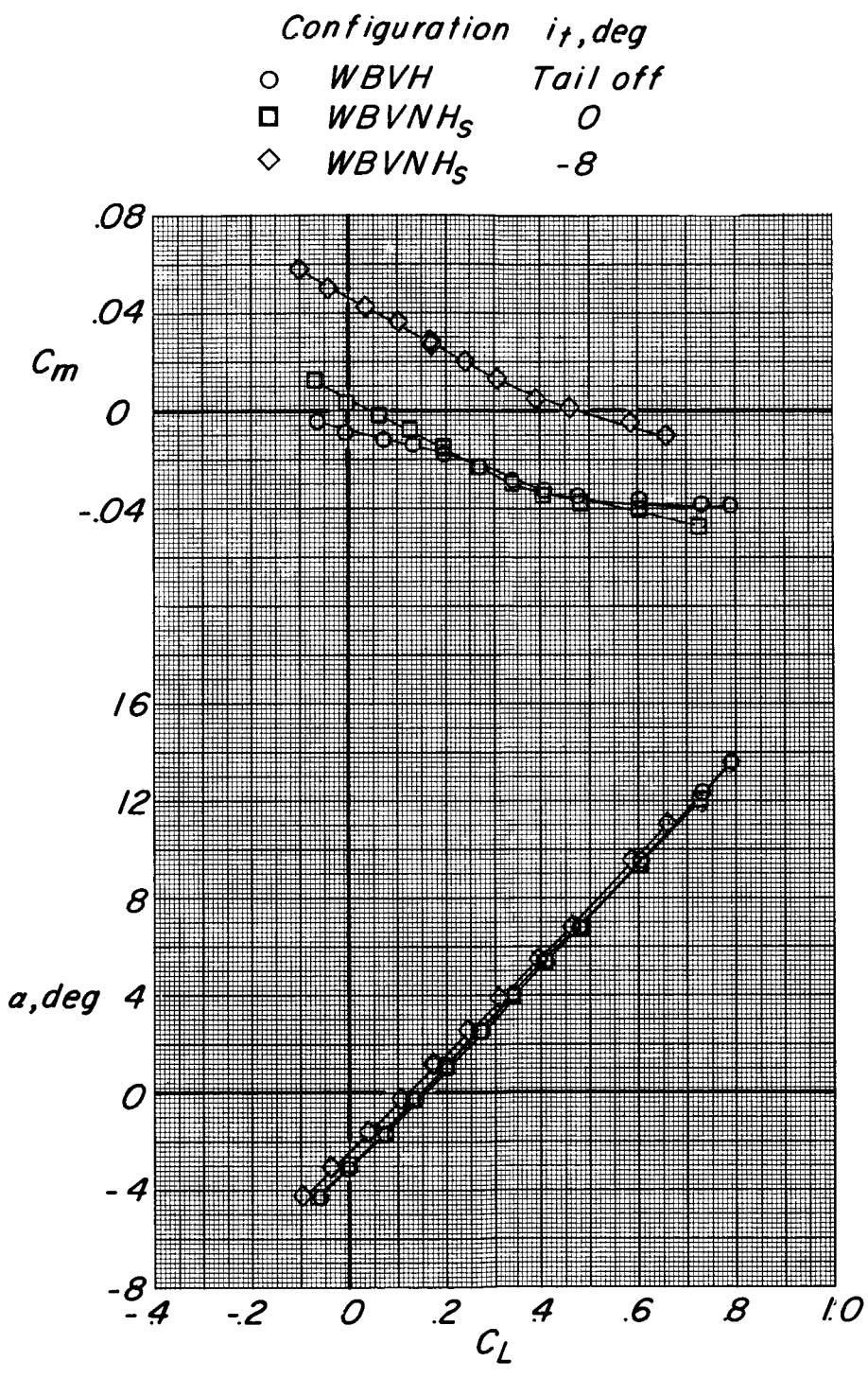

(f) M = 1.19.

Figure 5.- Continued.

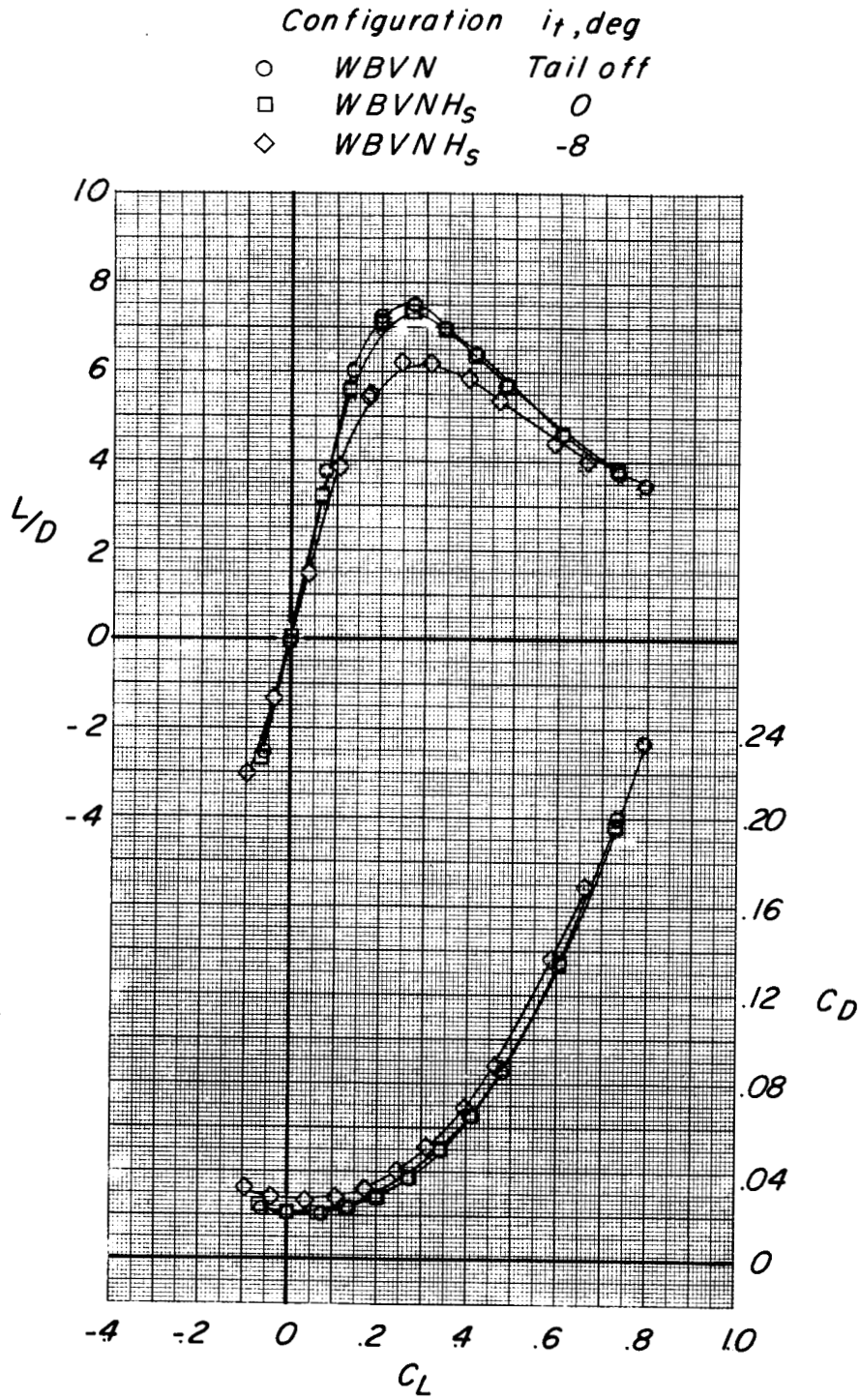

(f) Concluded.

Figure 5.- Continued.

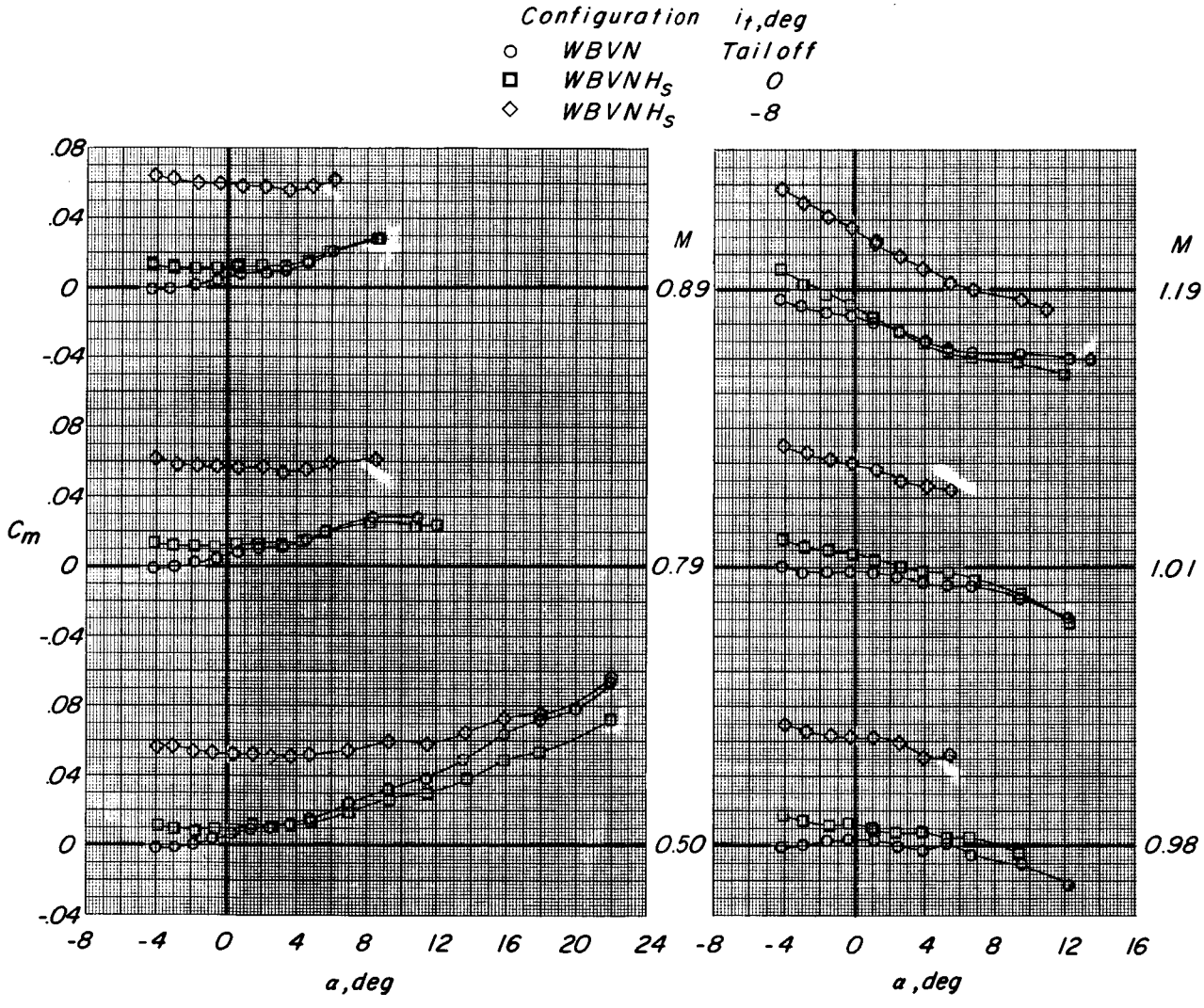

(g) C_m plotted against α.

Figure 5.- Concluded.

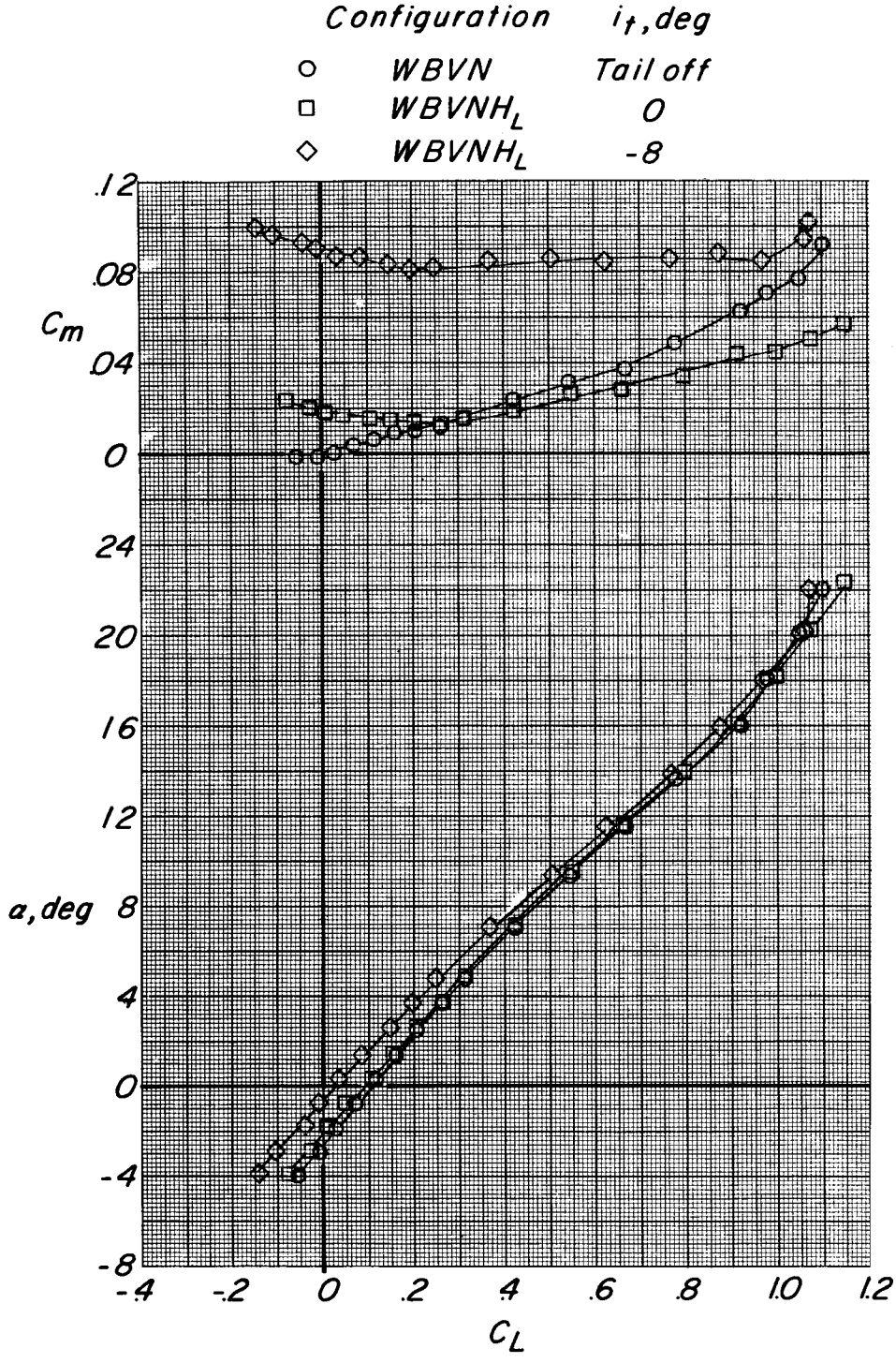

(a) M = 0.50.

Figure 6.- Effect of horizontal-tail deflection on the longitudinal characteristics of the model with the large horizontal tail.

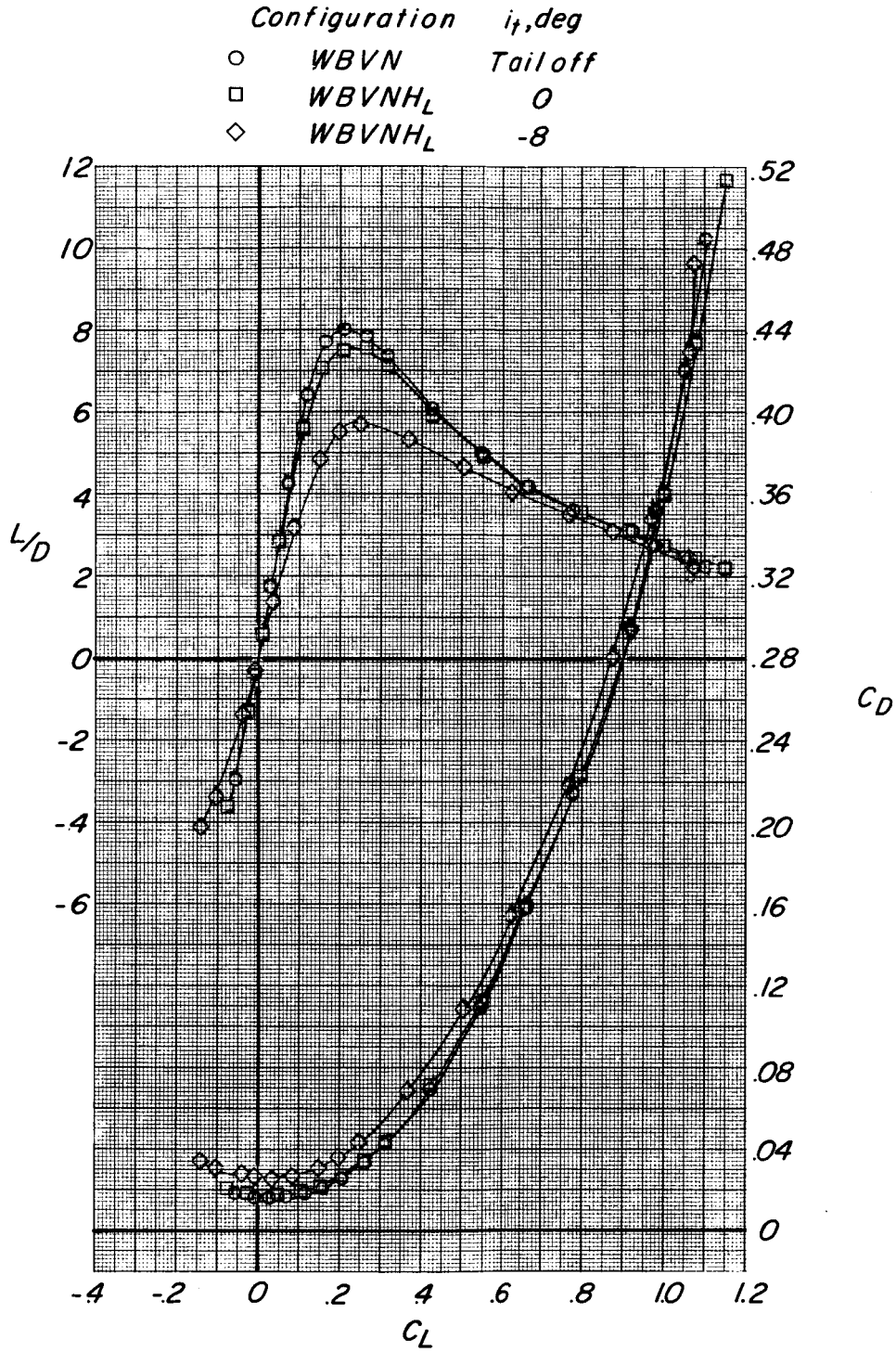

(a) Concluded.

Figure 6.- Continued.

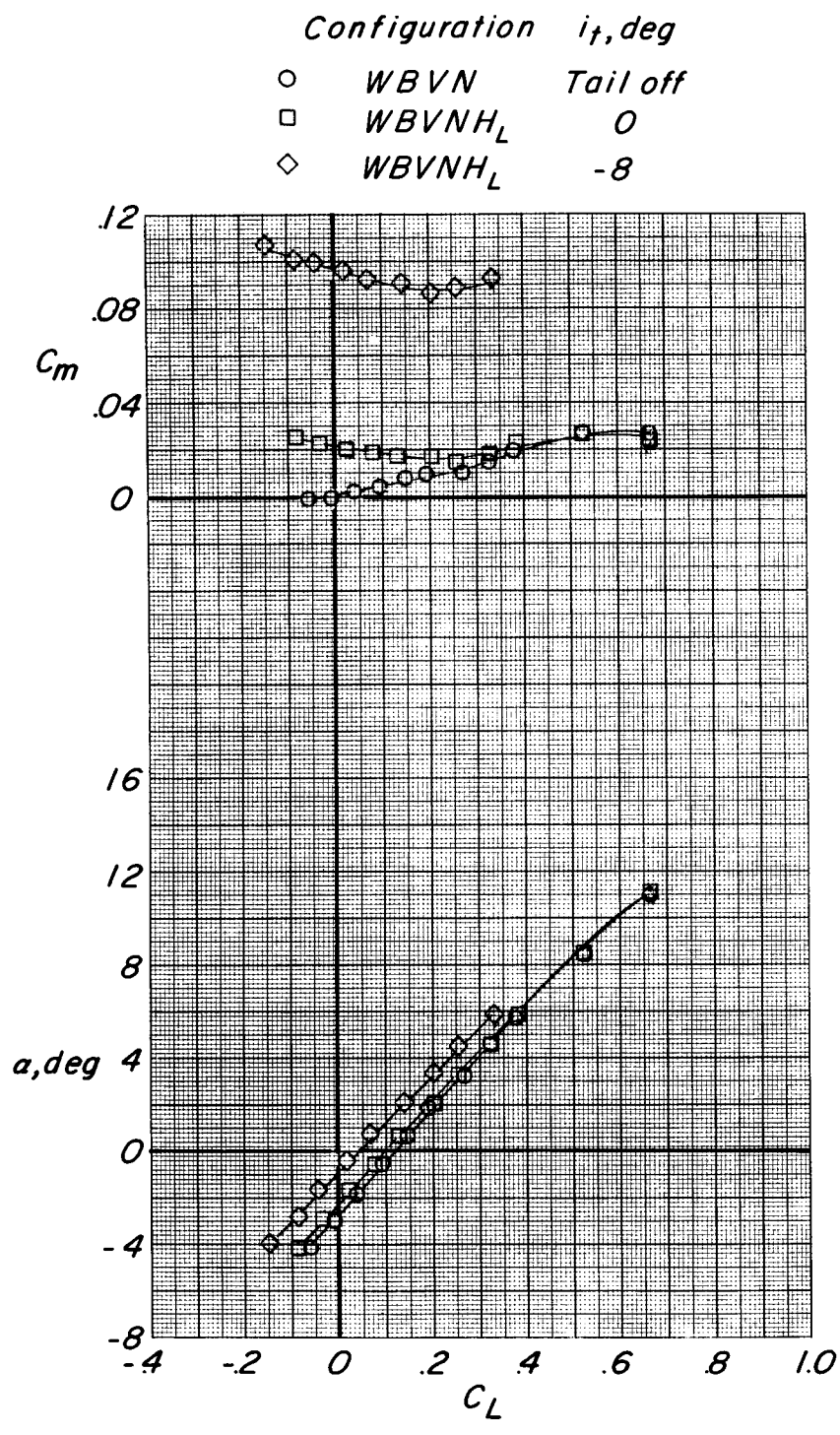

(b) M = 0.79.

Figure 6.- Continued.

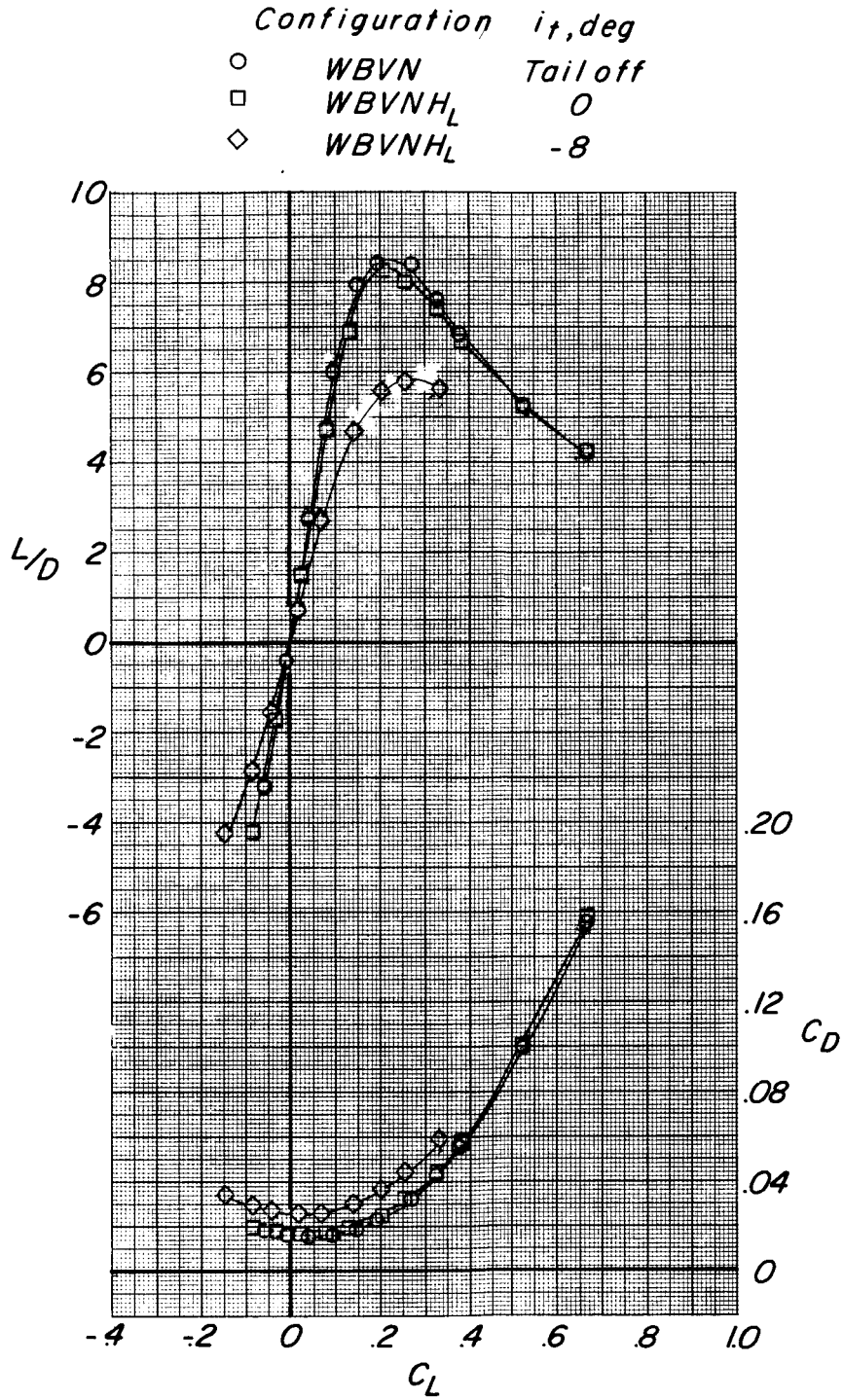

(b) Concluded.

Figure 6.- Continued.

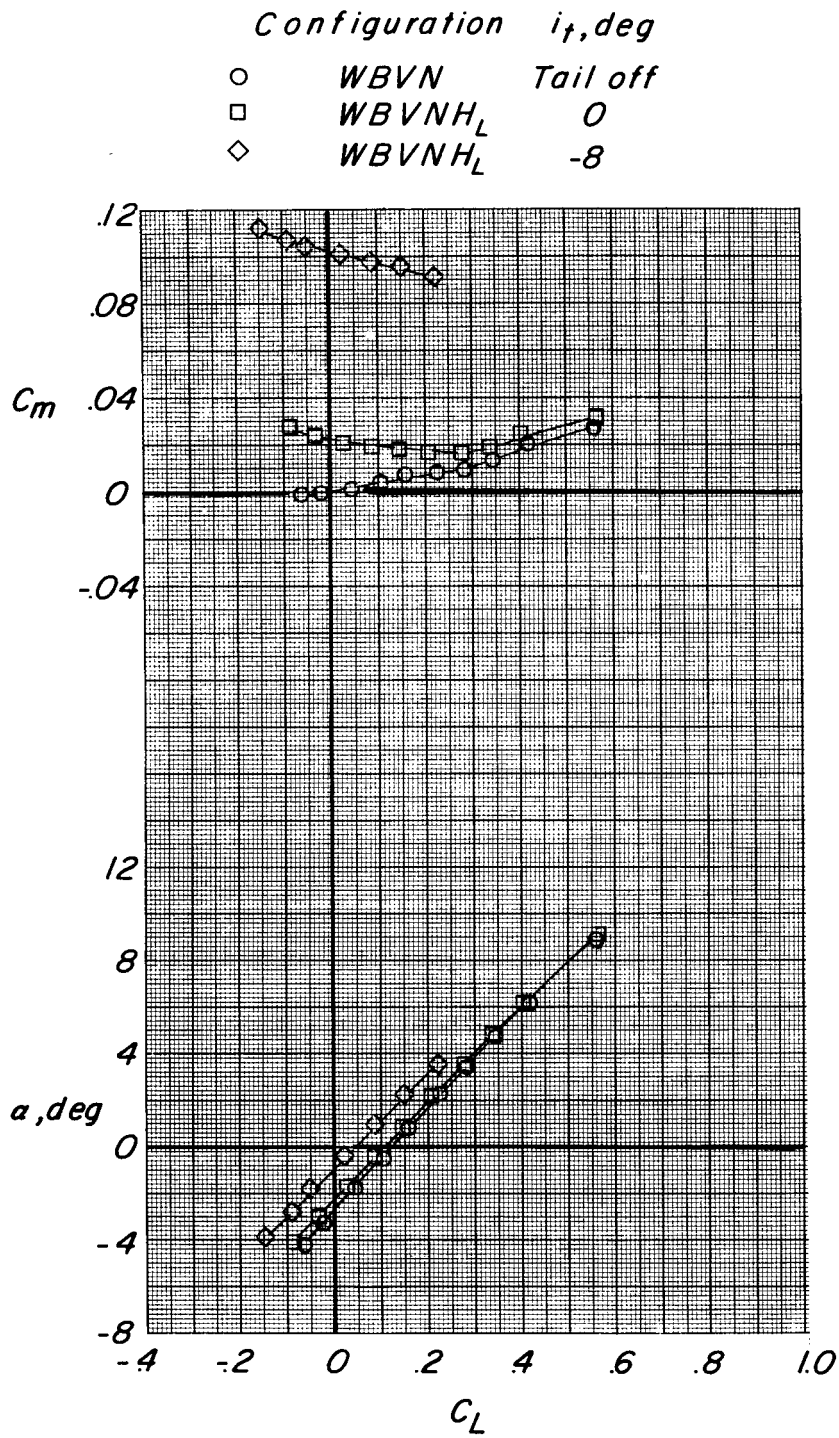

(c) M = 0.89.

Figure 6.- Continued.

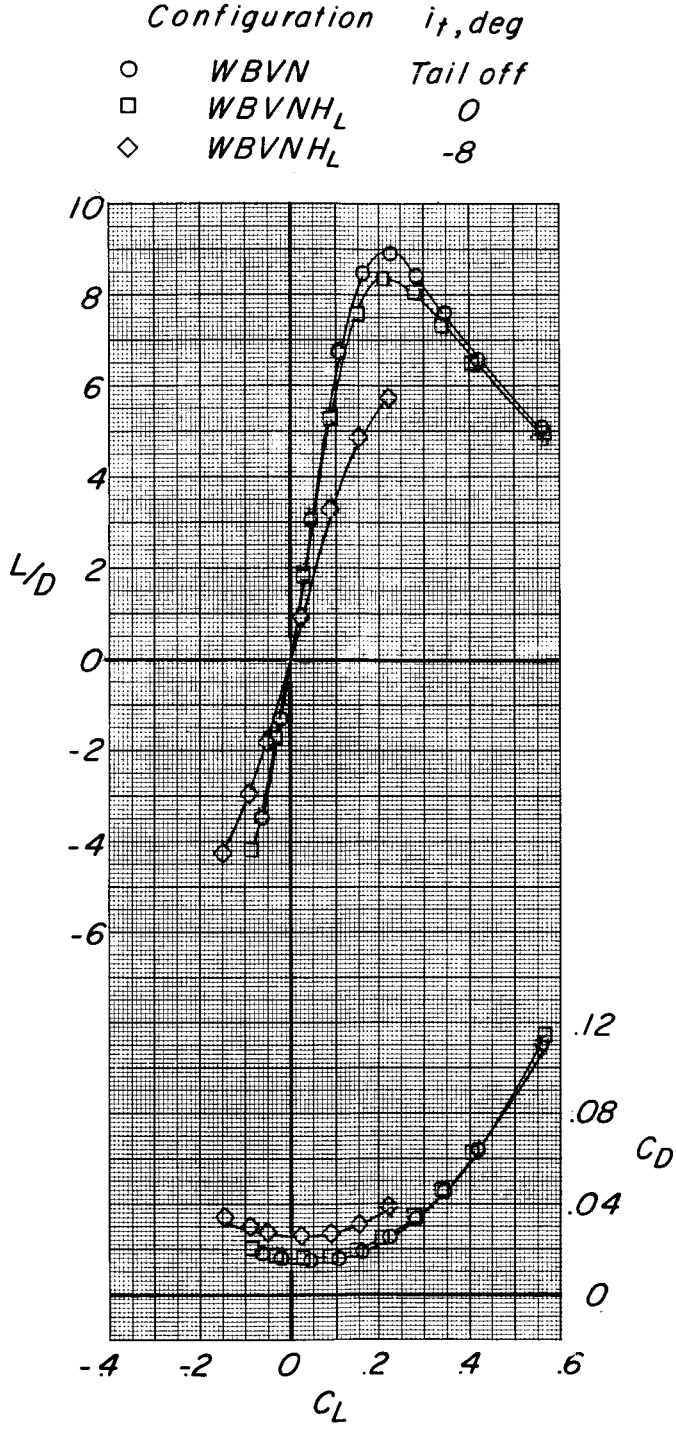

(c) Concluded.

Figure 6.- Continued.

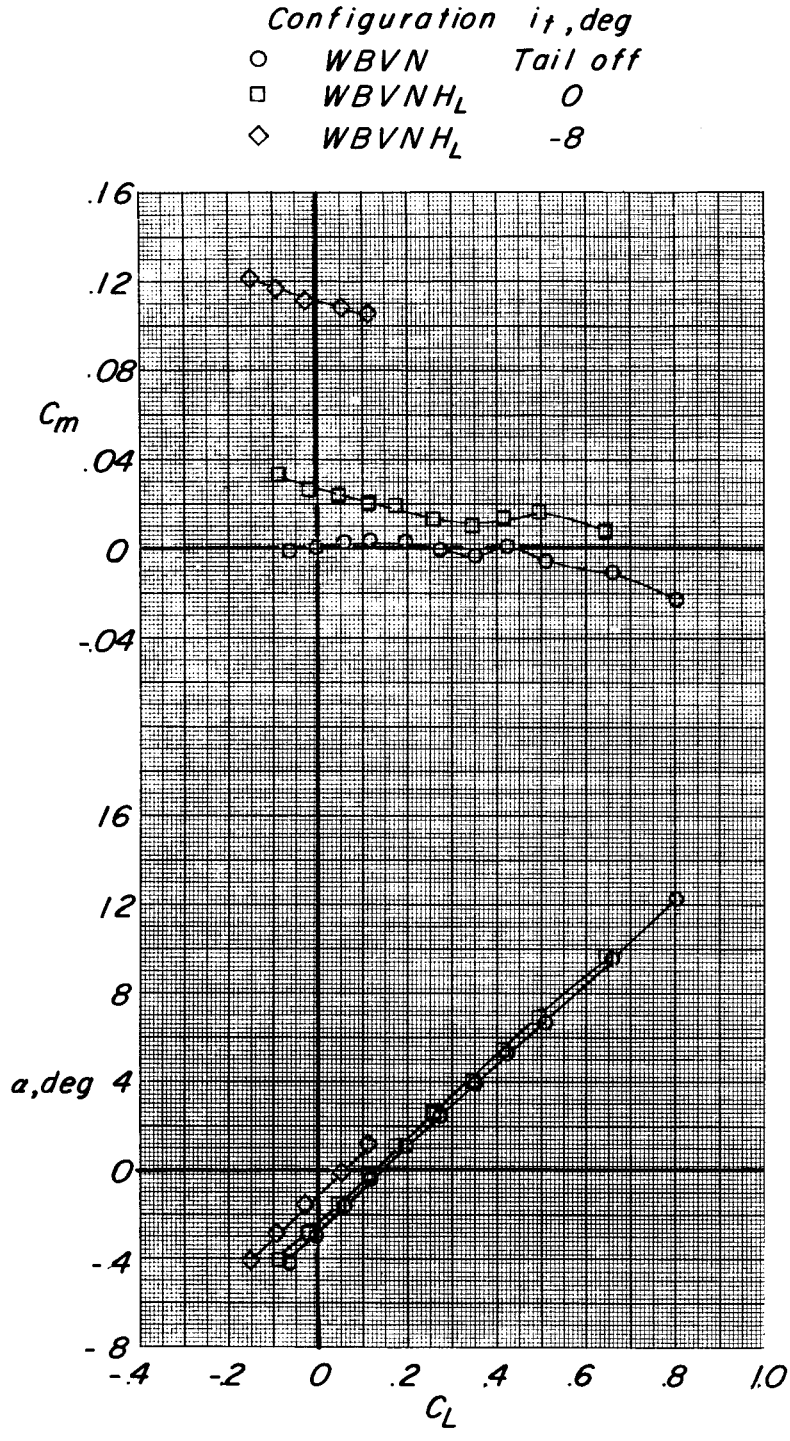

(d) M = 0.98.

Figure 6.- Continued.

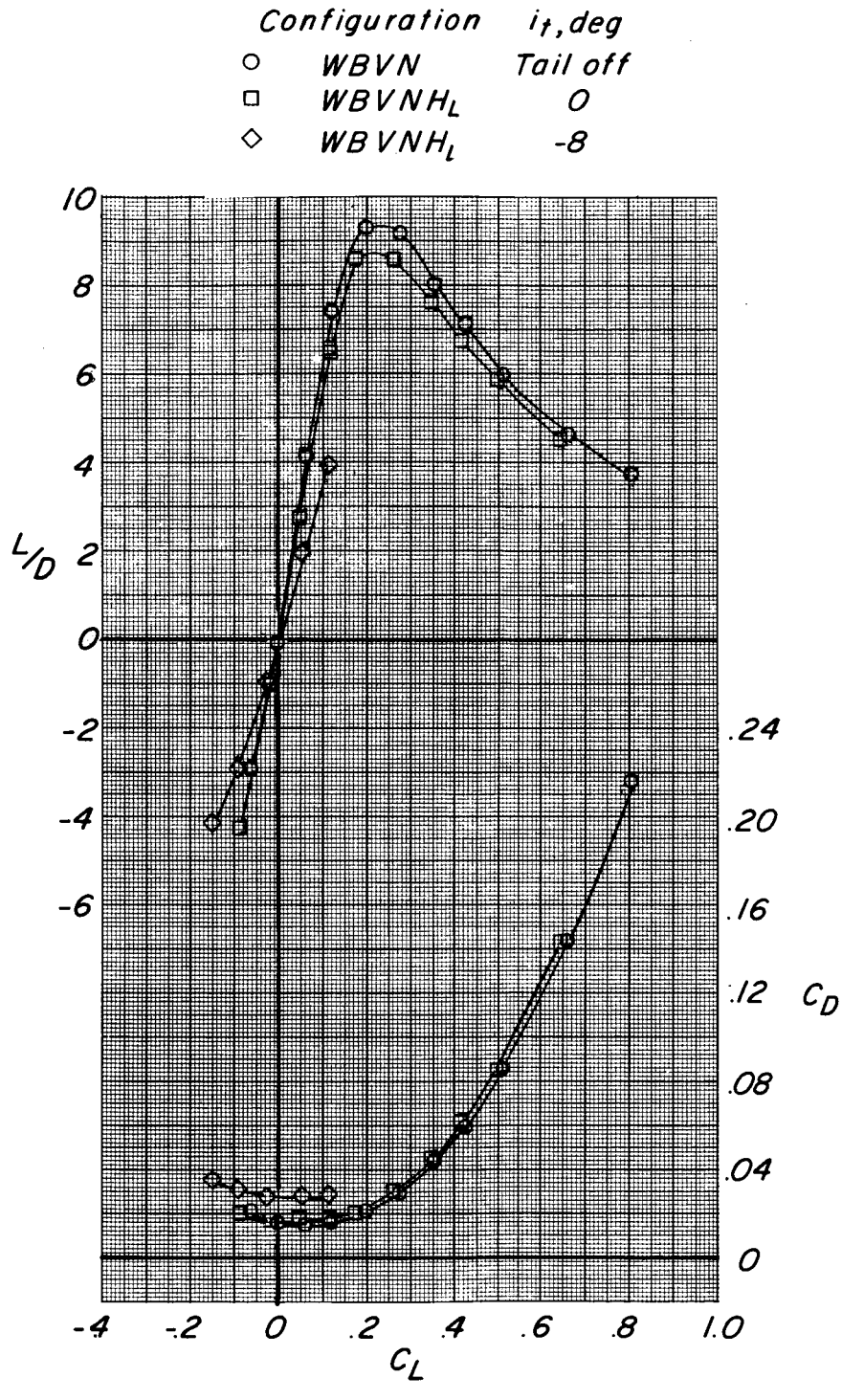

(d) Concluded.

Figure 6.- Continued.

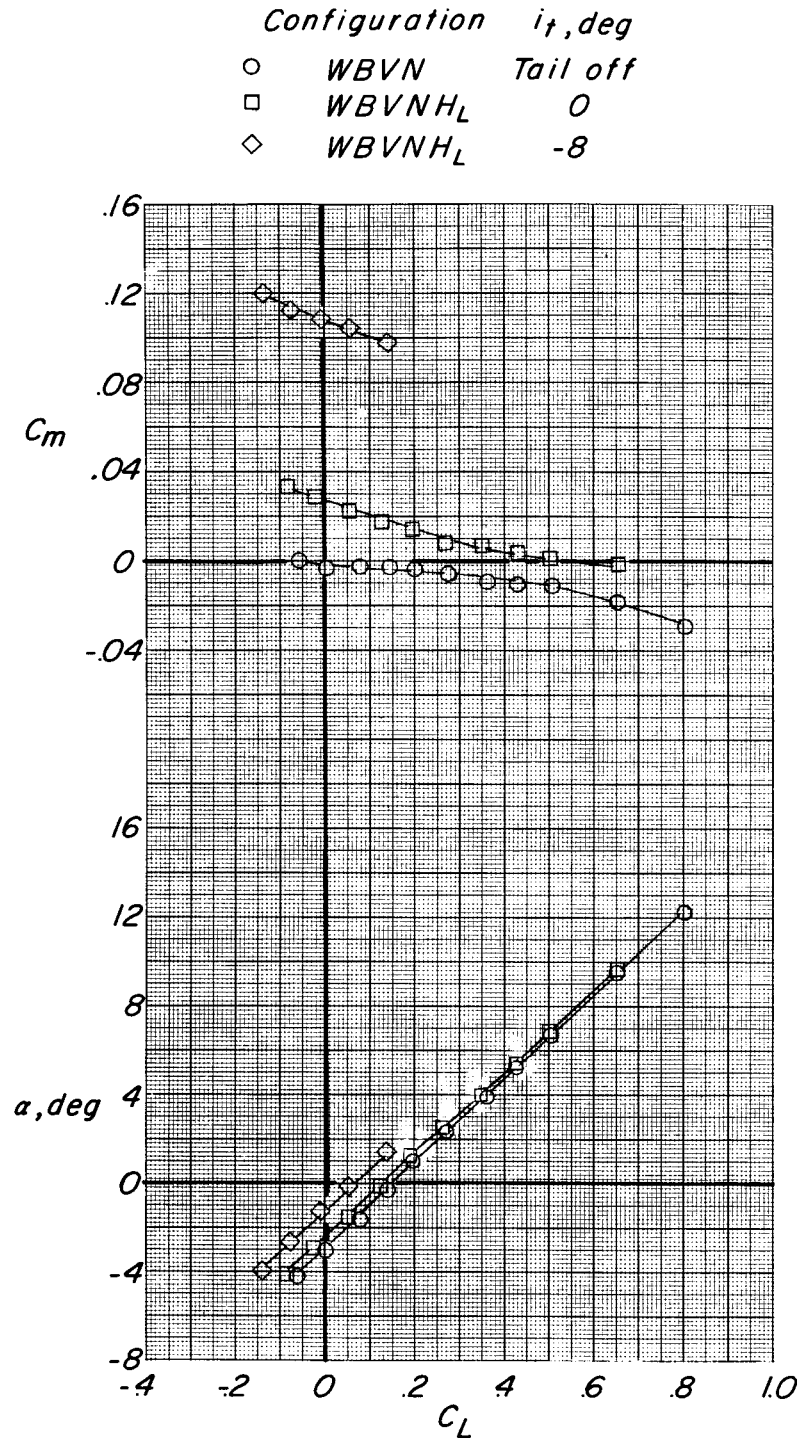

(e) M = 1.01.

Figure 6.- Continued.

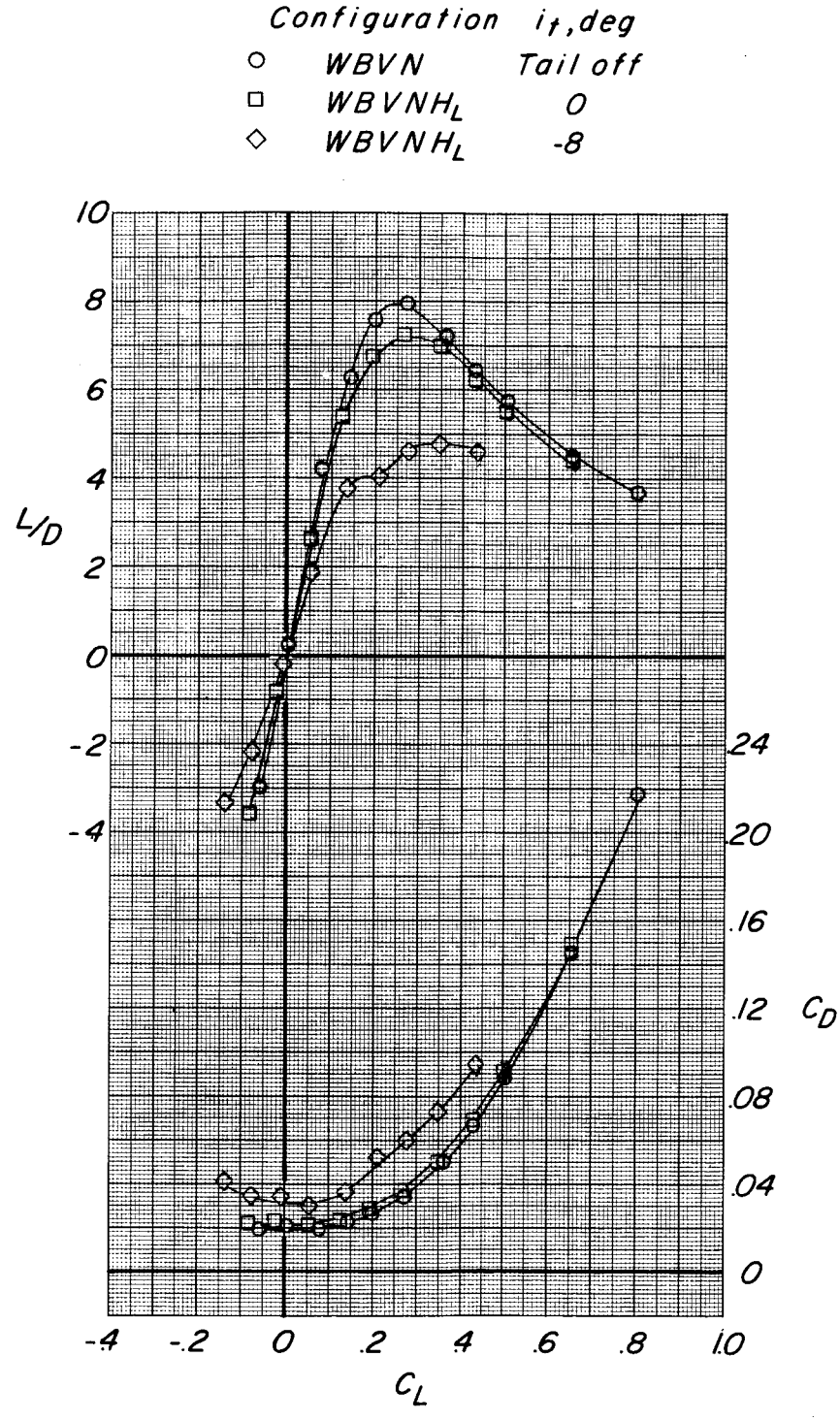

(e) Concluded.

Figure 6.- Continued.

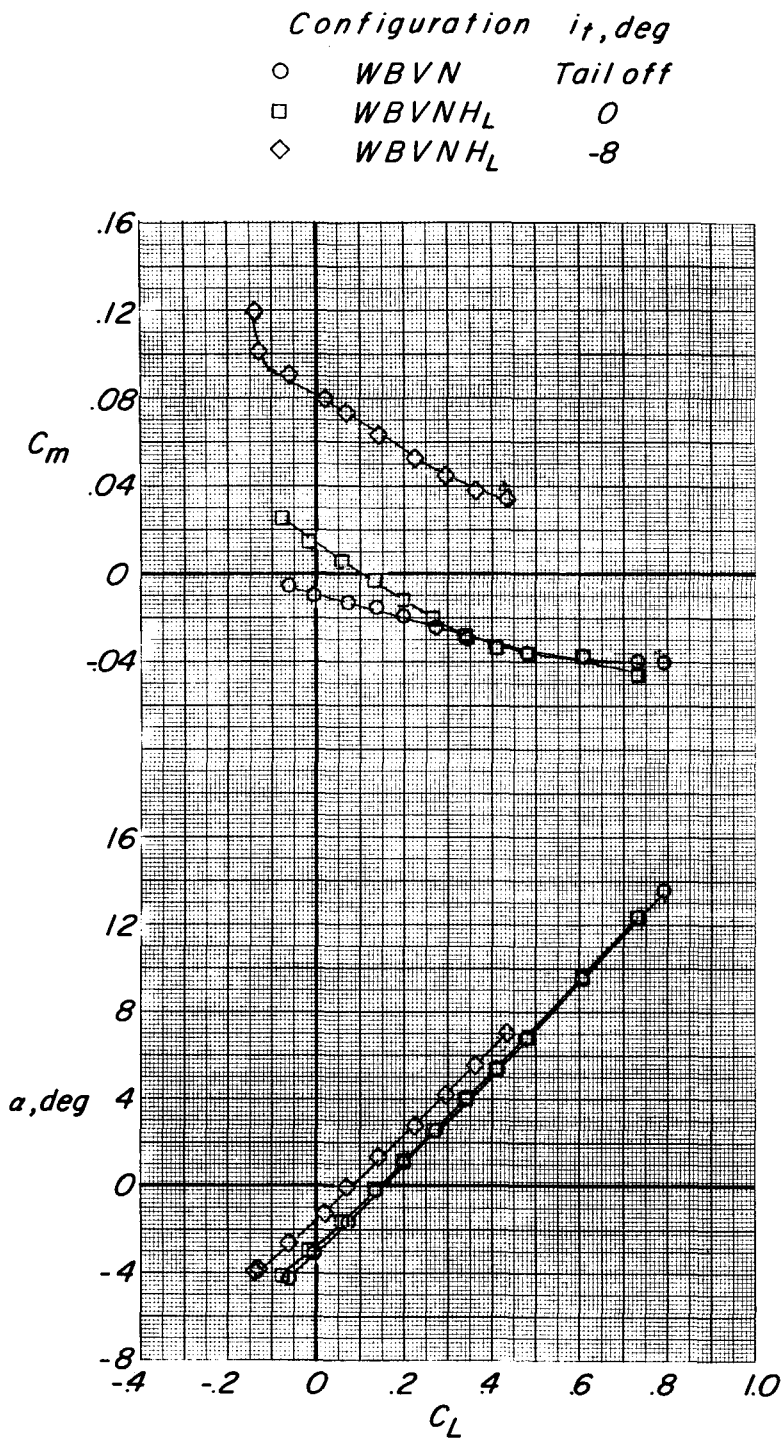

(f) M = 1.19.

Figure 6.- Continued.

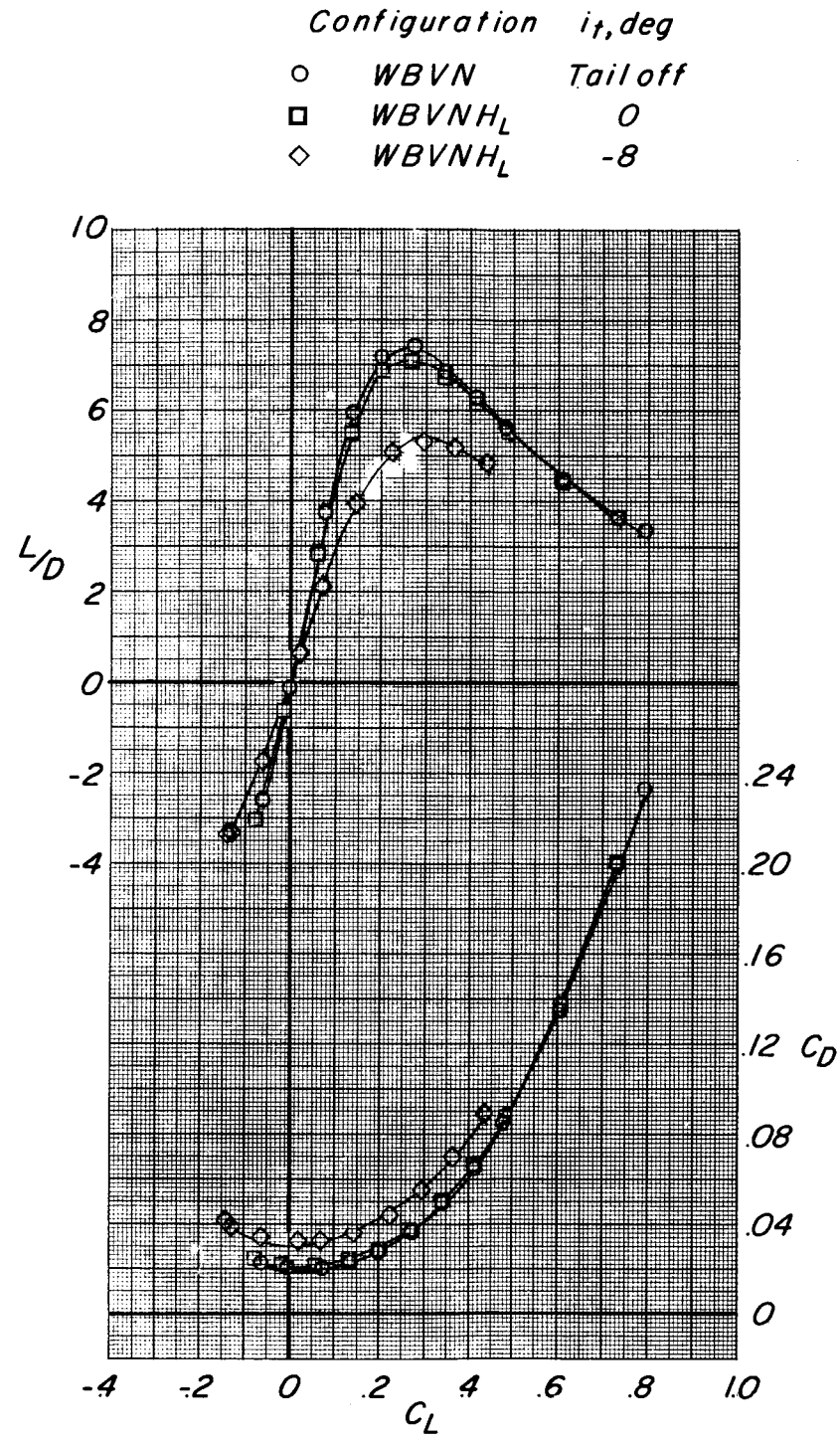

(f) Concluded.

Figure 6.- Continued.

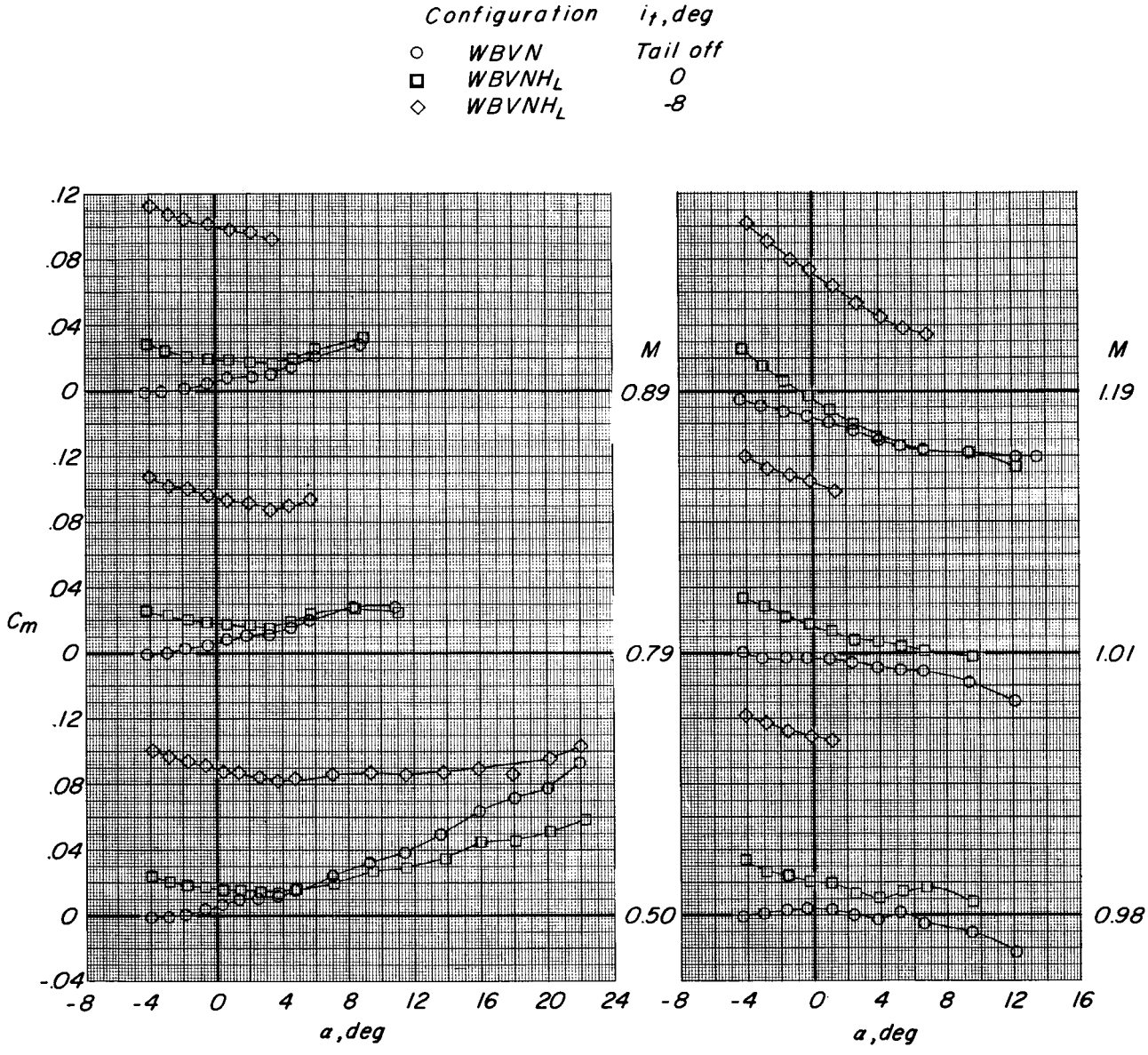

(g) C_m plotted against α.

Figure 6.- Concluded.

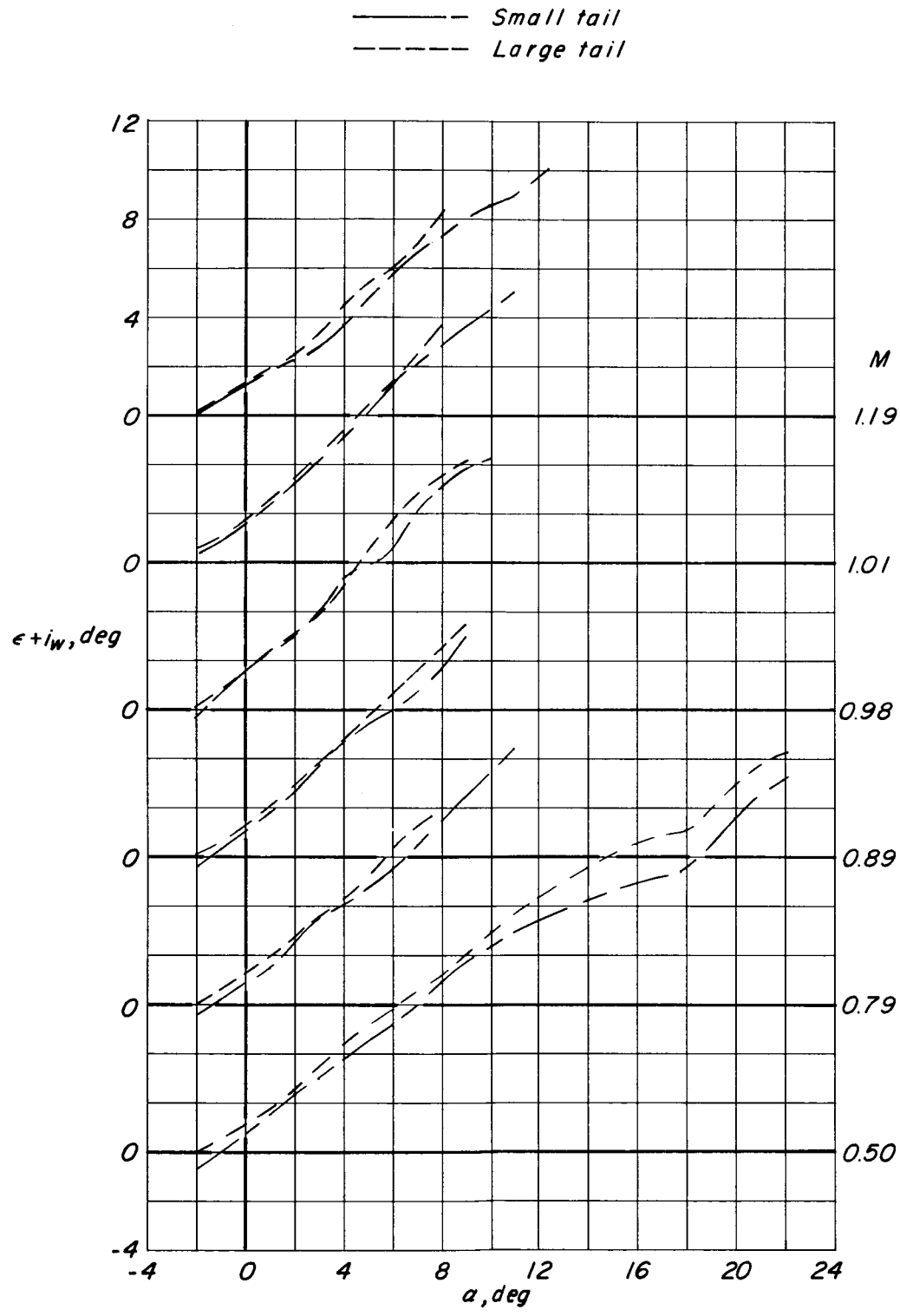

Figure 7.- Effect of horizontal-tail size on longitudinal control effectiveness. M = 0.50 to 1.19.

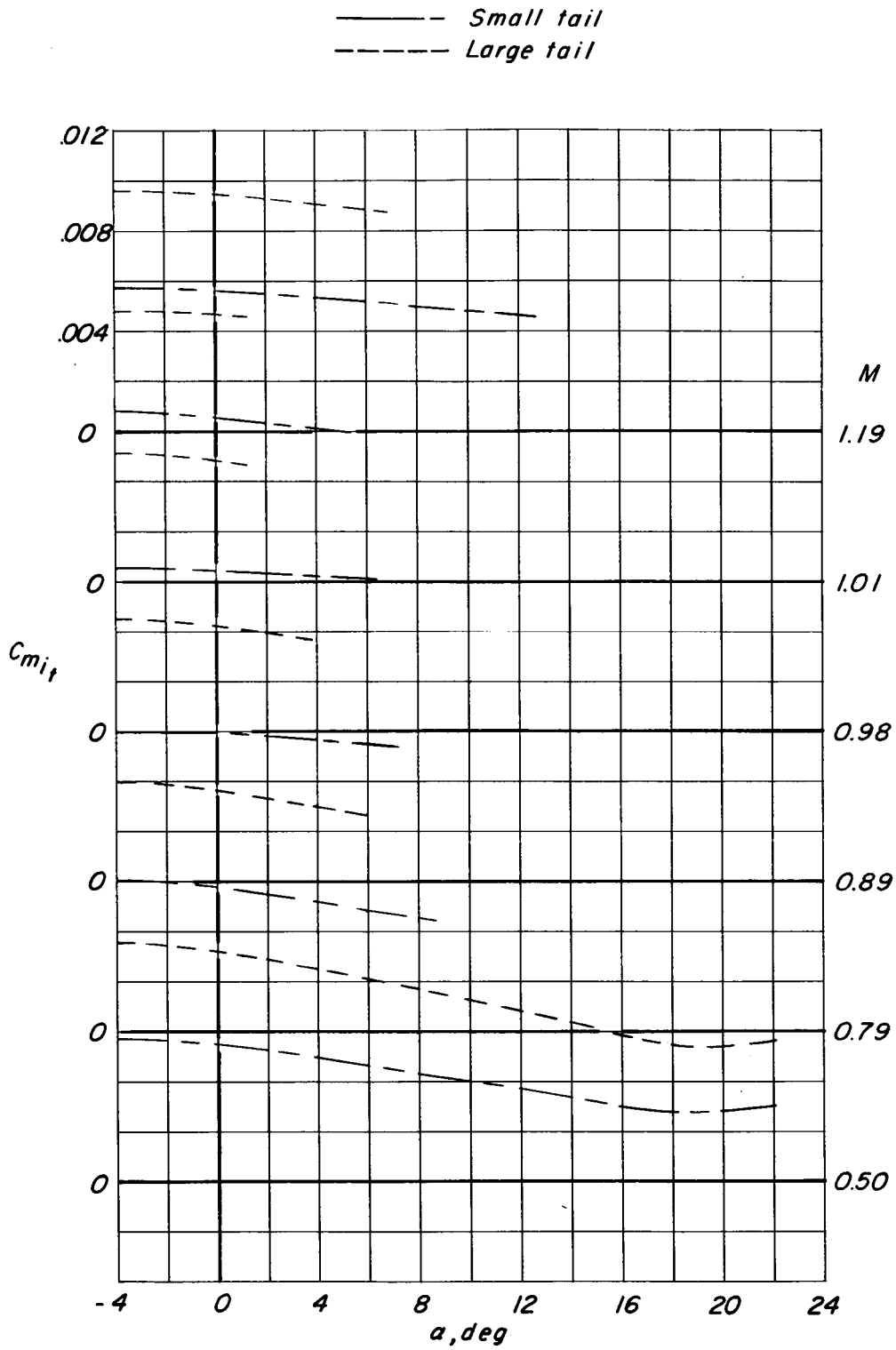

Figure 8.- Downwash characteristics of the model with the small horizontal tail and with the large horizontal tail. M = 0.50 to 1.19.

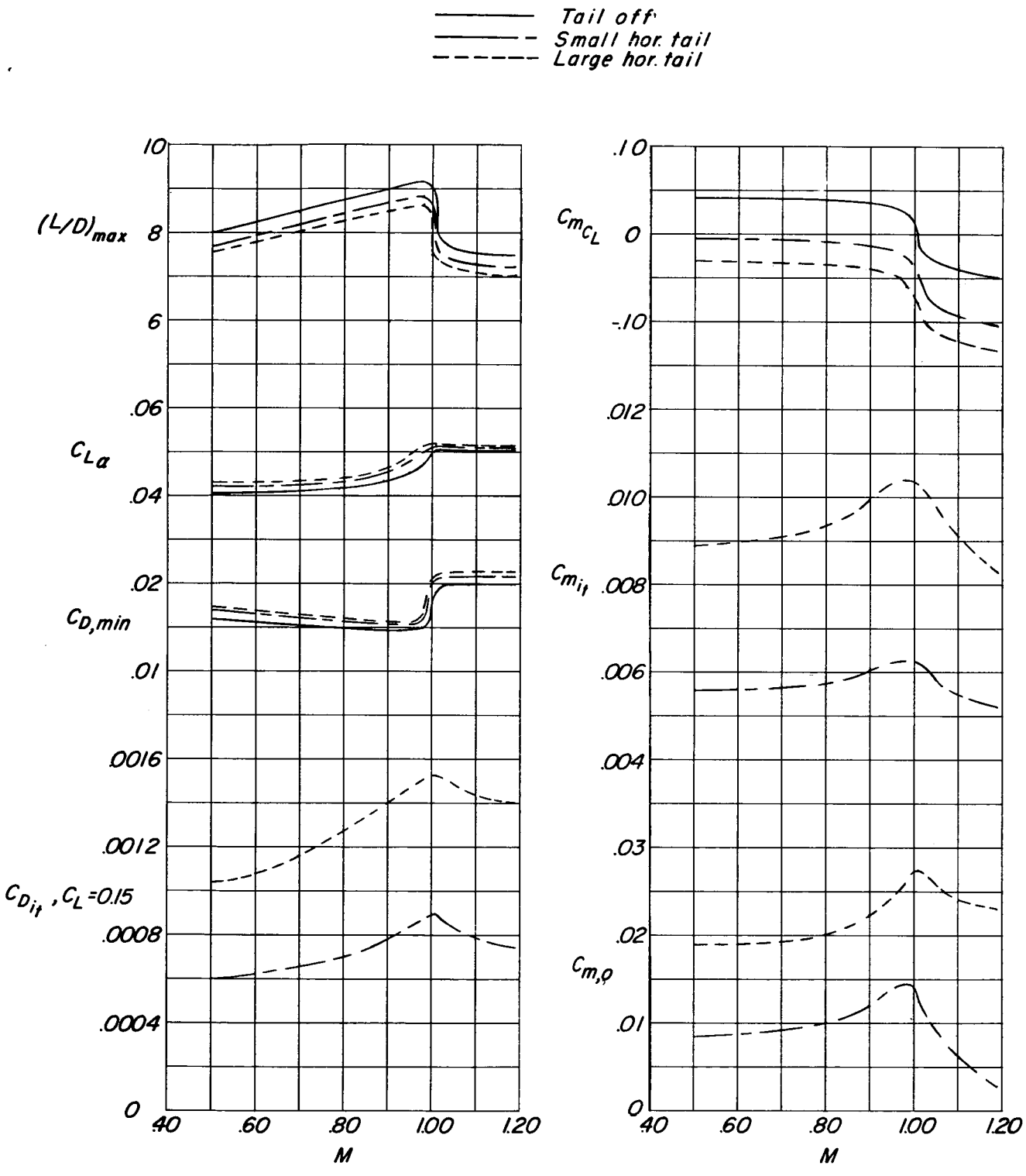

Figure 9.- Summary of the longitudinal characteristics of the model at Mach numbers from 0.50 to 1.19.